How *CLEC16A* modifies the function of thymic epithelial cells

-

Wie *CLEC16A* die Funktion von Thymus-Epithelzellen beeinflusst

Doctoral thesis for a medical doctoral degree

at the Graduate School of Life Sciences,

Julius-Maximilians-University of Wuerzburg,

Institute for Virology and Immunobiology

submitted by

Kevin Börner

from

Dresden

Wuerzburg, June 2019

Submitted on:

June 4th, 2019

……

Office stamp

Members of the Thesis Committee:

Chairperson: ……

Primary Supervisor: Prof. Dr. Thomas Hünig

Supervisor (Second): Prof. Dr. Stephan Kissler

Supervisor (Third): Prof. Dr. med. Hans-Peter Tony

Date of Public Defense: ……

Date of Receipt of Certificates: ……

The doctoral candidate is a licensed physician.

FOR MY FAMILY

Table of content

Sections marked with an asterisk (*) include data contributed by Dr. Cornelia Schuster or Prof. Dr. Stephan Kissler from experiments performed for the manuscript "The autoimmunity-associated gene CLEC16A modulates thymic epithelial autophagy and alters T cell selection" (Immunity, 2015). All data were used with explicit permission.

List of tables

List of figures

Figures marked with an asterisk (*) were generated by Dr. Cornelia Schuster as part of her work for the manuscript titled "The autoimmunity-associated gene CLEC16A modulates thymic epithelial cell autophagy and alters T cell selection" (Immunity, 2015). All figures were used with explicit permission.

Figure 1 was created and published by van Belle et al. in "Type 1 Diabetes: etiology, immunology, and therapeutic strategies" (Physiol Rev, 2011) and is used with the explicit permission by the American Physiological Society.

Abbreviations

DMEM	Dulbecco's Modified Eagle Medium
DPBS	Dulbecco's Phosphate-Buffered Saline
FBS	Fetal Bovine Serum
DNA	Deoxyribonucleic Acid
RNA	Ribonucleic Acid
shRNA	Small Hairpin RNA
mRNA	Messenger RNA
miRNA	Micro RNA
siRNA	Small Interfering RNA
shRNA	Small Hairpin RNA
dH_2O	Distilled Water
SOC	Super Optimal
PCR	Polymerase Chain Reaction
cDNA	Complementary DNA
GAPDH	Glyceraldehyde 3-Phosphate Dehydrogenase
TEC	Thymic Epithelial Cell
cTEC	Cortical Thymic Epithelial Cell
mTEC	Medullary Thymic Epithelial Cell
LC3	Microtubule-Associated Proteins 1A/1B Light Chain 3B
EBSS	Earle's Balanced Salt Solution
3MA	3-Methyladenine
RT	Room Temperature
BSA	Bovine Serum Albumin
SDS-PAGE	Sodium Dodecyl Sulfate Polyacrylamide Gel Electrophoresis
HCl	Hydrochloric Acid
TEMED	Tetramethylethylenediamine
APS	Ammonium Persulfate
TBS/T	Tris-Buffered Saline/Tween
IgG	Immunoglobulin G
HRP	Horseradish Peroxidase
CO_2	Carbon Dioxide

HBSS	Hank’s Balanced Salt Solution
FCS	Fetal Calf Serum
OCT	Optimum Cutting Temperature
H.E.	Hematoxylin / Eosin
BM	Bone Marrow
ER	Endoplasmic Reticulum
GA	Golgi Apparatus
IM	Isolation Membrane
aa	Amino Acids
TCR	T Cell Receptor
T1D	Type 1 Diabetes
T2D	Type 2 Diabetes
HLA	Human Leukocyte Antigen
AIRE	Autoimmune Regulator Protein
APECED	Autoimmune Polyendocrinopathy-Candidiasis-Ectodermal Dystrophy
GWAS	Genome-Wide Association Studies
MHC	Major Histocompatibility Complex
INS	Insulin
PTPN22	Protein Tyrosine Phosphatase, Non-Receptor Type 22
CTLA-4	Cytotoxic T-Lymphocyte-Associated Protein 4
CLEC16A	C-Type Lectin Domain Family 16 Member A
CV-B4	Coxsackie Virus B4
T_{reg}	T Regulatory Cells
NK	Natural Killer Cells
DC	Dendritic Cells
IAA	Insulin Antibodies
GAD65	Glutamic Acid Decarboxylase
IA-2	Tyrosine Phosphatase 2
ZnT8	Zinc Transporter
DPT-1	Diabetes Prevention Trial
CD	Cluster Of Differentiation
Th_1	T Helper Cell Type 1

Th_2	T Helper Cell Type 2
Th_{17}	T Helper Cell Type 17
TFH	T Follicular Helper Cells
IFNγ	Interferon Gamma
IL	Interleukin
CSII	Continuous Subcutaneous Insulin Injections
HbA1c	Glycated Hemoglobin
BCR	Beta Cell Receptor
MS	Multiple Sclerosis
SLE	Systemic Lupus Erythematosus
DN	Double Negative
DP	Double Positive
SP	Single Positive
TSSP	Thymic-Specific Serine Protease
TRA	Tissue Restricted Antigen
ATG	Autophagy Related Genes
CMA	Chaperone Mediated Autophagy
LIR	LC3-Interacting Region
UBA	Ubiquitin-Associated Domain
SNP	Single Nucleotide Polymorphism
CTLD	C-Type Lectin-Like Domain
ITAM	Immunoreceptor Tyrosine-Base Activation Motif
TM	Transmembrane Region
KD	Knockdown
KO	Knockout
RNAi	RNA Interference
RISC	RNA-Induced Silencing Complex
ESC	Embryonic Stem Cells
NOD	Non-Obese Diabetes Mouse
HSP60	Heat Shock Protein 60
SCID	Severe Combined Immunodeficiency
CY	Cyclophosphamide

IPGTT	Intraperitoneal Glucose Tolerance Test
eQTL	Expression Quantitative Trait Locus
APC	Antigen Presenting Cell
TAg	SV40 large T-Antigen
qPCR	quantitative PCR
CBD	Common Bile Duct

1. Introduction

1.1. Type 1 Diabetes

About 1 of 11 adults suffer from diabetes mellitus, a disease that has become the ninth major cause of death worldwide [1]. Diabetes mellitus is a chronic disease that is caused by a lack of or resistance to insulin. Insulin is a hormone produced by pancreatic β cells, which regulates blood glucose metabolism by promoting uptake of glucose into cells. Normal fasting blood glucose levels are less than 100 mg/dL (5.6 mmol/L) and vital for normal function of tissues [2]. A continuous elevation of blood glucose levels can lead to toxicity and chronic damage to tissues such as nerves and vessels. To monitor three-month plasma glucose concentrations and glucose control in patients, glycated hemoglobin (HbA_{1C}) has been established as a valuable diagnostic marker, as it is a form of hemoglobin that gets glycated proportionately based on blood glucose levels. 90% of all diabetes cases are attributable to Type 2 Diabetes (T2D), a chronic metabolic disease based on increased insulin resistance of the cells. Type 1 Diabetes (T1D), however, is a form of diabetes mellitus which is thought to be caused by an autoimmune-mediated destruction of β cells of the endocrine pancreas, culminating in a complete insulin deficiency and compromised glucose homeostasis. The vast majority of T1D cases is of autoimmune nature, while only a small minority of T1D cases are idiopathic with a distinct lack of autoimmunity [3]. Predominantly, T1D is a chronic disease of children and adolescents, but recent studies have shown that autoimmune diabetes can vary in age at onset and span across all age groups [4]. Core characteristics of T1D are the triad of polyuria, polydipsia and polyphagia, as well as hyperglycemia and the need for exogenous insulin substitution. Although the discoveries of insulin and other modern therapies have improved long term survival of patients with T1D greatly, the effects of macrovascular and microvascular complications can be detrimental for the patient. As prevalence and incidence rates rise, the burden of both T1D and T2D on patients and the health care system increases drastically. Currently, the estimated cost of T1D treatment accounts for 10% of the total health care costs in countries such as the UK [5]. Additionally, it was shown that the generic health-related quality of life in young children with T1D was significantly lowered compared to children without T1D of the same age [6]. Large epidemiological studies have shown that improved blood glucose control over the last decades has significantly lowered the risk of complications and cardiovascular disease in patients with T1D. However, the age adjusted relative risk of cardiovascular disease in children with T1D is still ten times greater than that of the general

population [7]. Despite great efforts and investments of today's society, many questions about epidemiology, pathogenesis and the effectiveness of current therapies and possible cures for T1D remain unanswered.

1.1.1. Epidemiology of Type 1 Diabetes

T1D is one of the most common autoimmune diseases in children and adolescents. There are two peaks of age at onset, the first at 5-7 years of age and the second during puberty. T1D accounts for approximately 5-10% of all diabetes cases around the world [1]. Its incidence rate varies greatly globally, with more than 60 cases per 100 000 people per year in Finland and less than 0.1 cases per 100 000 people per year in China. T1D accounts for more than 85% of all diabetes mellitus cases in youth under the age of 20 years. Data from large epidemiological studies such as DIAMOND and EURODIAB have shown that annual incidence rates of T1D are continuously increasing by 2-5% [8]. Such drastic rises in incidence cannot solely be attributed to genetic predisposition, but rather to a combination of genetic susceptibility and environmental influences.

1.1.2. Pathophysiology of Type 1 Diabetes

T1D is a heterogeneous disorder with variations in pathogenic processes, genetics and phenotypes. The majority of cases are autoimmune mediated, with patients showing either autoantibodies in their serum or genetic variations in genes that control immune functions. A small collective of T1D patients lack all signs of autoimmunity, with no clear understanding of pathogenesis. Recently, it has become more and more complicated to differentiate and diagnose T1D correctly, because prevalence of T2D in children has risen as obesity of the young is drastically increasing worldwide [9]. Generally, T1D is a result of autoimmune mediated destruction of pancreatic β cells and a lack of insulin secretion. Current hypotheses suggest a combination of genetic susceptibility and immunological and environmental factors as the cause for T1D.

T1D is a polygenic disease with almost 40 different gene loci identified to be involved in pathogenesis. There are a few genes with very large effect and many genes with smaller effects on risk of disease. Most prominently, the human leukocyte antigen (HLA) region on chromosome 6 makes up almost half of all genetic susceptibility for T1D. Both, HLA class I and

HLA class II alleles are significantly linked to T1D, with some alleles playing a predisposing (DRB1*03-DQB1*0201 [DR3]; DRB1*04-DQB1*0302 [DR4]) and others playing a protective (DQB1*0602) role [10, 11]. Notably, most gene loci associated with increased risk of T1D are involved in the immune response. Due to the autoimmune aspect of T1D, lymphatic tissues are thought to be heavily involved in pathogenesis.

In the thymus, presentation of antigen and central tolerance play crucial roles in maintaining immunological homeostasis. Naturally, overtly self-reactive immune cells are negatively selected (central tolerance). Self-reactive T cells that escape these mechanisms are usually suppressed in the periphery (peripheral tolerance). Dysfunction of these regulatory mechanisms may result in autoimmune disorder. For example, the autoimmune regulator protein AIRE is a transcription factor mainly expressed in the thymus, which regulates the expression of autoantigens and is linked to immune tolerance. It has been shown that patients with mutations of AIRE suffer from an autoimmune syndrome known as APECED or APS1, which is also associated with T1D [10]. In total, genome-wide association studies (GWAS) have identified 55 non-HLA gene loci to at least partially confer susceptibility, including *INS*, *PTPN22*, *CTLA-4* and amongst others a lectin-like gene called *CLEC16A*.

Despite the clear link between genetic susceptibility and risk of disease, the concordance rate in monozygotic twins is 30-50% [10], suggesting an influence of environmental factors. A plethora of such potential environmental factors have been investigated extensively, including nutrients, viruses, toxins and the microbiome. Epidemiological studies have linked viral infections, especially infections with enteroviruses such as coxsackie virus B4 (CV-B4), to T1D and autoimmunity. In some patients, CV-B4 was isolated from pancreatic tissue of patients with T1D, indicating a possible relation between disease and virus. Current hypotheses suggest an important role of CV-B4 in pathogenesis of T1D through activation of the innate immune system and autoimmunity by molecular mimicry [12, 13]. Additionally, the effect of diets and nutrition on disease development has been critically reviewed. Early exposure to cow's milk in an infant's diet may increase risk of autoimmunity and T1D [14]. This hypothesis was supported by a study that showed a reduction of T1D markers such as autoantibodies in children with genetic susceptibility after supplementing breast milk with ultra-hydrolyzed milk

formula [15]. Other factors such as vitamin D deficiency or reduced intake of omega-3 fatty acids may also be implicated in T1D pathogenesis.

In recent years, the gut microbiota has become a popular topic of research in the field of T1D pathogenesis. As modern day medicine shows greatly improved control of infectious disease in the western world, the incidence of autoimmune disorders is on the rise [16]. Most recently, it was found that patients with T1D show significant differences in their gut microbiota compositions compared to healthy controls [17]. If these changes in composition are caused by environmental factors such as diet and hygiene, and whether these changes are cause or result of T1D, needs to further be investigated.

The pathology and natural history of T1D have been extensively studied using pancreatic biopsies and entire organs of people with serological evidence of recent-onset of disease. Analyses of these tissues showed that more than 70% of pancreatic islets show a complete lack of insulin. About 20% of pancreatic islets still contain insulin but already display signs of inflammation (insulitis), and a small percentage of pancreatic islets show no sign of pathology [18]. Typically, pancreata of T1D patients show decreased weight, atrophy in the dorsal region, a lobular loss of β cells and heterogenous lobular insulitis. Histologically, pancreatic islets show a loss of β cells, which increases with the duration of disease and leads to reduced levels of insulin in the remaining β cells over time. Eventually, the remaining pancreatic islets are completely insulin-deficient, but show a preservation of all other hormone secreting cells, which suggests a selective loss of β cells in the pancreas. Immunostaining of pancreatic tissue of recent-onset patients shows infiltration of $CD8^+$ cytotoxic T cells as the most prevalent cell population in insulitis lesions, followed by $CD68^+$ macrophages, $CD4^+$ T cells and $CD20^+$ B cells. In contrast, $FoxP3^+$ T regulatory cells (T_{reg}) and natural killer cells (NK) are almost absent from insulitis lesions. Interestingly, once β cells are insulin-deficient, all subsets of immune cells are significantly reduced in islets. This indicates that there is some intrinsic stimulus during insulitis that promotes immune response and attracts immune cells [19].

Additionally, another typical feature of T1D compared with T2D is the presence of autoantibodies in the serum of patients. As a sign of autoimmunity, autoantibodies can be found in 70-80% of T1D patients at onset of disease [14]. The most common autoantibodies

in T1D are those against insulin (IAA), glutamic acid decarboxylase (GAD65), tyrosine phosphatase 2 (IA-2) and zinc transporter (ZnT8) [20]. Despite expansive information on the prevalent autoantibodies in T1D, it is still unclear whether these antibodies are cause or result of autoimmunity in the pancreas. So far, autoantibodies have mostly been of predictive or diagnostic value. In some large studies such as the Diabetes Prevention Trial (DPT-1) the 5 year risk of T1D was 25% for subjects with one antibody, 50% for subjects with two antibodies and more than 70% for subjects with three or more antibodies in their serum [21]. Although most theories disregard autoantibodies as pathogenic, some studies found an improvement in T1D patients after treatment with Rituximab, a B cell depleting drug, suggesting a potential role of autoantibodies in pathogenesis of T1D [22].

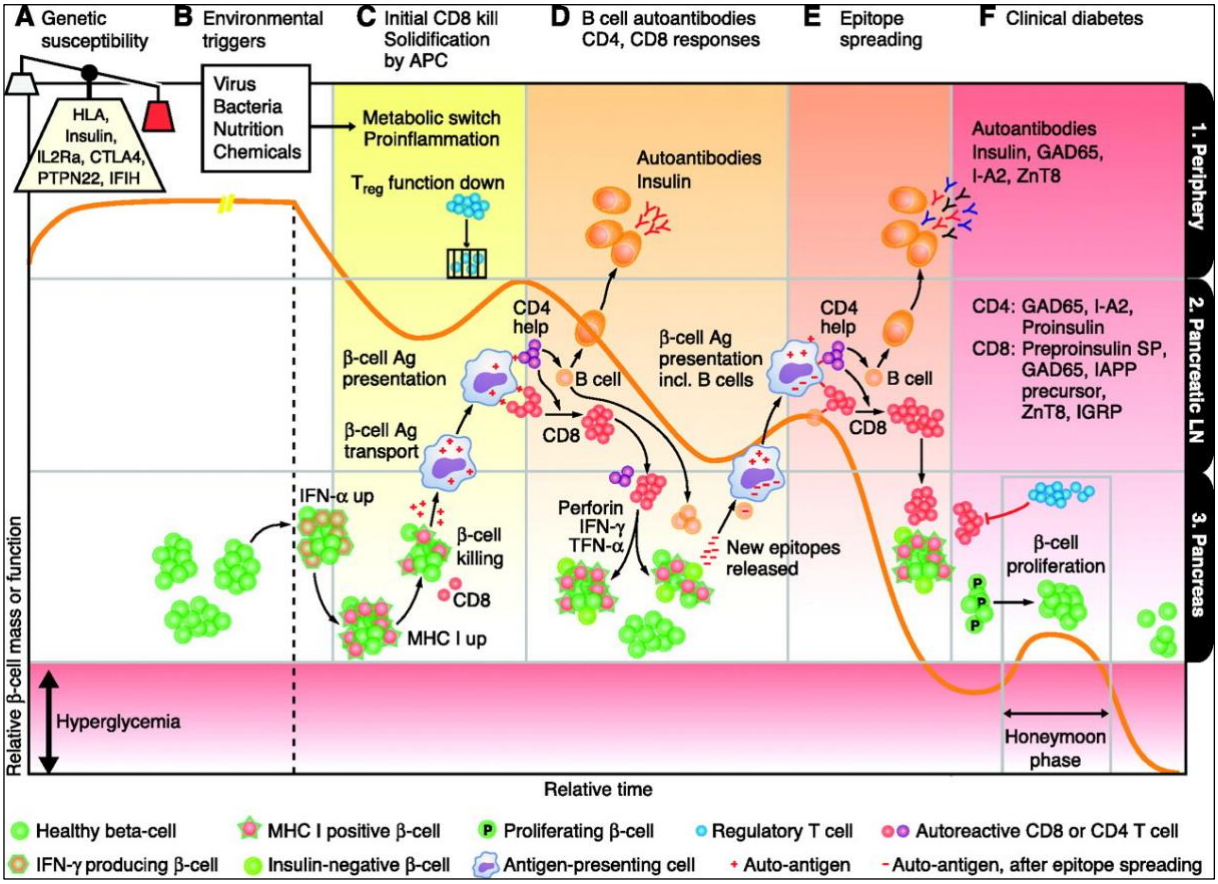

Figure 1 **Pathogenesis of Type 1 Diabetes, with permission, as published by van Belle et al.** [23]

Today, most theories agree that T1D is caused by a final pathway of cellular autoimmunity in which autoantigen-specific T cells destroy insulin producing β cells in the pancreas. Once autoreactive T cells are activated through antigen presentation by local antigen presenting cells (APCs), they differentiate into effector cells. To initiate and convey insulitis and T1D, both

$CD4^+$ and $CD8^+$ T cells are required. $CD4^+$ T cells are helper cells mainly required for activation and stimulation of $CD8^+$ T cells and B cells. There are multiple subsets of $CD4^+$ T cells. Th_1 cells exacerbate T1D by cell mediated immunity and the expression of pro-inflammatory chemokines such as IFNγ and IL-2. Th_2 cells protect from T1D by humoral immunity and the production the immunoregulatory chemokines IL-4 and IL-10. Th_{17} cells are pro-inflammatory T cells also involved in the pathogenesis of T1D, whereas T_{regs} are understood to serve as immunoregulatory and immunosuppressive cells [24]. $CD4^+$ T cells require the major histocompatibility class (MHC) II molecules for activation. On the other hand, $CD8^+$ T cells recognize antigen presented through the MHC class I pathway. Pancreatic β cells only express MHC class I molecules and no MHC class II molecules [25]. Studies have shown that non-obese diabetic (NOD) mice, which lacked MHC class I molecules, were protected from insulitis and T1D, which indicates that $CD8^+$ T cells are essential for T1D initiation [26]. Once activated, $CD8^+$ T cells proliferate into cytotoxic T cells. Cytotoxic $CD8^+$ cells can interact with pancreatic β cells directly through a cell-to-cell contact, or indirectly by releasing pro-inflammatory cytokines and perforin, which leads to the destruction of pancreatic β cells [24].

Over the past decade, $FoxP3^+$ T_{regs} were implicated in the pathogenesis of T1D. T_{regs} were found to suppress activation, proliferation and expansion of $CD4^+$ and $CD8^+$ T cells and therefore help to maintain peripheral tolerance [27]. Patients with T1D show a quantitative and qualitative deficit in T_{regs}, which could mean reduction in peripheral tolerance and an increase in immune response [14].

In summary, individuals with predisposing genetic susceptibility can develop T1D if triggered by concurrent environmental effects. $CD8^+$ T cells specific for pancreatic antigens attack pancreatic β cells, which die and release pancreatic antigen. These antigens are processed and presented by APCs, which stimulates and activates $CD4^+$ T cells and B cells. B cells differentiate into plasma cells and start producing autoantibodies. Meanwhile, environmental factors shape the inflammatory setting and suppress T_{regs}, and further enable pro-inflammatory immune cells. With the increasing cellular stress and destruction of pancreatic β cells, the production and secretion of insulin ceases and blood glucose levels rise.

1.1.3. Management of Type 1 Diabetes

In 1921, insulin was discovered as a breakthrough therapy for T1D. Since then, substitution of exogenous insulin has become the standard treatment of T1D patients. Despite the many advantages of insulin replacement therapy, persistent metabolic homeostasis cannot always be maintained, which in turn can lead to common micro- or macrovascular damage and complications such as retinopathy or cardiovascular disease. Therefore, a more rigorous blood glucose management is required. Today, modern treatment of T1D usually includes the use of insulin analogues and mechanical devices such as pumps and blood sugar monitors. There are different viable options for treatment of T1D. With multiple injections of insulin per day, the patient uses a long-acting basal insulin and a rapid-acting bolus insulin. In recent years, the use of continuous subcutaneous insulin injections (CSII) has become more popular, with studies showing a lower HbA_{1C} compared to multiple injections a day. Additionally, recent studies have shown that real-time blood glucose monitoring decreases time spent in hypoglycaemia and lowers HbA_{1C}. In combination, real-time blood glucose monitoring and CSII are now being used as sensor-augmented pump therapy. In the future, sensor-augmented pump therapy may be enhanced even further by algorithms which simulate a closed-loop system similar to an artificial pancreas [28, 29].

1.2. The immune system

Humans are constantly exposed to potentially damaging influences from the environment. As a host defense, the immune system has evolved to protect the human body from such harm. Its main task is to detect and eliminate infectious agents, known as pathogens, as well as keeping the body's own defective cells in check. Pathogenic microorganisms can differ greatly in their mechanisms of pathogenesis. Hence, the immune system comprises a variety of systems and processes, all of which interact with each other to protect from infection and disease. Without an immune system, the body would be left vulnerable to pathogens such as microbes, toxins and allergens. There are two major parts of the immune system, the innate and the adaptive system.

1.2.1. Innate immune system

The innate immune system is an immediate, yet unspecific response and can be considered a first line of defense. It exists in almost all living organisms. As a first layer of defense, physical

barriers such as the epithelium with tight cell-cell contacts, or the protective mucus barrier in the respiratory tract, stop pathogens from entering the body. Once these barriers are breached, the immediate innate response includes antimicrobial proteins such as defensins, which can bind to the cell membrane of a microbe and disrupt its stability. If a pathogen bypasses the initial defense, it encounters another layer of the innate immune system, the so-called complement system. This system is comprised of soluble proteins in blood and bodily fluids that can be activated directly by contact with pathogens or indirectly by contact with antibodies bound to pathogens. Once activated, a biochemical chain of reactions aids (or complements) the immune system in detecting, tagging and eliminating pathogens. Cells of the innate immune system can be divided into two groups. On the one hand, phagocytes (i.e. macrophages, neutrophils, dendritic cells) consume opsonized pathogens, destroying the threat and activating other parts of the immune system by releasing inflammatory mediators such as chemokines. On the other hand, natural killer cells are capable of inducing apoptosis directly in infected cells [30-33].

1.2.2. Adaptive immune system

Unlike the innate immune response, the adaptive immune system is highly specific to its target antigens and provides an immunological memory for re-infections. There are two major cell types involved in adaptive response: T lymphocytes (T cells) and B lymphocytes (B cells). All lymphocytes derive from the bone marrow, yet only B cells mature there. Naïve B cells differentiate into either plasma cells, which produce antibodies, or B memory cells. Precursor T cells migrate to the thymus, a site where complex selection and maturation takes place. At the end of development, T cells express either CD8 or CD4 as a surface protein. $CD8^+$ T cells leave the thymus as cytotoxic T cells, whereas $CD4^+$ T cells can develop into at least five different subsets of effector cells called Th_1, Th_2, $Th_{17,}$ T_{regs} and follicular helper cells (T_{FH}). After maturation, lymphocytes migrate into the bloodstream and spread to secondary lymphoid tissues, ready to encounter antigen.

A functioning immune system must be able to recognize millions of different pathogens at any time. In contrast to cells of the innate immune system, which express pattern recognition receptors that recognize features common to many pathogens, cells of the adaptive immune system each carry one receptor specific to a single antigen. Once an antigen-specific

lymphocyte gets activated, it proliferates into a clone of identical cells, all expressing the same antigen receptor. The highly diverse repertoire of antigen-specific receptor molecules in humans is encoded by genes, which are generated through somatic rearrangement of a few hundred gene elements during maturation in the bone marrow and thymus.

Although the B cell receptor (BCR) and T cell receptor (TCR) are evolutionarily quite similar, the way B cells and T cells recognize antigen is fundamentally different. B cells directly bind antigen with their BCR. In contrast, T cells only recognize antigens that have been processed and presented as peptides on the surface of APCs. Specifically, T cells will only recognize peptides if they are bound to a particular group of surface proteins encoded in a cluster of genes called the major histocompatibility complex or human leukocyte antigen complex. MHC molecules are assembled inside the cell and transported to the cell surface where they display a single processed peptide to T cells. There are two major classes: MHC class I and MHC class II. MHC class I molecules can be found on most human cells and present peptides derived from intracellular proteins, such a degraded viral protein. Peptide bound to MHC class I molecules can interact with $CD8^+$ cytotoxic T cells, which in turn activate and kill infected cells. In contrast, MHC class II molecules are mostly present on the surface of APCs (dendritic cells, macrophages) and display peptides previously internalized through phagocytosis or endocytosis. Peptide bound to MHC class II molecules activates $CD4^+$ T cells. These will release chemokines and other effector molecules to effect target cells directly or promote activation of other immune cells. Thus, T cells play a crucial role in both cell-mediated and humoral immune response [30-33].

1.2.3. The immune response

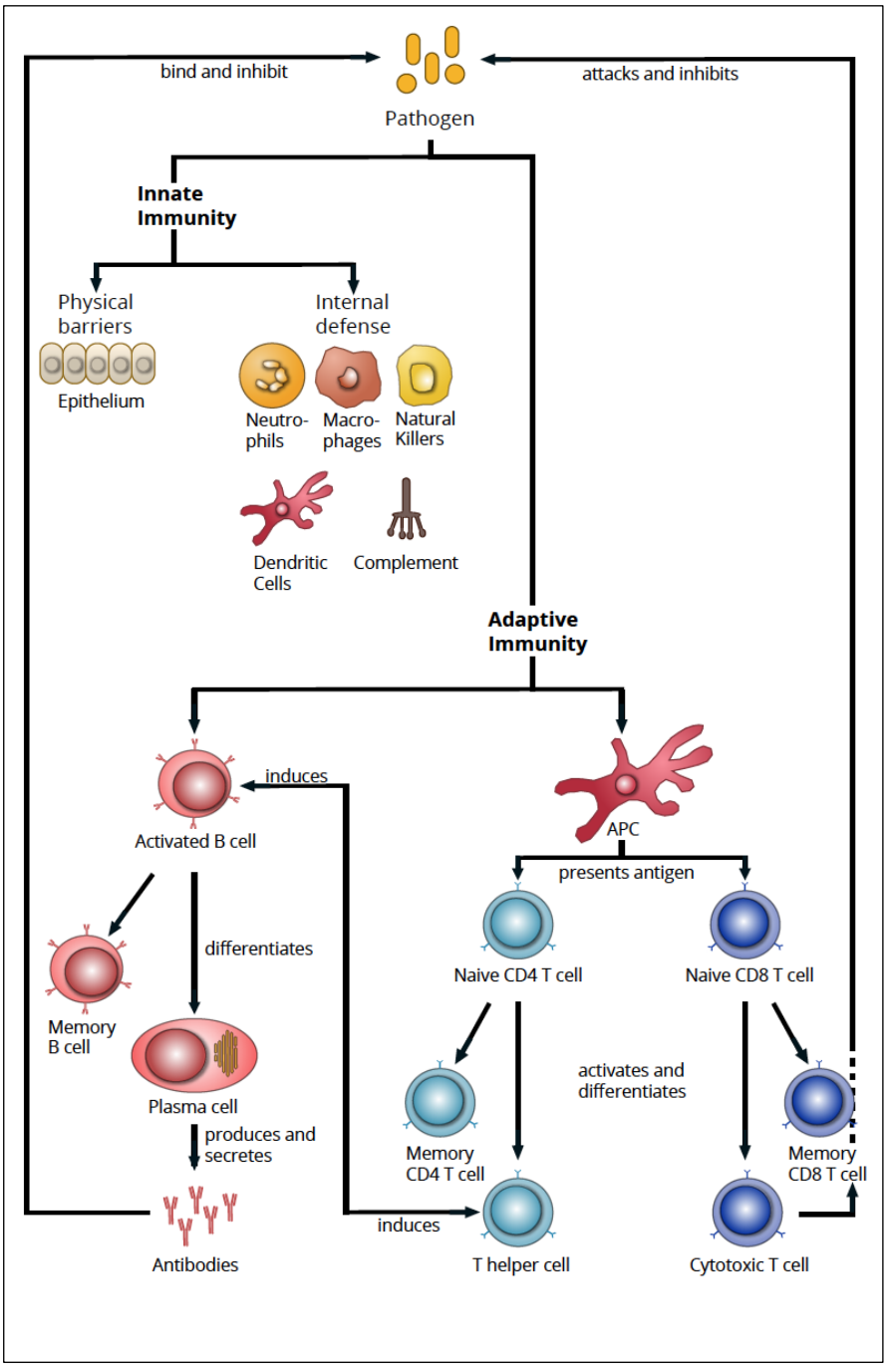

Figure 2 **Overview of the primary immune response**

The innate system is the first line of defense against infectious agents. Its components are of different nature: physical barriers (e.g. epithelium), immune cells (macrophages) and other molecules such as the complement system play a crucial role in innate immunity. The adaptive system can be divided into two systems, the humoral and cellular response. B cells differentiate into plasma cells and generate antigen specific antibodies. Antibodies can tag foreign agents and help eliminate pathogens. Some B cells differentiate into memory cells, which will reactivate quickly during a secondary response. T cells differentiate into a plethora of different

subpopulations, most prominently $CD4^+$ T helper cells and $CD8^+$ cytotoxic T cells. $CD4^+$ T helper cells stimulate other immune cells and mediate immune response, while $CD8^+$ cytotoxic T cells directly help eliminate pathogens. T cells can also differentiate into memory T cells for secondary responses.

1.3. Autoimmune disease

Autoimmune diseases such as T1D, Multiple Sclerosis (MS), Systemic Lupus Erythematosus (SLE), Crohn's Disease, Celiac Disease and others are considered a leading cause of death and disability worldwide, with a recently estimated prevalence of 7.6 - 9.4% in the general population [34]. Over the past decades, incidence rates for autoimmune diseases such as T1D have risen significantly [35], severely effecting both patient quality of life and health care systems [36], and making them a prime target for modern day research.

Multiple studies have shown an increased risk of autoimmune disease in monozygotic twins [37] and first-degree relatives of affected individuals [38], implying a genetic component in susceptibility for autoimmune disease. Additionally, environmental factors such as nutrition, tobacco smoking, infectious disease or the microbiota are known to be of critical importance in autoimmune disease [39, 40]. Today, autoimmune disease can be seen as a complex disorder that requires genetic predisposition and environmental factors to trigger autoimmunity and tissue damage. Yet, despite significant advances in our understanding of human autoimmunity, many questions considering etiology and pathogenesis of autoimmune disease remain unanswered.

1.3.1. Autoimmunity

The human immune system uses both innate and adaptive mechanisms to protect the body against a plethora of pathogenic organisms, as well as toxins and allergens. Its main goal is to detect foreign pathogenic antigens and to launch a powerful immune response to eliminate any threat. At the same time, excessive damage to self-tissue must be avoided. Critical to a functioning immune system is the ability to distinguish between self and non-self. Lack of self-discrimination leads to an uncoordinated immune response against self and results in autoimmunity. Autoimmunity can lead to chronic inflammation, tissue damage and autoimmune disease.

Generally, through a process of central tolerance, T cell differentiation in the thymus generates such a repertoire of T cells that induces strong immune response against foreign

antigen but maintains relatively weak responsiveness to self-peptide. This process starts with the maturation of progenitor thymocytes in the thymus.

1.3.2. T cell development

During T cell maturation in the thymus, thymocytes go through a series of developmental stages which can be characterized by the expression of certain cell surface proteins, most prominently the TCR complex (CD3 and the TCR chains) and the co-receptor proteins CD4 and CD8. The first cells migrating to the thymus do not bear any of these characteristic surface proteins. At this point, the precursor cells can give rise to two populations of T cells: a majority α:β T cell line and a minority δ:γ T cell line. After contact with stromal cells in the thymus, the progenitor cells commit to the T cell lineage but still lack the surface molecules CD4 and CD8. These so-called double negative (DN) T cells undergo another series of developmental stages ranging from DN1 to DN4, which are characterized by the up and down regulation of surface molecules such as CD25 and CD44 and gene rearrangement within the TCR β-chain locus. Eventually, DN4 cells start to express CD4 and CD8 and turn into double positive (DP) $CD4^+$ $CD8^+$ thymocytes. DP thymocytes express low levels of α:β TCRs with ranging affinities for antigen. At this point, the affinity of TCR to the self-peptide:MHC complex determines the fate of the thymocyte [33].

1.3.3. Positive and negative selection in the thymus

DP thymocytes are programmed to die by neglect, unless they are rescued by TCR signaling after binding self-peptide:MHC complex – a process called positive selection. Most DP thymocytes express TCRs with no affinity to self-peptide:MHC and die. Only about 1 - 5% of DP thymocytes express α:β TCRs with low affinity to self-peptide:MHC and survive. After positive selection, thymocytes express high levels of TCR and down regulate one of the two surface molecules, either CD4 or CD8, and mature into single positive (SP) $CD4^+$ or $CD8^+$ T cells. In contrast, other thymocytes express TCRs with high affinity to self-peptide:MHC complex and bind self-antigen too strongly. As a potential threat to self-tissue, thymocytes with high affinity TCRs to self-peptide are subject to negative selection, a process that eliminates highly reactive T cells [33, 41].

In order to understand the process of T cell maturation, it is important to discuss the anatomical and functional compartments of the thymus. There are two major regions in the thymus: an outer cortex containing mostly DP and DN thymocytes and a central medulla harboring mostly SP thymocytes. Although most of the thymus comprises progenitor thymocytes, there are a number of stromal cells such as macrophages, dendritic cells (DCs) and epithelial cells. Positive selection of α:β TCR thymocytes takes place in the cortex and is highly dependent on a particular class of APCs known as cortical thymic epithelial cells (cTECs). Previously, it was thought that cTECs were important for positive selection due to an abundance in expression of MHC molecules and close proximity to developing thymocytes. Recently, however, it was shown that antigen processing in cTECs may play a vital role in positive selection [42]. MHC class I antigen presentation in cTECs involves a distinct proteasome subunit called β5t. Mice lacking β5t in the thymus were shown to have a severely reduced pool of positively selected $CD8^+$ T cells [43]. Additionally, MHC class II antigen presentation in cTECs involves uniquely expressed proteases such as the thymus-specific serine protease (TSSP) and cathepsin L. Mice deficient of TSSP or cathepsin L showed a significantly impaired selection and immune response of $CD4^+$ T cells [44, 45]. Furthermore, it was shown that MHC class II antigen presentation in cTECs is highly dependent on macroautophagy, a process where intracellular components are degraded and recycled [46, 47].

While the cortex plays an important role in early T cell development and positive selection, the thymic medulla is involved in tolerance induction and the deletion of hyperreactive α:β TCR thymocytes. Medullary thymic epithelial cells (mTECs) are critical to tolerance induction, as they are capable of promiscuous gene expression of tissue-restricted antigens (TRAs) [48]. mTECs can present endogenously expressed self-antigen directly to T cells through MHC class II loading and induce negative selection of both $CD4^+$ and $CD8^+$ T cells [49, 50]. There are at least two ways how mTECs can load self-antigen onto MHC class II molecules. First, contents of the endoplasmic reticulum (ER) can leak into the MHC class II loading pathway. Second, just as in cTECs, antigen presentation of endogenous self-peptide in mTECs has been reported to heavily depend on macroautophagy [47]. Athymic mice which had received thymic transplants deficient in macroautophagy showed severe immune-mediated tissue damage, indicating a crucial role of autophagy in TECs, T cell selection, tolerance and autoimmunity [46].

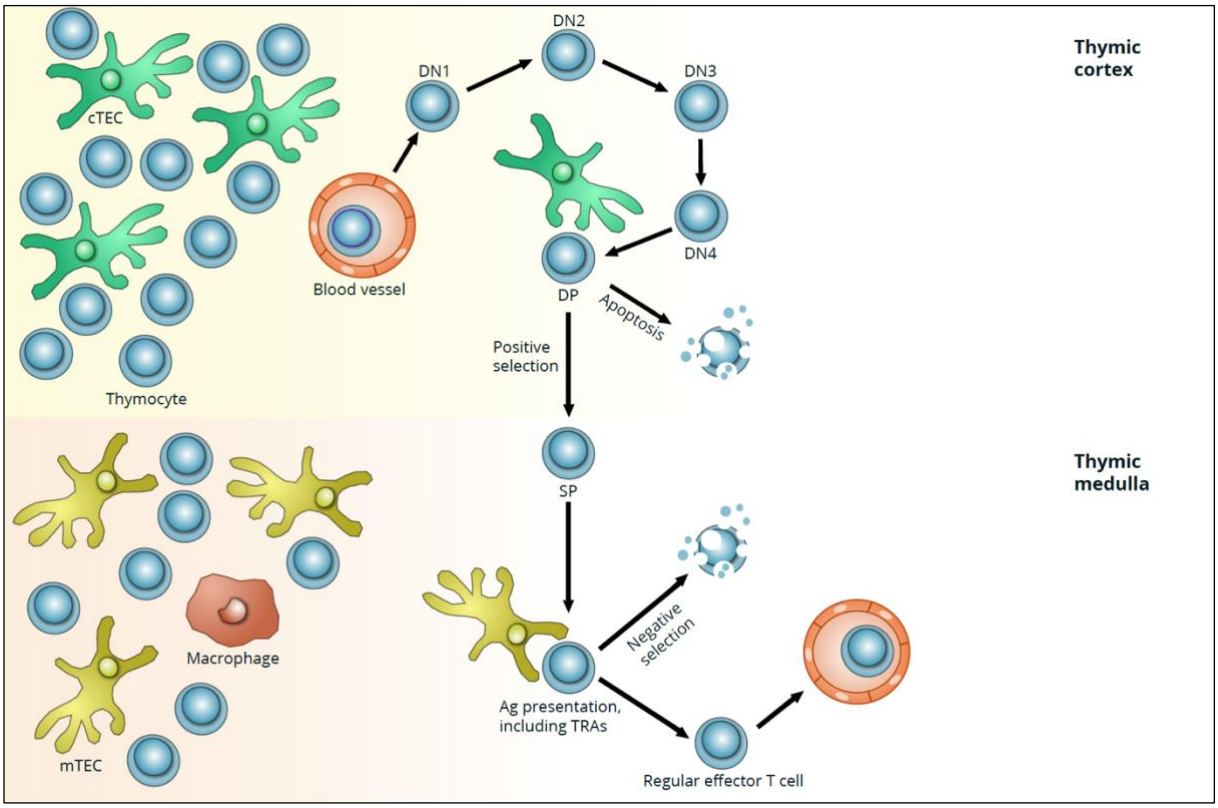

Figure 3 T cell selection in the thymus

Naïve thymocytes enter the thymus through vessels in the subcapsular cortical region, where they encounter a network of cortical epithelial cells (cTEC). At first, T cell precursors are double negative (DN) and express neither CD4 nor CD8. As the thymocytes progress through the four DN stages, β-chain rearrangement takes place. Once β-chain rearrangement is completed, thymocytes will proliferate and express CD4 and CD8 and become double positive (DP). DP thymocytes move deeper into the thymic cortex, where they are presented with antigen via MHC molecules on cTECs. Cells that bind with self-peptide:MHC survive (positive selection), while most other cells die by neglect. Cells that survive positive selection migrate towards the medulla, where they are presented with tissue-restricted antigens (TRAs) by medullary thymic epithelial cells (mTECs) and interact with other antigen presenting cells (APCs). Cells that bind too strongly to self-peptide receive an apoptotic signal and die. The remaining cells exit the thymus as effector T cells [51-53].

1.4. Autophagy

Autophagy is a protein degradation process essential to maintaining cellular homeostasis. It is a constitutive process that is also highly inducible through stress such as starvation. Evolutionary, it is well conserved from yeast to mammals [54]. Autophagy is required to rid cells of abundant protein, aggregates, organelles and nutrients. It serves as a recycling and fuelling mechanism within the cell. Recent studies show its involvement in tumor suppression, immunity, adaption to starvation or other stressors [55]. Since the discovery of autophagy-

related genes (ATGs) in yeast, there is a greater mechanistical understanding of autophagy [56]. Recently, polymorphisms of autophagy related genes have been linked to disease such as neurodegenerative or autoimmune disease. There are three types of autophagy: microautophagy (as seen in yeast), chaperone-mediated autophagy (CMA) and macroautophagy (from here on called 'autophagy').

1.4.1. Macroautophagy

Autophagy has long been thought to be a non-selective process. Recent studies, however, suggest there are also highly specific degradation processes mediated by autophagy [57]. First, an isolation membrane (also called phagophore) encloses intracellular material to form a double-membrane vesicle, called the autophagosome. Next, autophagosomes fuse with lysosomes to form an autophagolysosome. Finally, enzymes contained within the autophagolysosome degrade the previously engulfed cytoplasmic material (see Figure 4). Currently, at least 41 ATGs have been identified. ATG proteins are critical in regulating initiation, maturation, fusion and degradation. A core ATG protein is ATG5, which is indispensable in autophagosome formation. A knockdown (KD) or knockout (KO) of *ATG5* can result in downregulation or complete inhibition of autophagy. Hence, *ATG5* is a commonly used marker for autophagy.

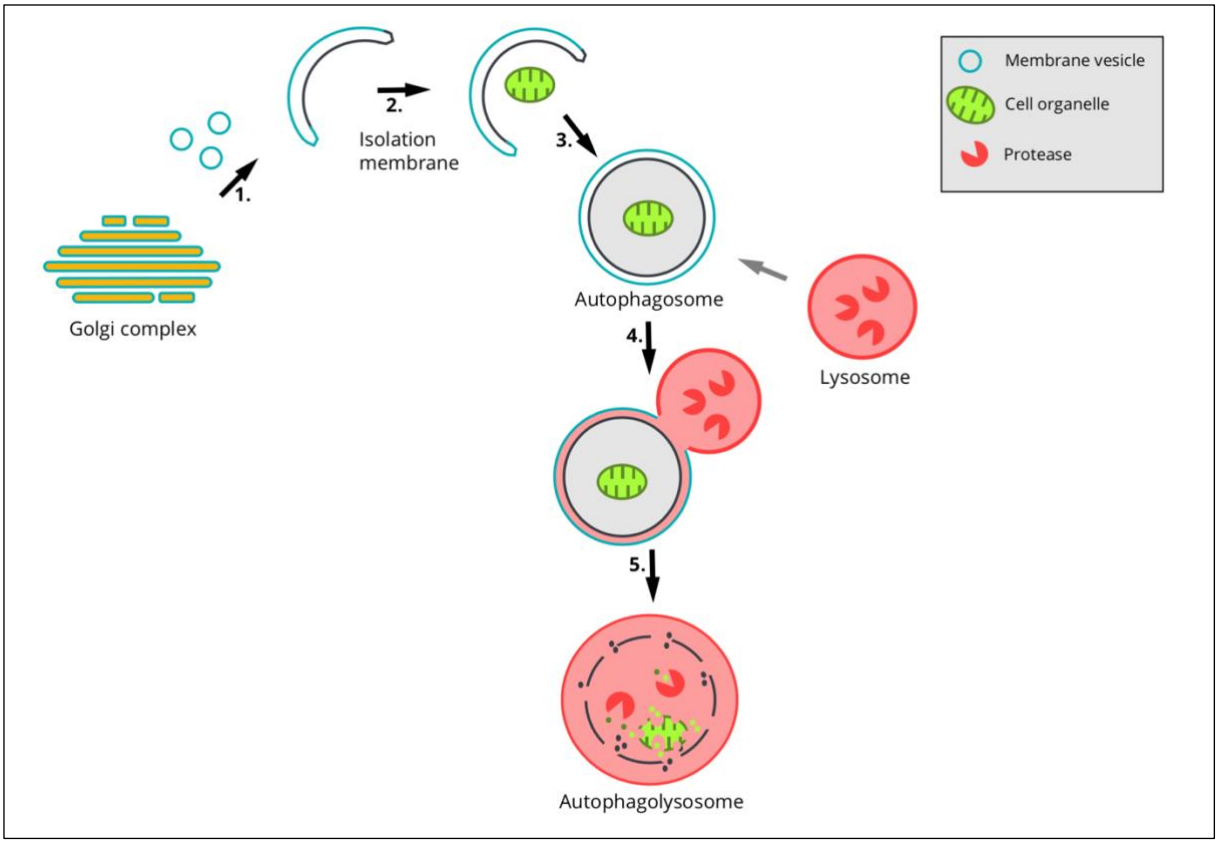

Figure 4 Overview of autophagy

Pre-existing organelles such as the Golgi body (or endoplasmic reticulum, mitochondria) supply lipids and membrane vesicles to support the formation of an isolation membrane, also called phagophore. The phagophore encloses organelles and cytoplasm to form a vesicle called autophagosome, a process which is highly dependent on ATGs, e.g. *ATG5*. Also, the *Clec16a* ortholog *ema* in Drosophila has been shown to be crucial for autophagosome formation and maturation. The outer membrane of the autophagosome subsequently fuses with a lysosome to form an autophagolysosome. The engulfed organelles are degraded by lysosomal enzymes into peptides. These peptides can be re-purposed within the cell or presented as antigens [58, 59].

1.4.2. Autophagy in autoimmunity

Lymphocytes are crucial to adaptive immunity. One way to activate lymphocytes is through antigen presentation via MHC class I and MHC class II molecules (see Chapter 1.2.2.). For regular activation of lymphocytes, MHC molecules are loaded with peptides previously processed by protein degradation systems such as the ubiquitin-proteasome or autophagy. Studies have demonstrated that autophagy can promote antigen presentation through MHC class I and MHC class II molecules and affects activation of T cells [60, 61]. Additionally, it was reported that autophagy deficiency in thymic epithelial cells impairs MHC class II antigen presentation and therefore shapes the selection of autoreactive T cells [46].

1.4.3. Autophagy in thymic epithelial cells

In contrast to most other cells, TECs show a high rate of constitutive autophagy. Additionally, they are the only non-hematopoietic cells which express MHC class II molecules constitutively. It was demonstrated that presentation of self-antigen through MCH class II molecules on TECs is essential for the selection of a functional T cell repertoire [46]. Regular APCs mainly display extracellular peptides on MHC class II molecules previously processed through endocytosis. TECs, however, are highly inefficient in processing and presenting extracellular peptides through the MHC class II pathway [46]. This suggests that TECs use other systems to load MHC class II molecules, systems such as autophagy. The protein H2-DM is involved in antigen presentation on APCs, mostly through the MHC class II pathway. In further studies, autophagy markers in TECs colocalized with H2-DM$^+$ lysosomal compartments, suggesting a possible intersection of the autophagy pathway with the MHC class II loading process [62]. Additionally, it was found that genetic interference with autophagy strictly in TECs led to an altered T cell repertoire and severe multi-organ inflammation in mice. Remarkably, in that study, impaired autophagy led to altered MHC ligands on cTECs and altered TRAs in mTECs, underlining a possible effect of autophagy on T cell selection [46]. Despite these findings, it remains unclear how exactly impaired autophagy leads to an altered T cell repertoire and autoimmunity.

1.4.4. Monitoring autophagy

To this day, monitoring autophagy remains complicated. With a recent surge of interest in the field, especially since Yoshinori Ohsumi received the *Nobel Prize in Physiology or Medicine* for his work on autophagy in 2016, an increasing number of assays and techniques have been developed to investigate the process. There are two major ways of monitoring autophagy: direct observation of autophagy-related structures in the cell and quantification of turnover of autophagy related proteins. Considering that autophagy is a highly complex and dynamic process, it is important to measure autophagic activity. This comprises the formation of autophagosomes, but also the entire flow of autophagic structures, including transportation and release of autophagic substrates. Currently, the most common way to monitor autophagic flux is to quantify the levels of certain proteins, most prominently LC3 and p62 [59, 63].

1.4.4.1. The microtubule-associated protein 1 light chain 3 – LC3

As the homolog of *Atg8*, the microtubule-associated protein 1 light chain 3 (*MAP1LC3B*) encodes for one of the most commonly used markers for autophagy called LC3 [64]. In mammals, there are three known isoforms of LC3, in particular LC3A, LC3B and LC3C. The isoform LC3B (from here on called LC3) has been studied intensively and has been found to play a crucial role in the formation of autophagosomes [65]. There are two forms of the ubiquitin-like protein LC3. First, proLC3 is cleaved by the ATG4 protease to become LC3-I with a glycine residue. Then, in a ubiquitination-like process, LC3-I gets modified by ATG7, ATG3 and the ATG16L complex with phosphatidylethanolamine to become LC3-II [65, 66]. While LC3-I is a soluble fraction in the cytoplasm, LC3-II is bound to most autophagic membranes, including the phagophore and the autophagosome. Specifically, LC3-II localizes with both the outer and the inner membrane of the autophagosome. Once the autophagosome fuses with a lysosome, the LC3-II bound to the outer membrane of the autophagosome gets cleaved by ATG4 protease and converted back to LC3-I [64, 66]. The LC3-II on the inner part of the autophagosome gets degraded by lysosomal proteases as part of autophagy.

The amount of LC3-II is closely tied to the formation of autophagosomes and usually a good indicator of autophagy. One way to investigate autophagy is to study LC3-positive structures using an anti-LC3 antibody and immunofluorescence [63, 66]. Under nourished conditions, there are only few LC3-positive structures. In contrast, under starved conditions, there is a significant increase in LC3-positive structures, indicating an induction of autophagy. Although LC3-positive structures can signal an increase in autophagy and the formation of autophagosomes, they can also be a result of impaired autophagy and an accumulation of autophagosomes due to reduced degradation of vesicles.

A more commonly used approach of studying autophagy is protein detection via the Western blot technique [63, 64, 66]. LC3-I and LC3-II can be separated due to different mobility in SDS-PAGE. LC3-I can usually be detected at 16kD and LC3-II at roughly 14kD [64]. Although immunoblotting is a widely used method, there are pitfalls to this technique, and it can be difficult to interpret results. For example, LC3-I and LC3-II show different immunoreactivity with LC3-II binding more strongly to antibodies than LC3-I. Furthermore, after starvation, the amount of LC3-I decreases and the amount of LC3-II increases, as more autophagosomes are

formed and more LC3-I is converted to LC3-II. Levels of LC3-II, however, are dynamic and cannot be used for studies, as the outer-membrane LC3-II is converted back to LC3-I and the inner-membrane LC3-II is further degraded by autophagy. Hence, in order to measure autophagic turnover, lysosomal inhibitors such as pepstatin A or E64d are used to arrest autophagy and stop lysosomal degradation of LC3-II [64, 66]. Degradation of LC3-II is mostly inhibited while LC3-I remains unaffected by protease inhibitors. With this approach, it is possible to measure autophagic flux in the form of an LC3-II/LC3-I ratio. Normally, after treatment with protease inhibitors, starved wild type cells show a high LC3-II/LC3-I ratio, as autophagy is induced, and LC3-II accumulates due to inhibition of further degradation. In contrast, when autophagy is genetically impaired (*Atg5* knockout), cells show a significantly lower LC3-II/LC3-I ratio [66]. In summary, analysis of autophagy assays can be difficult, but generally, if there is an increase in LC3-II after treatment with protease inhibitors, there is functional autophagic flux.

1.4.4.2. The autophagosome cargo protein p62

An alternative way to study autophagy is to measure levels of p62, a protein encoded by *SQSTM1*. p62 is a multifunctional protein with an LC3-interacting region (LIR) and a C-terminal ubiquitin-associated domain (UBA), playing an important role in autophagy as well as the proteasomal degradation of proteins [67]. p62 serves as a receptor for selective autophagy [68]. It can bind LC3 and deliver polyubiquitinated cargo proteins to autophagosomes, serving as a substrate of autophagy [64, 67]. It has been established that autophagy reduces levels of p62, while the inhibition of autophagy increases levels of p62 [69]. Although levels of p62 are highly dependent on autophagy, they can also be altered by transcriptional regulation and inhibition of proteasomal degradation. Therefore, results of p62 studies are usually interpreted and presented in combination with other methods, such as LC3-II turnover studies.

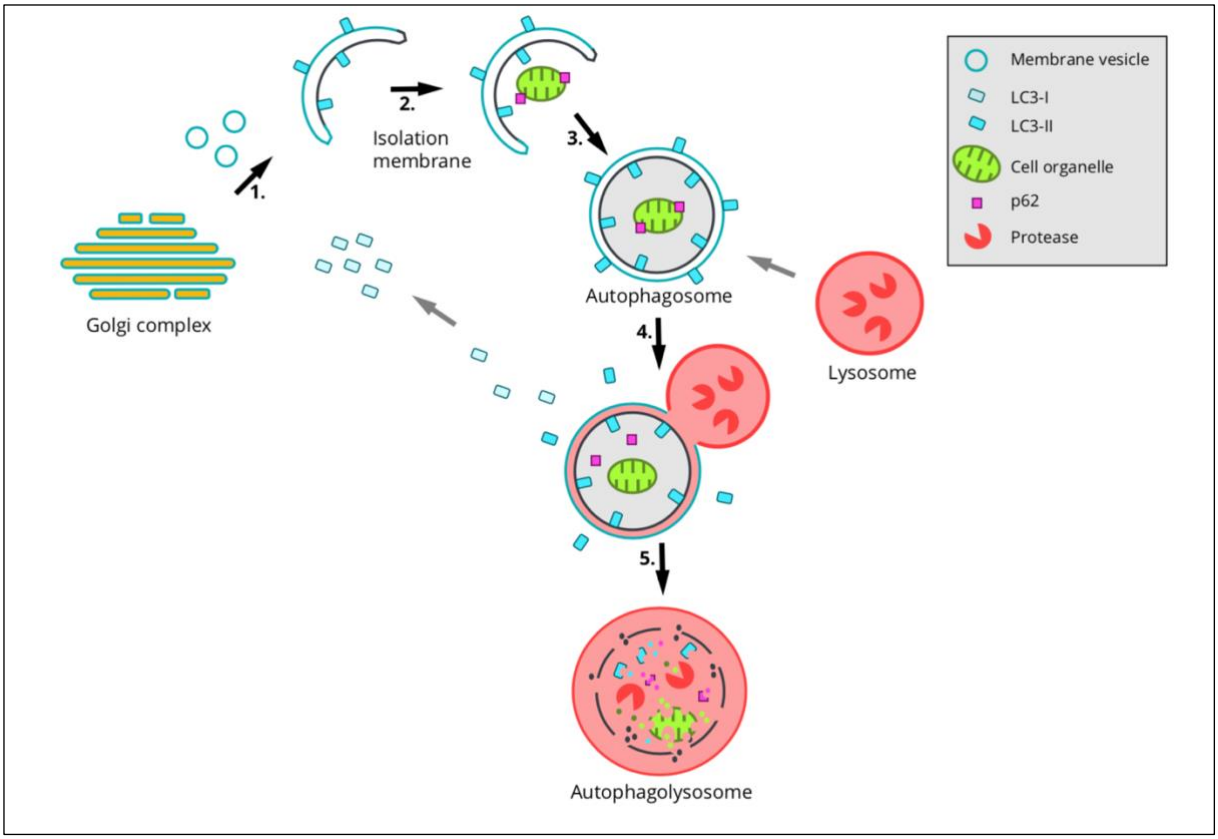

Figure 5 **The autophagy markers LC3 and p62**

LC3 plays a major role in autophagosome formation. LC3-I is the soluble cytosolic form, while LC3-II is bound to most autophagic membranes, especially the inner and outer membrane of the autophagosome. LC3-II on the outer membrane gets cleaved by ATG4 and converted back to LC3-I. The inner membrane fraction of LC3-II gets degraded during autophagy [64, 70, 71]. p62 is a direct substrate of autophagy, that can recruit cargo proteins to the autophagosome, and is degraded by the autophagic process [67, 69].

1.5. The C-type lectin domain family 16 member A - CLEC16A

Recent genome-wide association studies have identified *CLEC16A* as a new risk allele for T1D. *CLEC16A* (also *KIAA0350*) is a gene located within the chromosome 16p13 region and encodes for a C-type lectin domain family 16 member A protein. *CLEC16A* variation has been associated with a variety of autoimmune diseases. Two single nucleotide polymorphisms (SNPs) in particular, rs12708716 and rs2903692, are located on introns of *CLEC16A* and are most significantly linked with T1D [72, 73]. Furthermore, *CLEC16A* variants have been found to confer susceptibility for other autoimmune diseases such as MS, SLE, celiac disease, Crohn's disease, primary biliary cirrhosis, alopecia areata, juvenile idiopathic arthritis, rheumatoid arthritis and primary adrenal insufficiency [74-81]. Despite this clear link to autoimmunity the function of *CLEC16A* is still unknown.

1.5.1. Characteristics of *CLEC16A*

The full-length gene *CLEC16A* encodes a protein of 1053 amino acids (aa) and consists of 24 exons. There are thirteen transcript variants and at least three isoforms, two long and one short isoform [82, 83]. *CLEC16A* is markedly expressed in a variety of different immune cells, as well as other tissues such as brain, testes, thymus and intestine [84]. CLEC16A is part of the C-type lectin family. Proteins of this family typically express a C-type lectin-like domain (CTLD), which mediates Ca^{2+}-dependent carbohydrate binding and subsequently facilitates pathogen recognition processes within the immune system [85]. After binding a ligand, CTLDs induce signal pathways through an immunoreceptor tyrosine-base activation motif (ITAM). ITAMs are highly conserved and can be found in most leukocytes associating with most immunoreceptors such as the TCR [86]. Due to its short length (only 23 aa), the CTLD of *CLEC16A* is most likely not capable of folding into a fully functional carbohydrate recognition domain. CTLDs, however, have been shown to have evolved and also bind other ligands such as lipids and (glycol-)proteins. Today, it is unclear whether the CTLD of *CLEC16A* is capable of interaction with ligands. However, further studies have revealed a potential ITAM in *CLEC16A* (aa 483-499), implicating the gene in immunoregulation. Additionally, *CLEC16A* contains a highly conserved, uncharacterized domain called FPL (aa 51-199) and a potential transmembrane region (TM) at amino acids 308-330 [84].

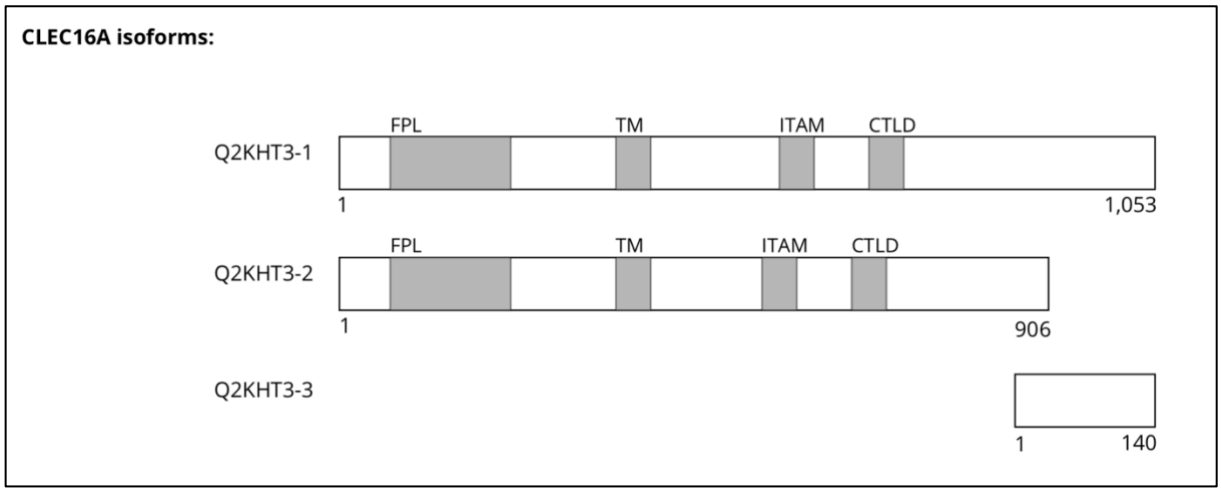

Figure 6 ***CLEC16A*** **isoforms, based on Berge et al. [82, 84]**

Schematic visualization of the three known isoforms of *CLEC16A* including their respective domains (FPL, TM, ITAM, CTLD): Q2KHT3-1 – 3.

1.5.2. The 16p13 gene locus

GWAS have found more than 40 new chromosomal regions that confer a low to moderate risk of T1D [87]. One of these regions is the chromosome 16p13.13 locus, which harbors *CLEC16A* and its neighboring genes *CIITA*, *SOCS1* and *DEXI* [72]. The MHC class II transactivator (CIITA) regulates gene expression of HLA class II molecules [88] and SOCS1 is a suppressor of cytokine signaling, which regulates immune cell homeostasis and inflammation [89]. Additionally, *DEXI* has been identified as a novelty immunoregulatory gene which is upregulated by stimulation with dexamethasone, an anti-inflammatory and immunosuppressive drug [90]. Despite the identification of the 16p13.13 locus as a chromosomal region linked to autoimmunity, the specific mechanisms of susceptibility remain unknown. Recently, chromosome confirmation capture could show physical proximity and interaction between intron 19 of *CLEC16A* (including SNPs associated with T1D) and the promoter region of *DEXI* [90]. Furthermore, it was reported that *DEXI* serves as an enhancer for *CIITA* expression [73]. Additionally, it was reported that there is significant correlation between the expression of *CLEC16A* and *SOCS1* and *DEXI* in the thymus [91]. As the causal variants are associated with *CLEC16A*, these findings suggest that genetic variation in *CLEC16A* could regulate expression of itself and its neighboring genes and modulate risk of T1D.

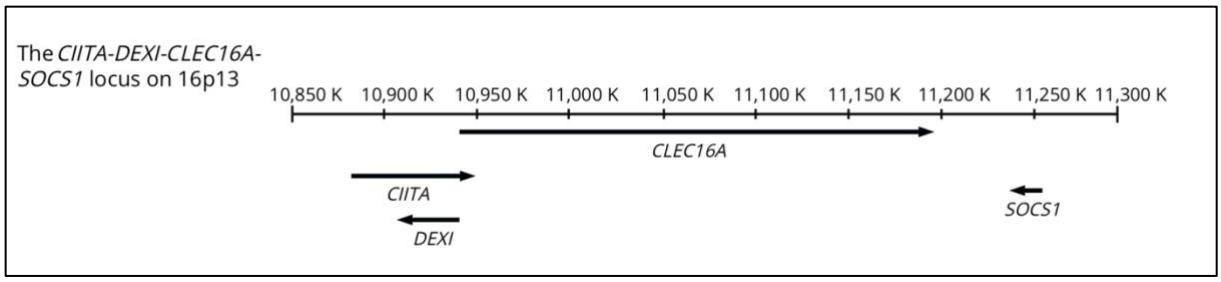

Figure 7 Neighboring genes on chromosome 16p13

Schematic visualization of the 16p13 genetic locus including *CLEC16A* and its neighboring genes *CIITA*, *DEXI* and *SOCS1*. Based on the Human Genome Resources database at NCBI [92].

1.5.3. *CLEC16A* in autophagy

CLEC16A is the human ortholog of the Drosophila gene *ema* (endosomal maturation defective). It has been reported that Ema is an endosomal membrane protein required for endosomal maturation [93]. In *ema* mutants, endosomal maturation fails to progress, and late endosomes and lysosomes are unable to fuse [93]. Moreover, *ema* was found to modulate size and function of autophagosomes in Drosophila fat cells [58]. Under starved conditions,

Ema localizes to the Golgi complex and is then recruited to the autophagosome, together with the Golgi protein Lva (lava lamp) [58]. Although fusion of autophagosomes with lysosomes was generally functional in *ema* mutants, there was a significant reduction in the size of autophagosomes [58]. Strikingly, the human ortholog *CLEC16A* could rescue autophagy in *ema* mutants, implicating the autoimmunity-associated gene *CLEC16A* in autophagy [58, 93].

1.6. Gene knockdown models

An increasing number of genes have been associated with autoimmune disease, yet very little is known about their function or specific effect on susceptibility. Studying the knockdown of these genes is a valuable tool to better understand the link between susceptibility genes and their individual contribution to disease pathogenesis.

RNA interference (RNAi) is a well conserved, sequence-specific and post-transcriptional gene silencing mechanism of cells used to defend against pathogenic nucleic acids. RNAi takes place when a small RNA strand pairs with a complementary messenger RNA (mRNA) strand. There are two kinds of RNA which can facilitate RNAi: microRNA (miRNA) and small interfering RNA (siRNA). miRNA derives from small RNA regions that fold upon themselves to form small hairpin RNA (shRNA). siRNA stems from longer double stranded RNA (dsRNA) regions. For RNAi, first, dsRNA/shRNA gets processed into siRNA/miRNA by RNase enzymes called Drosha and Dicer. Second, siRNA/miRNA gets loaded onto the RNA-induced silencing complex (RISC), which unwinds the duplex and facilitates hybridization of siRNA/miRNA with a complementary mRNA strand. As a result, the targeted mRNA is silenced through one of two ways: (1) cleavage and degradation by an RNase called Argonaute or (2) inhibition of translation [94-97].

RNAi can also be induced experimentally and used to create a gene knockdown. Compared to a complete knockout, a gene knockdown silences a specific gene and reduces its expression, similar to how genetic variations associated with autoimmune disease present a reduced effect on gene expression. A gene KO typically requires embryonic stem cells (ESCs). Considering the technical difficulty of retrieving and maintaining ESC lines, another option is to cross breed KO animals with animals of the standard strain. This, however, is a very lengthy process with the potential of introducing other confounding variants. Alternatively, KD by RNAi is a viable and widely used method for studying the phenotype of certain risk alleles.

Gene KD can be achieved by the introduction of dsRNA or constructs which express shRNA and works both *in vitro* as well as *in vivo*. RNAi gene silencing can be used in almost any mouse strain or disease model. It is highly inducible and reversible, and it allows specific targeting of a single splice variant or sequence of only moderate silencing effect. However, it can be difficult to select a proper target sequence. Additionally, RNAi only causes a gene KD, which can be problematic when a certain phenotype only manifests after complete loss of the gene. Lastly, RNAi can lead to off-targeting, which is an unintended KD at an undesired location that can also potentially cause a measurable phenotype. This can be controlled for by using two independent shRNA sequences [94, 98]. Overall, RNAi is a valuable and widely accepted tool for studying autoimmunity-associated gene variants.

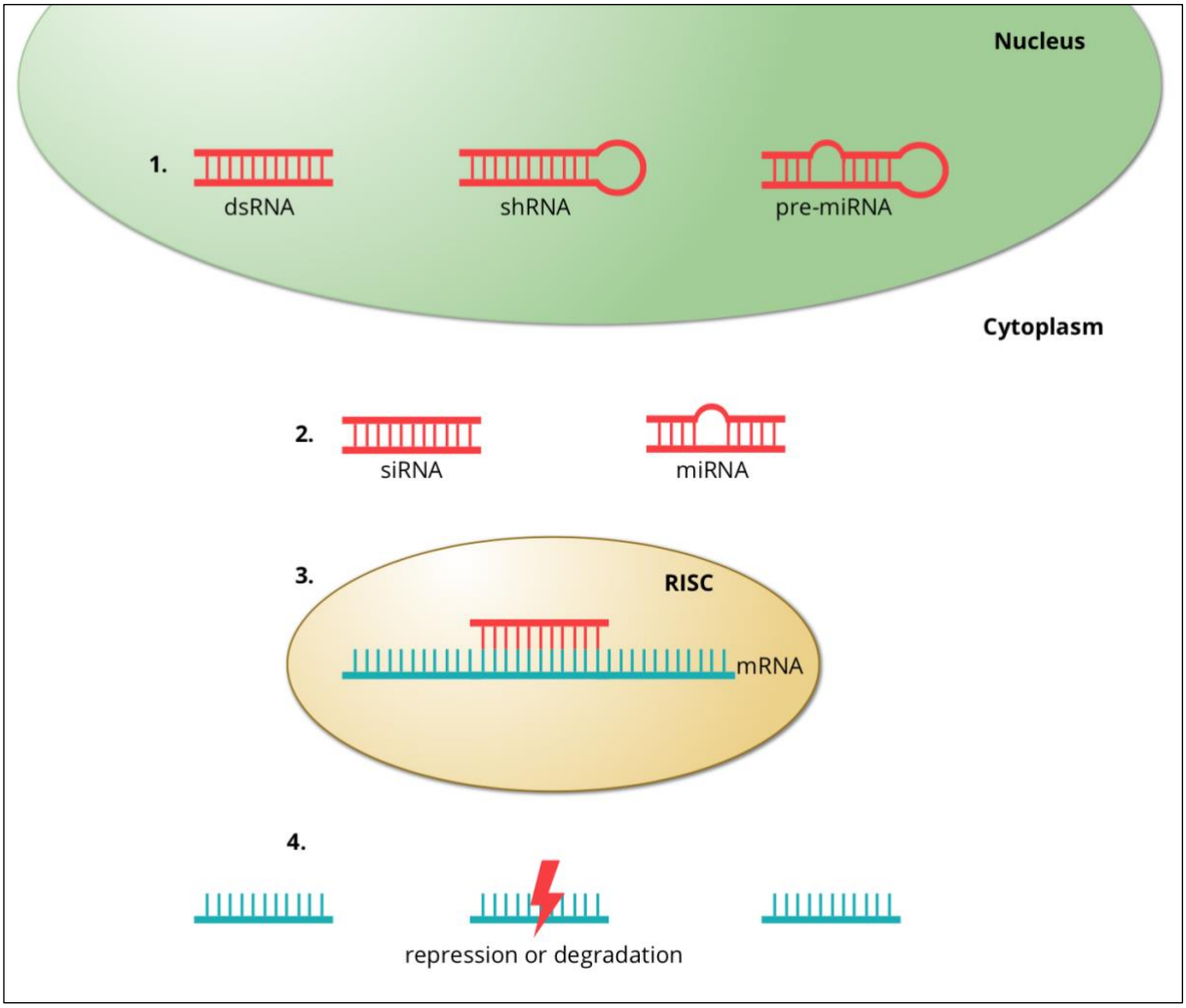

Figure 8 **Overview of the RNA interference pathway**

(1.) Double stranded RNA molecules such as shRNA and pre-miRNA are cleaved and transported to the cytoplasm as short doubled-stranded fragments. (2.) siRNA and miRNA are separated into single strands and loaded onto the RISC. (3.) Single-strand fragments bind mRNA and block protein translation by (4.) either cleavage of mRNA or inhibition of translation.

1.6.1. *In vitro* experiments with HeLa, HEK293T and MJC1 cells

In vitro experiments are the basis of modern-day research. *In vitro* studies are performed on components of an organism, which are taken out of their original complex environment, to simplify a biological system and allow for a more detailed investigation of individual processes. Naturally, results of these studies can be difficult to translate back into the context of a whole organism. This can become even more problematic when working with cancer cells, which, by nature, show some form of transformation and therefore a phenotype that is not identical to the original organism. An advantage of *in vitro* studies is that they are highly specific. Human cells, for instance, can be studied directly without the need to rely on other organisms such as animal models. Due to their simplicity and reproducibility, *in vitro* studies have been optimized very well, which in turn offers great practicability and a high turnout of information. Here, *in vitro* work was performed on HeLa, HEK293T and MJC1 cells (see Chapter 2.1).

1.6.2. *In vivo* studies with the NOD mouse

In vivo studies are the pinnacle of today's research as it allows for studies to be conducted within the living organism. Preferably, *in vivo* studies should be performed on humans as that is the relevant organism in clinical research. Most commonly, however, experimental animal models are used for *in vivo* research. Mouse models are the leading animal model for studying human disease. Mice are genetically and physiologically very similar to humans. Additionally, they are small and economically advantageous. Furthermore, mice can be genetically modified and inbred to create identical strains. Nevertheless, mouse models are less reliable to study human disease, than the human system itself. Naturally, animal studies are frequently discussed and questioned as their results have to be taken with caution. Regardless, the mouse model is an invaluable tool to further understand evolutionarily conserved mechanisms [99, 100]. For this project, the non-obese diabetic (NOD) mouse was used as the experimental model for *in vivo* studies.

2. Methods and Material

2.1. HEK293T, HeLa and MJC1 cells

Human Embryonic Kidney cells (HEK293) are derived from human kidney cells. They were initially transformed with adenovirus 5 and held in culture. Today, HEK293 are commonly used in research due to their reliable growth and aptitude for transfection. For this work, a highly transfectable cell line called HEK293T was used. These cells contain a mutant variant of the oncoprotein SV40 large T-antigen (TAg). Thus, DNA plasmids carrying the SV40 promoter get replicated in high numbers, which ensures a high turnout of viral protein [101].

HeLa are the most commonly used human cells in biomedical research. These cells were originally cervical cancer cells taken from a patient called Henrietta Lacks in 1951. They were the first cells to be "immortal", meaning cells would not die after multiple divisions, and the first cells to be successfully cloned. To this day, HeLa can be used for a plethora of experiments with the boon of being a human cell line [102]. For this work, HeLa cells were transduced with lentivirus previously produced by HEK293T to create a gene KD through RNAi. The lentivirus carried plasmids encoding for shRNA that would be able to interfere with *CLEC16A* or *ATG5* sequences, respectively.

MJC1 cells resemble cortical thymic epithelial cells. For the generation of MJC1, cells were retrieved from thymi of newborn mice and digested. Second, $EpCAM^{+}CD45^{-}$ cells were sorted. Third, $Ly\text{-}51^{+}UEA1^{-}$ cells were sorted and isolated as cTECs. MJC1 cells were used in this work to study the effect of impaired autophagy on TECs. These cells had kindly been generated by Dr. Mi-Jeong Kim and were provided by the Serwold Lab.

All cells were grown in cell culture and sub-cultured for their respective experiments. Cells were microscopically checked regularly to ensure healthy growth and discarded at any sign of unnatural development. HEK293T cells were primarily used to produce shRNA lentivirus. HeLa and MJC1 cells were infected with lentivirus encoding neomycin resistance and shRNA targeting *CLEC16A* and *ATG5* sequences (for HeLa), or puromycin resistance and shRNA targeting *Clec16a* and *Atg5* sequences (for MJC1), respectively. The latter was performed by the Kissler Lab prior to this work. ATG5 plays an important role in the formation of autophagosomes [103] and therefore served as a positive control for impaired autophagy.

2.1.1. Cell culture

Cell cultures were kept and treated in aseptic environments. All cell lines were cultured in serum-positive media (500 ml DMEM with 10 % fetal bovine serum, 100 µg/ml penicillin/streptomycin, 2 mmol/l glutamine) and grown in 10 cm petri dishes at 37 °C and 5 % CO_2. Cells were split every one to three days at a confluency of 70-80 %. After discarding old media, the plate was washed with 10 ml DPBS. Cells were then lysed for 2-10 min using 2 ml 0.05 % Trypsin-EDTA at 37 °C. To stop lysis and create a cell suspension, previously warmed 8 ml serum-positive DMEM media were added. The cell suspension was then transferred to a 10 ml tube and centrifuged at 1400 rpm for 4 min at 4 °C. After discarding the supernatant, the cell pellet was dissolved in 10 ml serum-positive DMEM. Depending on the desired dilution, 0.5 – 2 ml of the cell suspension was then transferred back onto a 10 cm petri dish and filled up to 10 ml with serum-positive DMEM.

2.1.2. Cell count

Experiments were generally carried out with cells at a confluency of 70-80 % and a target count of approximately $2x10^6$ (10 cm dish) cells or $0.3x10^6$ (6-well plate) cells, respectively. Cells were washed, trypsinized and filled up to 10 ml with serum-positive DMEM (see 2.1.1). To count cells, 90 µl Trypan Blue were added to 10 µl of the cell suspension. 10 µl were taken from the mixture and then transferred to the counting chamber. Using a hand tally counter, living cells were counted in each of the 16 squares. To calculate the number of cells/ml, the average cell count (per square) was multiplied by 10^4 and then multiplied by 10 to correct for the 1:10 dilution. The targeted cell count in its respective volume was then transferred to 10 cm petri dishes or 6-well plates and filled up with serum-positive DMEM.

Table 1 Material for HEK293, HeLa, MJC1

HEK293T Cells	**Joslin Diabetes Center**
HeLa Cells	**Joslin Diabetes Center**
MJC1 Cells	**Joslin Diabetes Center**
0,05 % Trypsin	**Gibco**
DMEM	**Gibco**
DPBS	**HyClone**

Penicillin/Streptomycin	**Gibco**
Glutamine	**Gibco**
Fetal Bovine Serum	**Gibco**
Trypan Blue Solution	**Corning**
Counting Chamber	**Hausser Scientific**
Tissue Culture Dish	**Fisher Scientific**

2.1.3. Gene knockdown in HeLa

2.1.3.1. Transformation of bacteria with *CLEC16A* and *ATG5.7* DNA

Transformation of bacteria is a process used to replicate plasmids by introducing DNA into a cell. The *CLEC16A* and *ATG5.7* plasmids also encoded for antibiotic resistance and were provided by the Kissler Lab. 25 µl NovaBlue Singles competent E. coli bacteria were thawed and mixed with approximately 1 µl plasmid (approximately 1 ng DNA) from the stock, which had previously been diluted with dH_2O at a ratio 1:250. After 10 minutes of incubation on ice, the cell/DNA mixture was heat-shocked at 42°C for 30 seconds and then put back on ice for an additional 2 minutes. 30 µl of SOC medium were added to the tubes in order to obtain maximal transformation efficiency. The transformation was then spread on LB-Ampicillin agar plates and incubated overnight at 37 °C. Only bacteria successfully transformed were able to survive due to their inherent resistance to antibiotics. The next day, a single surviving colony was picked using a pipette tip and incubated in 5 ml LB-Ampicillin media shaking at 220 rpm for roughly 8 h at 37 °C.

2.1.3.2. Plasmid preparation

Bacteria were harvested the next day and centrifuged at 5000 rpm for 10 min at 4 °C. To extract DNA a Maxiprep Kit was used following the manual. Afterwards, DNA concentration was measured, which equaled 1.00 µg/µl for *CLEC16A* and 0.95 µg/µl for *ATG5.7*.

2.1.3.3. shRNA lentivirus production for HeLa cells

HEK293T cells were used as packaging cells to produce lentivirus encoding antibiotics resistance and shRNA. Depending on the plasmid, shRNA targeted *CLEC16A*, *ATG5.7* or a luciferase gene which was not present in either human or mouse cells and served as a control. For lentivirus production, 10 µg DNA were added to an envelope mixture containing 1.75 µg

pCMV-VSV-G, 2.33 µg pMDLg/pRRE, 1.75 µg pRSV-Rev and 2.9 µg pAdv/TERT plasmids. 35 µl FuGENE and 600 µl serum-free DMEM were added per Eppendorf tube to transfect plasmid into the cells. The mixture was incubated for 30 min at room temperature (RT) and then added to HEK293T cells, which had been split 1:2 the day before.

2.1.3.4. Transduction of HeLa cells with lentivirus

Peak virus production is usually achieved 24 - 48 h post transfection. After 48 h at 37 °C and 5% CO_2, supernatant from the cells was centrifuged at 4000 rpm for 4 min at 4 °C to get rid of cell debris. Then, the supernatant was filtered using a 0.45 µm low protein-binding filters. At this point, the supernatant containing lentivirus could be used to transduce target cells and was mixed with media at a 1:1 ratio. HeLa cells on a 6-well plate were immediately transduced with 2 ml lentivirus mixture encoding antibiotics resistance and shRNA. The target sequence for *CLEC16A* in HeLa cells was *GACTGATGATGTCCTGGATCTG*. In MJC1 cells, two *Clec16a* KD lines were created with the target sequences *CACCTTGTACGTCATTTCTATA* (K3 line) or *GAGTGTCCACCTTGTACGTCAT* (K5 line). As the positive control, *ATG5/Atg5.7* KD, the target sequence was *GCAGAACCATACTATTTGCT*. As the negative control, cells (HeLa and MJC1) were infected with lentivirus encoding for a puromycin resistance and shRNA of a luciferase not present in human or murine cells.

2.1.3.5. Selection of successfully transfected HeLa cells

The transfected DNA plasmid also contained a *neo(R)* gene. *Neo(R)* is a commonly used gene that encodes antibiotics resistance for neomycin and G418 (Geneticin) and serves as a selectable marker in cell biology. Only cells that were successfully transfected carried the vector including the *neo(R)* gene. After treatment with G418, vector(+) cells survived due to their antibiotics resistance, while vector(-) cells died in culture. The effective concentration of G418 varies greatly with different cell types. Therefore, the optimal concentration of G418 for selection was determined by titrating and treating HeLa cells with different concentrations of G418 ranging from 400 µg/ml to 1500 µg/ml. Cell survival was monitored microscopically over a 4-day period. At a concentration of 1500 µg/ml all non-transfected HeLa cells died, while lower concentrations did not sufficiently kill HeLa cells. Hence, 1500 µg/ml G418 were used for the selection of transfected HeLa-neo cells. After treatment with G418 over 9 days, the

remaining HeLa cells were considered to be vector(+) HeLa-neo cells. Over the course of these studies HeLa-neo cells were regularly (re-)treated with G418 to ensure purity.

2.1.3.6. Validating knockdown efficiency by quantitative PCR

Gene knockdown verification can be tested in multiple ways, for instance on the mRNA level via real-time PCR or the protein level via Western Blot. Methods such as real-time quantitative PCR (qPCR) have been shown to be efficient tools for verification of gene knockdown after siRNA gene silencing [104]. PCR is a commonly used technique based on thermal cycling and enzymatic replication of a specific DNA sequence. As a result, the template DNA is amplified exponentially and can be used for DNA quantification. With qPCR, amplification and detection of DNA are combined into one step and it is possible to quantify the target sequence in real time based on fluorescent dye staining. In this study, qPCR was used to detect knockdown in HeLa cells.

As starting material, RNA was isolated from *CLEC16A* KD, *ATG5.7* KD and control HeLa-neo cells using the High Pure RNA Isolation Kit following the manual. RNA was eluted with 30 µl RNase-free water. 0.88 µg RNA was then used to create cDNA with the SuperScript First-Strand Synthesis System following its manual step-by-step. cDNA was either stored at -20 °C or used for PCR immediately.

This experiment aimed to measure mRNA expression levels of *CLEC16A* and *ATG5.7* in HeLa cells. While RNA expression variation may be of biological cause, there is also a possibility of technical variance. To minimize technical variance and to normalize qPCR data, the ubiquitously expressed *GAPDH* gene was used as a reference gene, and standard operating techniques were used in all qPCR experiments. For qPCR, previously produced cDNA was diluted with dH2O at a ratio 1:20. For each sample, a master mix specific to the target sequence was created consisting of 1 µl forward primer, 1 µl reverse primer and 10 µl SYBR green. 8 µl of diluted cDNA were then plated on a 96-well plate before 12 µl master mix were added to a well. Wells purely filled with dH2O served as control. The plate was sealed, put on a vortex and centrifuged quickly before running the qPCR program. All data were analyzed using the software Graphpad Prism.

2.1.4. The OVA-LCR3 construct

2.1.4.1. Transduction of MJC1 cells with dsRed-LC3 constructs

To investigate the effect of impaired autophagy in TEC on the stimulation of OT-II thymocytes, the Kissler Lab had cloned a dsRed-LC3 fragment of a previously published dsRed-LC3-GFP construct [105]. The Kissler Lab had amplified it and incorporated a sequence for the $OVA_{323-339}$ peptide and reverse primers that would either leave LC3 intact or introduce a point mutation at position 120 that would switch in alanine for glycine. These fragments were then used to produce vectors encoding either dsRed-LC3 (control), dsRed-OVA-LC3 or dsRed-OVA-$LC3_{G120A}$ (mutated) [106].

For this thesis, lentiviral particles were produced for each plasmid combining 20 µg vector DNA, 3 µg pCMV-VSV-G, 4 µg pMDLg/pRRE, 3 µg pRSV-Rev and 5 µg pAdv/TERT. 70 µl FuGENE and 1200 µl serum-free DMEM were added to each Eppendorf tube. The mixture was incubated for 30 min at RT and then added to HEK293T cells, which had been split 1:3.5 the day before. After 48 h, the supernatant was retrieved, and the plates were checked for immunofluorescence to validate successful transfection. The supernatant was then centrifuged and filtered as mentioned in 2.1.3.4 before ultra-centrifuging at 25000 rpm for 90 min at 4 °C. All supernatant was discarded and 100 µl PBS were added. The tube was stored at 4 °C overnight. The next day, the lentivirus was re-suspended in 100 µl PBS and added to 4 ml serum-positive DMEM. Finally, 1 ml virus/DMEM mixture was added to MJC1 cells to create the desired cell lines.

2.1.4.2. Sorting transduced MJC1 cells with flow cytometry

Flow cytometry is a widely used technique to characterize and analyze cell subpopulations within a heterogeneous cell group. Cells can be analyzed by cell size and granularity or by the expression of cell surface proteins through fluorochrome staining. Three days after transfection, the MJC1 cells were sorted using a MACSQuant Analyzer depending on whether or not they were expressing dsRed. All data were analyzed with the software FlowJo. Approximately 200.000 cells of each cell line were retrieved as dsRed-positive cells and plated onto 24-well plates.

Table 2 Material for transformation and transfection

NovaBlue Competent Cells	**Novagen**
CLEC16A, *ATG5.7*, *CTRL* plasmid	**Kissler Lab**
dH2O	**Gibco**
SOC Medium	**Invitrogen**
Eppendorf Safe-Lock Tubes	**Eppendorf**
Agar plates	**Kissler Lab**
LB-Ampicillin	**Kissler Lab**
New Brunswich Classic C24 Incubator	**New Brunswick Scientific**
NucleoBond Xtra Maxi Kit	**Macherey-Nagel**
NanoDrop ND-1000 Spectrophotometer	**NanoDrop Technologies**
pCMV-VSV-G	**Addgene**
pMDLg/pRRE	**Addgene**
pRSV-Rev	**Addgene**
pAdv/TERT	**Addgene**
FuGENE	**Promega**
Millex-HV Syringe Filter Unit, 0.45 µg, PVDF, 33 mm, gamma sterilized	**Millipore-Sigma**
G418	**ThermoFisher Scientific**
High Pure RNA Isolation Kit	**Roche**
RNase free water	**Qiagen**
SuperScript First-Strand Synthesis Kit	**Invitrogen**
fwPrimer_*CLEC16A*	**5'-CCTGATTTGGGGCGATCAAAA-3'**
rvPrimer_*CLEC16A*	**5'-CATAACGGCCTGATTTCTGCC-3'**
fwPrimer_*ATG5.7*	**5'-CACCCCTGAAATGGCATTATCC-3'**
rvPrimer_*ATG5.7*	**5'-TGGACAGTGTAGAAGGTCCTTT-3'**
fwPrimer_*Actin Beta 1*	**5'-GGCTGTATTCCCCTCCATCG-3'**
rvPrimer_*Actin Beta 1*	**5'-CCAGTTGGTAACAATGCCATGT-3'**
fwPrimer_*GAPDH*	**5'-AGCTTGTCATCAACGGGAAG-3'**
rvPrimer_*GAPDH*	**5'-TTTGATGTTAGTGGGGTCTCG-3'**
Power SYBR Green	**ThermoFisher Scientific**
Prism software	**Graphpad**

ABI 7900	**Applied Biosystems**
dsRed-LC3, dsRed-OVA-LC3, dsRed-OVA-LC3$_{G120A}$	**Kissler Lab**
MACSQuant Analyzer	**Miltenyi Biotec**
FlowJo	**Tree Star Inc.**

2.2. Detection of autophagy

2.2.1. Initiation and inhibition of autophagy in HeLa

Mammalian autophagy is a highly complex bulk degradation process that can be interfered with at a variety of steps. The most commonly studied trigger of autophagy is nutrient starvation. Additionally, autophagy can be induced with Rapamycin [107]. In contrast, protease inhibitors such as Pepstatin A, E64d, Bafilomycin A1 and 3-Methyladenine (3MA) can be used to inhibit autophagy [107]. For this project, autophagy was induced by starvation. HeLa cells were washed with PBS and then incubated with 10 ml EBSS at 37 °C for different time spans ranging from 4 - 48 h. Controls were incubated with 10 ml serum-positive DMEM. Depending on the experiments, further chemical inhibitors or inducers were added, as mentioned above. In these cases, HeLa cells were treated with either a single drug or a combination of the following: E64d (10µg/ml), Pepstatin A (10 µg/ml), Bafilomycin A1 (50-100 nM), 3MA (200 µM) or Rapamycin in different concentrations [108, 109].

Table 3 Material for initiation and inhibition of autophagy in HeLa

EBSS	**Gibco**
E64d	**Sigma**
Pepstatin A	**Sigma**
Bafilomycin A1	**Sigma**
Rapamycin	**Invitrogen**
3-Methyladenine	**Sigma**

2.2.2. Immunoblot

The immunoblot is a fast and highly sensitive assay for detection, quantification and characterization of proteins. Once extracted from tissue or cells, protein samples of equal amounts are loaded onto a gel and separated by electrophoresis depending on their

respective molecular size. Separated proteins are then transferred onto a nitrocellulose membrane. Here, the target protein is bound by a primary antibody, which in turn is bound by a secondary antibody linked to a reporter enzyme. The enzyme then reacts with a matching luminescent substrate. Light is emitted and captured on an autoradiography film. When detected, the target protein can be seen as a stained band.

2.2.2.1. Preparing the lysates

HeLa cells were centrifuged at 1400 rpm for 4 min at 4 °C and mixed with RIPA lysis buffer to lyse cells and extract proteins. Cells were put on ice for 15 min and then centrifuged at 16000 g for 10 min at 4 °C to get rid of cell debris. 5 µl supernatant and 5 µl lysis buffer were mixed with 150 µl Pierce 660 nm Protein Assay Reagent and incubated for 5 min at RT. The absorbance of all samples was measured at 660 nm with the Synergy Mx Microplate Reader. As controls, 10 µl lysis buffer were mixed with 150 µl Pierce 660 nm Protein Assays Reagent. The average absorbance of the controls was subtracted from the individual absorbance of each sample. Protein concentration was calculated using the Bovine Serum Albumin (BSA) standard curve. All samples were diluted with 4x Laemmli buffer at a ratio 3:1 and cooked for 3 min at 95 °C. Samples were then either stored at -20 °C or used immediately.

2.2.2.2. SDS-PAGE

Sodium dodecyl sulfate (SDS) binds entire peptide backbones with its negative charges and negates the protein's intrinsic charge, conferring equal charge for every protein. Based on this, proteins can simply be separated by mass after application of an electric field in SDS-PAGE. The SDS-PAGE gel is divided into a separating gel and a stacking gel. The percentage of acrylamide depends on the molecular weight of the target protein. Given the molecular weight of LC3 (15 kD), p62 (47 kd) and actin (42 kD) a 12 % acrylamide gel was generally used for the experiments. The separating gel was produced by mixing 3.2 ml dH2O with 4.0 ml 30 % acrylamide, 2.6 ml 1.5 M Tris-HCl (pH 8.8) and 100 µl 10 % SDS in a small beaker. Immediately before pouring the gel, 10 µl TEMED and freshly made 100 µl 10 % APS were added to the mixture. The thoroughly mixed solution was then pipetted between two 1.0 mm spacer plates held by the casting frame. H_2O was added to make the top of the gel horizontal. The separating gel solidified within 20 - 30 min. After discarding the H_2O, the stacking gel was pipetted onto the separating gel and a 12-well or 15-well comb was inserted. The 4 % stacking

gel was made by mixing 2.975 ml H_2O with 670 µl 30 % acrylamide, 1.25 ml 0.5 M Tris-HCl (pH 6.8) and 50 µl 10 % SDS. Before pouring the gel, 5 µl TEMED and freshly made 50 µl 10 % APS were added to the mixture. The stacking gel solidified within 20 - 30 min. Gels were either used immediately or stored at 4 °C wrapped in wet paper towels and sealed for no longer than one week. For electrophoresis, gels were loaded with equal amounts of protein ranging from 10 – 30 µg consistent within each respective experiment. Samples were cooked at 95 °C for 5 - 10 min before electrophoresis. Additionally, 8 µl protein marker were loaded onto the first lane. Proteins were then separated using a buffer-filled mini-PROTEAN Tetra Cell system running at 80 - 120 V until the migration front reached the bottom of the gel.

2.2.2.3. Western Blot

After separation by SDS-PAGE, proteins were transferred from the gel to a nitrocellulose membrane using a Mini Trans-Blot Electrophoretic Transfer Cell. For transfer, gel and membrane were sandwiched (from cathode to anode: foam pad, filter paper, gel, membrane, filter paper, foam pad) in 4 °C transfer buffer, ensuring no bubbles had formed between gel and membrane. The gel-membrane sandwich was then placed within the Transfer Cell and submerged in 4 °C transfer buffer. To create an electrical field, 75 V were applied for 60 min at 4 °C. Within this field, all negatively charged proteins moved towards the anode and were bound by the membrane. Experiments were continued only if successful transfer was visually confirmed.

2.2.2.4. Immunodetection

To prevent unspecific binding of the primary or secondary antibody to the membrane, TBS/T 5 % Milk (1 % Tween, 5 % milk powder) was used to block the membrane. For this, the membrane was placed on a shaker for 30 min at 40 Hz and RT. While washing the membrane with TBS/T for 5 min, the primary antibody was prepared. The primary antibody was diluted in TBS/T at a 1:500 ratio (LC3, p62, ACTIN) or 1:250 (CLEC16A, DEXI), respectively. Membranes were cut and placed in sealed plastic for individual incubation, before adding the primary antibody. At 4 °C, the primary antibody was constantly agitated and incubated overnight. The next day, all membranes were washed several times in TBS/T for 5 min per wash to remove residual primary antibody. After washing, secondary antibodies were diluted at 1:5000 (anti-mouse for ACTIN, anti-rabbit for LC3, P62 and CLEC16A), added to the membranes and

incubated for 1 h rocking at 40 Hz and RT. After incubation, the membranes were washed in TBS/T three times for at least 5 min per wash. All secondary antibodies were conjugated with horseradish peroxidase as a reporter enzyme, which would react with 1 ml 1:1 chemilumiscent stubstrate that was added to each membrane. The membranes were placed into an autoradiography cassette. In the dark room, an autoradiography film was placed inside the cassette and exposed, ranging from 10 s to 15 min, before being developed.

2.2.2.5. Data analysis

To quantify the amount of expressed protein, autoradiography films were scanned in 16-bit grayscale and 600 dpi. Pixel intensity was then analyzed in ImageJ64 and data was presented with Graphpad Prism.

Table 4 Material for immunoblotting

RIPA lysis and extraction buffer	**Thermo Scientific**
Pierce 660 nm Protein Assay Reagent	**Thermo Scientific**
Synergy Mx Microplate Reader	**Biotek**
4x Laemmli Buffer	**Bio-Rad**
30 % Acrylamide	**Bio-Rad**
1.5 M Tris-HCl, pH 8.8	**Bio-Rad**
0.5 M Tris-HCl, pH 6.8	**Bio-Rad**
10 % SDS	**Bio-Rad**
TEMED	**Bio-Rad**
APS	**Bio-Rad**
1 mm / 1.5 mm spacer plates	**Bio-Rad**
12-well / 15-well comb	**Bio-Rad**
mini-PROTEAN Tetra Cell System	**Bio-Rad**
PowerPac Basic Power Supply	**Bio-Rad**
Precision Plus Protein Standard	**Bio-Rad**
Running Buffer	**Kissler Lab**
mini Trans-Blot Cell	**Bio-Rad**
Foam Pads	**Bio-Rad**
Blot Absorbent Filter Paper	**Bio-Rad**

Nitrocellulose membrane	**Bio-Rad**
Transfer Buffer	**Kissler Lab**
Milk Powder	**Fisher Scientific**
Tween	**Fisher Scientific**
TBS	**Kissler Lab**
Mini Rocker	**Bio-Rad**
β-ACTIN Antibody	**Santa Cruz**
LC3B Antibody	**Santa Cruz**
P62 Antibody	**GeneTex**
CLEC16A Antibody	**Novus Biologicals**
DEXI Antibody	**Novus Biologicals**
Anti-Rabbit IgG HRP-linked	**GE Healthcare UK**
Anti-Mouse IgG HRP-linked	**GE Heathcare UK**
Chemiluminescent Substrate	**Fisher Scientific**
Autoradiography Cassette	**Fisher Scientific**
Autoradiography Film	**Fisher Scientific**
X-Ray Machine	**Konica Minolta**
Scanner	**HP**
ImageJ64	**NIH**

2.3. The NOD *Clec16a* KD Mouse

The most prominent experimental animal model for studying T1D is the non-obese diabetic (NOD) mouse model. The NOD strain was created almost 40 years ago as a descendant of a cataract-prone strain [110]. Since then, the NOD mouse has been established as an excellent model for human autoimmune diabetes (T1D) as well as other autoimmune diseases. The power of the NOD strain is that it develops spontaneous autoimmune diabetes very similar to the human T1D, with autoreactive $CD4^+$ and $CD8^+$ cells and autoantibodies [111]. Antigens recognized by autoreactive T cells in human and NOD mice include insulin, GAD, IA-2 and the heat shock protein 60 (Hsp60) [112]. Similar to T1D in human, diabetes in NOD mice is a polygenetic disorder, as there are multiple gene loci linked to susceptibility. One major contributor to genetic susceptibility in this strain is the MHC haplotype called $H\text{-}2^{g7}$ [113], which affects T cell selection directly. There are other contributors, too, such as a defective

system of macrophages and natural killer cells. Furthermore, autoantibodies against antigens such as insulin and GAD can be found in NOD animals [114]. Nonetheless, autoimmune diabetes in the NOD strain is mostly dependent on autoreactive $CD4^+$ and $CD8^+$ cells. Evidently, disease can be induced by transfer of purified $CD4^+$ and $CD8^+$ cells and inhibited by alteration of T cells, whereas transfer of autoantibodies does not seem to induce autoimmune diabetes [111].

Generally, onset of spontaneous autoimmune diabetes in the NOD mouse occurs at 12 – 14 weeks of age [111]. Female NOD mice show a higher incidence rate of approximately 80% compared to males with an incidence rate of 20 – 30% [115, 116]. At 3 – 7 months of age, 80% of female NOD animals and 50% of male NOD animals demonstrate insulin dependency [113]. Histologically, as early as 3 – 4 weeks of age, NOD mice show lymphocytic infiltrates surrounding pancreatic islets (peri-insulitis). Later, at approximately 10 weeks of age, these infiltrates afflict the pancreatic islets and cause severe insulitis, similar to T1D in humans [111, 117].

Prior to this work, *Clec16a* KD NOD mice had been generated by the Kissler Lab [106]. In summary, *Clec16a* KD was generated by the Kissler Lab via lentiviral transgenesis. For this, lentivirus encoding for shRNA and a GFP reporter was injected into NOD zygotes. For the K3 KD line, the pLBM vector [118] was used with its target sequence CACCTTGTACGTCATTTCTATA. K5 KD mice were generated with a pUGM vector and GAGTGTCCACCTTGTACGTCAT as the target sequence. Successful KD was checked by GFP expression levels. All KD animals were kept as homozygous, GFP positive animals. As a control group, WT NOD mice were used. OT-II TCRα-/- mice were provided by the Serwold Lab [106]. Mice were held in the animal facility of the Joslin Diabetes Center and treated appropriately under Animal Welfare Rules and Regulations. Experimental procedures on animals were approved by the Institutional Animal Care and Use Committee.

2.3.1. Levels of gene expression in tissue

To study the expression and co-expression of *Clec16a* and its neighboring genes located on the 16p13.3 locus, different murine tissues were collected and used for qPCR.

2.3.1.1. Collecting and preparing organs

For each experiment, three mice (n=3) were used of each genotype (K3, K5 and WT), consistent within all experiments. Mice were euthanized, using CO_2 to provide a painless, rapid and stress-free death. Then, the animals were pinned down and dissected using micro-dissection scissors and tweezers. To reach the cranial, thoracic and abdominal cavity, fur and skin were dissected and rib cage and skull were opened carefully. The desired organs were cautiously prepared without damaging tissue or vessels. Tissue samples were collected from thymus, heart, inguinal lymph nodes, spleen, pancreas, liver, kidney and brain. After collection, organs were homogenized in TRIzol and stored at -80 °C for further use.

2.3.1.2. RNA extraction from organ tissue

After thawing the organ samples, 200 µl Chloroform and 1 ml TRIzol were added. The tubes were shaken vigorously, incubated for 2 min at RT and centrifuged at 12000 g for 15 min at 4 °C. The upper aqueous supernatant was collected and transferred to a new tube. 500 µl isopropanol and 1 ml Trizol were added, before shaking again for 15 sec, incubating for 10 min at RT and centrifuging at 12000 g for 10 min at 4 °C. The supernatant was retrieved and washed with 1 ml 75 % ethanol. The sample was spun at 7500 g for 5 min at 4 °C and air-dried for 5 min. Pellets were re-suspended in dH_2O and placed on a shaker for 15 min at 37 °C. RNA concentrations were then measured using the NanoDrop machine.

2.3.1.3. Islets isolation

Murine pancreatic islets were isolated according to a slightly modified protocol [119]. After sacrificing the animals, a V-incision was made to open the abdominal cavity. Bowel and liver were moved to the side cautiously to expose the pancreas and the common bile duct (CBD). Bulldog Clamps were placed on both sides of the duodenum. The gall bladder was punctured with a 1 ml syringe and collagenase solution (HBSS, 10 % FCS, 0.5 mg/ml collagenase) was applied to the CBD in order to distend the duct. The CBD was then catheterized with a 10 ml syringe and 3 ml collagenase solution were injected into the pancreas. When done correctly, the pancreas would assume more than three times its original size. The pancreas was removed and placed in a pre-cooled falcon tube containing 1 ml collagenase solution. After organ harvest, the falcon tubes were incubated at 37 °C for 17 min and shaken to dissolve the pancreas. 12 ml washing solution (HBSS + 10 % FCS) were added and the mix was flushed

through the cell strainer. All samples were centrifuged at 4 °C until the centrifuge reached 1500 rpm, then the supernatant was carefully discarded. After repeating this step twice, the pellet was re-suspended with 5 ml Histopaque-1077. 10 ml washing solution were carefully added without disturbing the gradient. All samples were centrifuged at 2400 rpm for 10 min with the break turned off. At this point, pancreatic islets could be identified as the layer floating between the Histopaque-1077 and the washing solution. All islets were carefully aspirated and transferred into a new falcon tube. Again, samples were centrifuged at 4 °C until the centrifuge reached 1500 rpm and the supernatant was carefully discarded. The pellet was re-suspended in 200 µl PBS and 400 µl Lysis/Binding Buffer and the samples were stored at -80 °C. For RNA extraction, the High Pure RNA Isolation Kit was used according to the manual as previously described in chapter 2.1.3.6.

2.3.1.4. Measuring gene expressing with qPCR

RNA was isolated from murine pancreatic islets and other murine tissue. 1.00 µg RNA was used to create cDNA and qPCR was performed as previously described (chapter 2.1.3.6.), with *β-Actin* as the reference gene, to measure mRNA expression levels of *Clec16a* and its neighboring genes *Dexi*, *Socs1* and *CIIta*.

Table 5 Material for measuring gene expression in organ tissue

NOD mouse	**Joslin Diabetes Center**
CO_2	**Joslin Diabetes Center**
Ethanol	**Fisher Scientific**
Micro-Dissection Scissors	**Biomedical Research Instruments**
Tweezers	**Biomedical Research Instruments**
TRIzol Reagent	**Fisher Scientific**
TissueLyser II	**Qiagen**
Chloroform	**Fisher Scientific**
Isopropanol	**Sigma-Aldrich**
Bulldog Clamp	**Biomedical Research Instruments**
Syringe 1 ml, 10 ml	**Sigma-Aldrich**
HBSS, 10 % FCS	**Gibco**
Collagenase	**Fisher Scientific**

Histopaque-1077	**Sigma-Aldrich**
Lysis/Binding Buffer	**Fisher Scientific**

2.3.2. Intraperitoneal glucose tolerance test

The intraperitoneal glucose tolerance test is used to study metabolic function by measuring glucose clearance after intraperitoneal injection of glucose. For this experiment, six animals of each genotype (K3, K5 and WT) were matched by sex, weight and age. Mice were fasted for 16 h overnight with no access to food, but with a sufficient supply of water. All mice were weighed for baseline body mass. A 20 % glucose solution (2 g glucose / kg body weight, in PBS) was prepared and the volume for intraperitoneal injection was calculated: V (µl) = 10 x body weight (g). To measure blood glucose levels, mice were restrained with their tail exposed. The tip of the tail was scratched with a sterilized scalpel and a drop of blood was placed on the test strip of the blood glucose meter. The first sample was taken at t = 0 min and recorded as the baseline value. After the first measurement, the abdominal area was washed with 70 % ethanol. The animal was grabbed firmly by the back and glucose solution was injected intraperitoneally with a sterile needle at an angle of approximately 45 ° near the ventral axis, avoiding epigastric vessels and away from liver and kidneys. Blood glucose levels were then measured, as described above, at t = 15, 30, 60, 90 and 120 min. Data was presented as a depiction of blood glucose levels over time after intraperitoneal injection.

Table 6 Material for the intraperitoneal glucose tolerance test

Beta-D-Glucose	**Sigma Aldrich**
ACCU-CHEK Aviva	**ACCU-CHEK**
ACCU-CHECK test strips	**ACCU-CHEK**
Single-Use Needles	**BD Medical**
Animal Weighing Scale	**Kent Scientific**

2.3.3. Insulitis Score

To investigate the lymphocytic infiltration of pancreatic islets in *Clec16a* KD and WT animals, pancreata of female NOD mice were collected at 4, 6, 8 and 10 weeks of age and frozen in OCT Compound by the Kissler Lab. Pancreatic tissue was cut into 7 µm cryosections and stained with hematoxylin and eosin. The degree of lymphocytic infiltration was studied with a light

microscope and pancreatic islets were scored as having no infiltration, moderate infiltration or severe infiltration [120].

2.3.3.1. H.E. Staining

Cryosections were washed in PBS before staining with hematoxylin for 1 min. Sections were rinsed with water and hematoxylin was fixed in acid water. After rinsing with water, sections were dunked in 0.2 % Ammonium Hydroxide Solution. After washing with water, sections were rinsed with 95 % ethanol and stained with Eosin Y for 30 s. Dehydration was performed in 95% (twice) and 100 % (thrice) Ethanol. Slides were preserved in Xylene, mounted with Cytoseal 60 medium and covered with cover slips. Images for analysis were acquired using a light microscope equipped with a digital camera.

2.3.3.2. Scoring pancreatic islet inflammation

2 - 5 animals of each genotype and age combination were used for the experiment. Six sections per pancreas were manually analyzed and over 3500 islets were scored in total. Insulitis was scored as no infiltration, moderate infiltration (peripheral, or < 50 % of the islet) and severe infiltration (>50 % of the islet) [120]. Data was manually tallied and analyzed.

Table 7 Material for insulitis scoring

Beta-D-Glucose	**Sigma Aldrich**
ACCU-CHEK Aviva	**ACCU-CHEK**
ACCU-CHECK test strips	**ACCU-CHEK**
Single-Use Needles	**BD Medical**
Animal Weighing Scale	**Kent Scientific**
Light Microscope	**Zeiss**
Digital Camera	**Olympus**

2.3.4. Thymic Transplantation

To show that the effect of *Clec16a* KD was specific to the thymus, NOD WT mice were thymectomized and irradiated, then reconstituted with lineage-depleted NOD WT bone marrow cells and transplanted with either NOD WT or *Clec16a* KD E14 thymic lobes.

Cyclophosphamide was injected to accelerate disease onset. Animals were then regularly monitored for glycosuria.

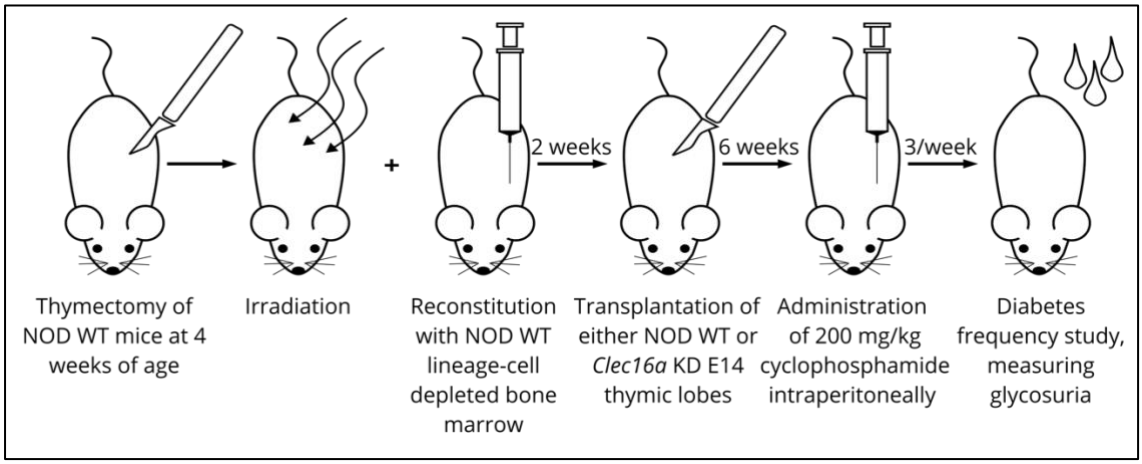

Figure 9 Thymic transplantation, schematic overview

Thymectomized NOD WT mice of 4 weeks of age were purchased from Jackson Laboratory. Subsequently, mice were irradiated and reconstituted with NOD WT lineage-cell depleted bone marrow by members of the Kissler Lab. 2 weeks later, thymic transplantation was performed as part of this thesis and E14 lobes were transplanted under the kidney capsule. 6 weeks later cyclophosphamide was injected to accelerate onset of diabetes. Thrice per week mice were tested for glycosuria.

2.3.4.1. Thymectomy and irradiation

Thymectomies were performed on NOD WT mice at 4 weeks of age by Surgical Services at Jackson Laboratories. The animals were subsequently irradiated at 900 rad by members of the Kissler Lab to eliminate endogenous hematopoietic cells and prepare for bone marrow transplantation.

2.3.4.2. Generation of bone marrow chimeras

To retrieve donor bone marrow, NOD WT donor mice were euthanized. The animals were dissected using forceps and scissors. Tibia and femur bones were removed, rinsed in 70 % ethanol and collected in cold PBS. Excess muscle and other tissue were removed, and the ends of the bones were cut off. Tibial and femoral shafts were flushed using a syringe with a 29G x ½ needle and bone marrow cells were collected. Bone marrow cells were pooled, and the density was adjusted to 5 x 10^6 / ml PBS. A MACS lineage depletion kit was used by members of the Kissler Lab to retrieve lineage-depleted BM cells. 200 µl of lineage-depleted BM cells were then injected intravenously into irradiated recipient mice.

2.3.4.3. Preparation of E14 thymic lobes

Pregnant donor mice were euthanized and sprayed with 70 % ethanol. The abdominal wall was cut and the peritoneum severed to reveal the uterus. The uterus was then separated from ligaments, removed from the abdominal cavity, transferred to a petri dish and cut lengthwise to expose and remove all embryos. Under the dissecting microscope, embryos were operated on and thymic lobes were collected in media.

2.3.4.4. Transplantation of E14 thymic lobes

After two weeks, the previously thymectomized BM chimeric recipient mice were anaesthetized with isoflurane. After anaesthetics had taken effect, the left flank was shaved. The skin was swabbed with iodine and wiped with 70 % Ethanol. After locating the left kidney underneath the skin, a small incision was made to expose the peritoneum. The peritoneum was opened carefully with an incision, keeping the incision small enough to prevent the exposed kidney from sliding back into the abdominal cavity. By pushing on both sides of the incision, the kidney was elevated and popped out of the abdomen. Kidneys were constantly kept moist using saline solution and fixated through clamps on each side of the incision. Using a 23G needle, the kidney capsule was then carefully scratched to create a small opening in the tissue. The embryonic thymus was placed in the opening and carefully pushed underneath the remaining capsule using forceps. Minimal bleeding was stopped using a dry cotton tipped swab. After re-moistening, clamps were removed, and the kidney was carefully placed back into the abdominal cavity. The peritoneum was closed using 5-0 silk sutures. Skin was pulled together and stapled two to three times. After the procedure, mice were placed underneath a heating lamp until full recovery.

2.3.4.5. Diabetes frequency study

Six weeks after surgery, all mice were injected with 200 mg/kg cyclophosphamide intraperitoneally to accelerate disease progression. Onset of diabetes was monitored regularly thrice per week by measuring glycosuria using Diastix. Mice with consecutive glucose levels of more than 250 mg/dL were considered diabetic.

Table 8 Material for thymic transplantations

thymectomized NOD mice	**Jackson Laboratories**
43855F Cabinet X-ray System – CP160 Option	**Faxitron X-ray Corporation**
Standard scissors	**Kent Scientific**
Dissecting forceps, tissue forceps	**Kent Scientific**
Syringe with 29 G x ½ needle	**Fisher Scientific**
23G needle	**Fisher Scientific**
MACS lineage depletion kit	**Miltenyi Biotec**
Brooder Heat Lamp – Model GP095B	**Brooder**
Dissecting microscope	**Fisher Scientific**
Animal clipper	**Braintree Scientific**
Cotton swaps	**CVS**
Iodine solution	**Fisher Scientific**
Scalpel handle and blades	**Kent Scientific**
Micro Bulldog clamp	**Kent Scientific**
Saline solution	**Jackson Laboratories**
Silk sutures	**Jackson Laboratories**
Stapler and staples	**Jackson Laboratories**
Diastix	**Jackson Laboratories**

3. Results

The following chapter partially contains data compiled and analyzed by Dr. Cornelia Schuster and Prof. Dr. Stephan Kissler (both members of the Kissler Lab, who supervised the author of this thesis), which was generated for the manuscript *"The autoimmunity-associated gene CLEC16A modulates thymic epithelial cell autophagy and alters T cell selection"* (*Immunity, 2015, Schuster et al.*). That data served as a foundation and framework for this thesis, and thus provides necessary context for the experiments and sub-experiments that were performed by the author of this thesis. Hence their inclusion in the following chapter. Data or figures generated by members of Kissler Lab will be marked with an asterisk (*) to clearly separate them from the work specifically done by the author of this thesis.

3.1. *In vivo* results

3.1.1. * *Clec16a* knockdown protects NOD mice from autoimmune diabetes

To study the role of *CLEC16A* in the pathogenesis of T1D, the Kissler Lab had generated a *Clec16a* KD NOD mouse model prior to this work (see Chapter 2.3). Lentiviral transgenesis had been used to introduce shRNA and a reporter GFP into the animals. GFP expression levels were checked in all animals to validate transgene expression (data not shown) [106]. Figure 1 is exemplary of various methods used by the Kissler Lab to validate an effective gene KD. As an example, there were significantly decreased expression levels of *Clec16a* mRNA in the spleen of KD animals relative to WT animals (Figure 1A). Furthermore, significantly reduced protein expression levels of *Clec16a* were found in the thymus of KD animals compared with WT animals (Figure 1B), as well as the spleen (data not shown).

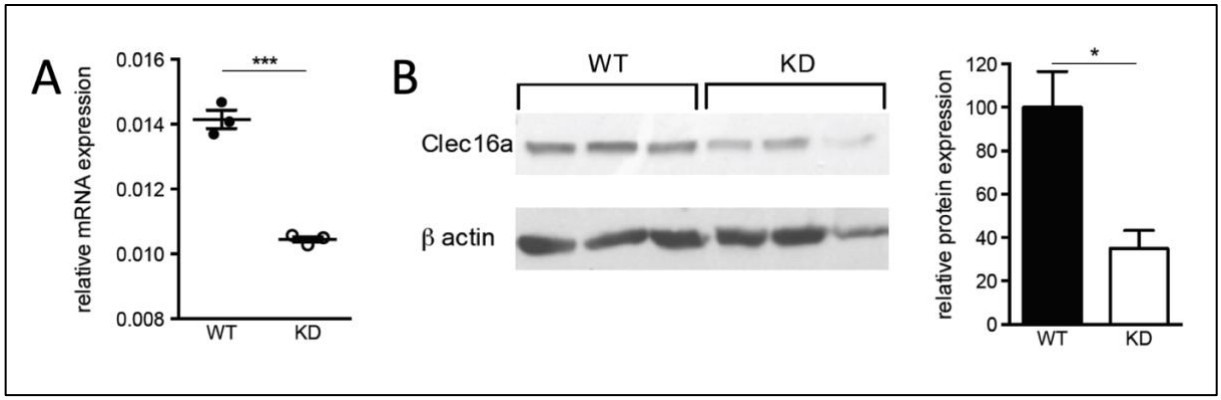

Figure 10 *** *Clec16a* knockdown efficiency in NOD mice, as published by Schuster et al.**

(A) Relative expression of *Clec16a* mRNA in the spleen of WT and K3 KD mice. Significant reduction of mRNA expression levels in KD animals. *** $p < 0.001$, two-tailed t-test, data representative of 5 experiments. (B) Western Blot with *β-actin* as loading control. *Clec16a* protein levels in the thymus of WT (n = 3) and KD (n = 3) animals. Significant reduction of protein levels in KD animals. * $p < 0.05$, two-tailed t-test, similar results in spleen (not shown) [106].

Transgenic mice developed expectedly with no visual change in phenotype. Most remarkably, however, Schuster et al. could demonstrate that *Clec16a* KD NOD animals were almost completely protected from autoimmune diabetes. To study disease protection, diabetes frequency studies were performed as described in Chapter 2.3.4.5. Briefly, blood glucose levels in animals were monitored regularly and diabetes was diagnosed when blood glucose levels were higher than 250 mg/dL in two consecutive measurements. As seen in Figure 2A, almost no *Clec16a* KD NOD mice suffered from autoimmune diabetes, while more than 60% of WT animals developed disease. Similar results were found after diabetes induction was accelerated via cyclophosphamide (CY) in *Clec16a* KD animals vs. WT animals [121] (data not shown). To see whether disease protection could be mediated by the immune system, Schuster et al. transferred splenocytes into immunodeficient NOD.SCID [122] mice which lacked both T and B lymphocytes. After transferring splenocytes from WT and *Clec16a* KD animals into NOD.SCID mice, animals injected with *Clec16a* KD splenocytes were indeed protected from CY induced diabetes (Figure 2B). Contrary, as displayed in Figure 2C, transfer of WT splenocytes into *Clec16a* KD NOD.SCID reinstated disease susceptibility, suggesting a protective effect of transgenic lymphocytes as opposed to changes in the pancreatic tissue. Specifically, the Schuster et al. identified the transgenic T cell population as the mediator of disease protection by reconstituting NOD.SCID animals with transgenic B and T lymphocytes and only seeing disease protection limited to mice which were injected with transgenic T cells (Figure 1D) [106].

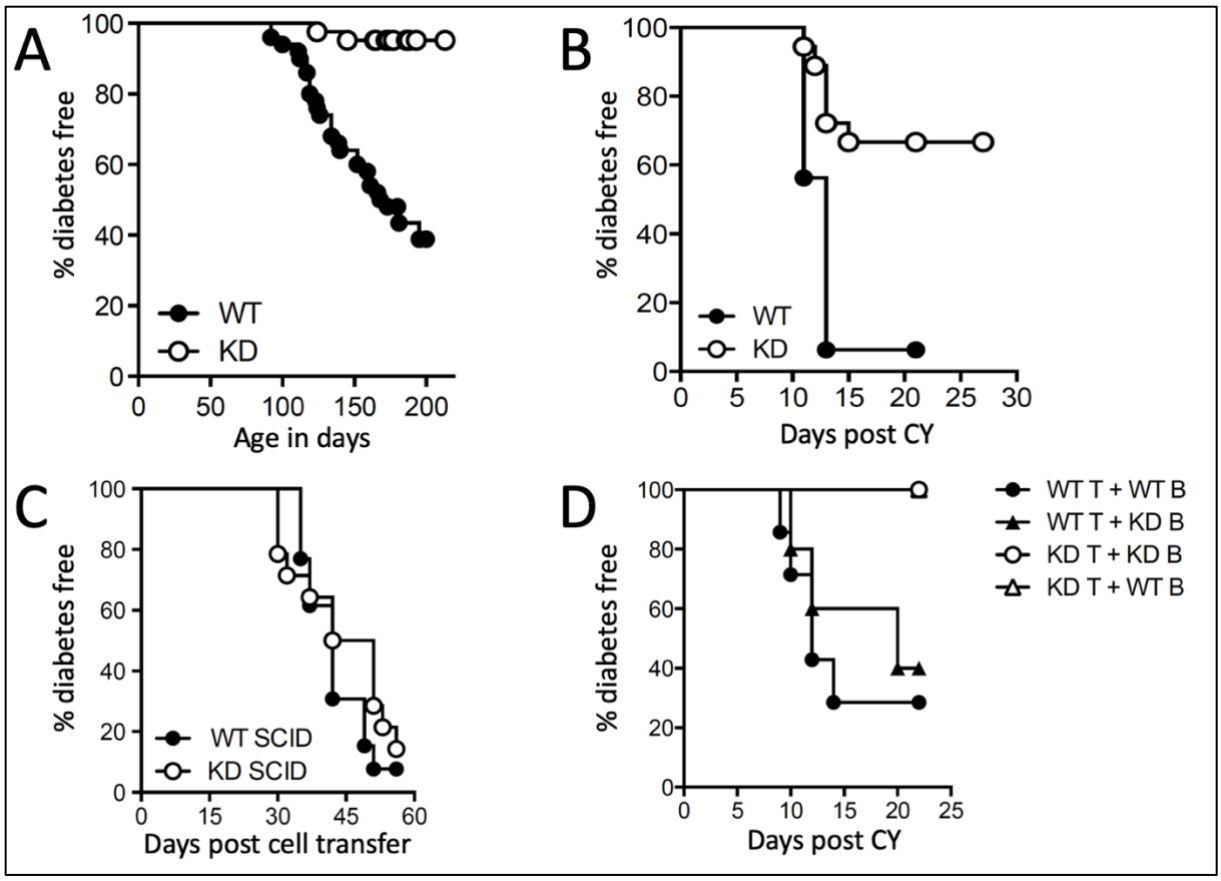

Figure 11 *** *Clec16a* knockdown protects from autoimmune diabetes due to less diabetogenic T lymphocytes, as published by Schuster et al.**

(A) Diabetes frequency study in WT (n=50) and *Clec16a* KD (n=42) animals. Significantly more KD animals are protected from diabetes, p <0.01. (B) Diabetes frequency study induced by CY in NOD.SCID mice reconstituted with splenocytes of WT (n=16) or *Clec16a* KD (n=18) animals. Significant protection of disease after injection with KD splenocytes, p <0.01. (C) Diabetes frequency study in WT NOD.SCID (n=13) vs. *Clec16a* KD NOD.SCID (n=14) mice reconstituted with WT splenocytes with no difference in disease frequency p = 0.36, Fisher's exact test. (D) Diabetes frequency study, induced by CY, in NOD.SCID mice reconstituted with T and B lymphocytes in the following combinations WT/WT, WT/KD, KD/KD and KD/WT, respectively. Significant disease protection in both animal groups injected with KD T cell groups, p < 0.01. For A, B and D data were analyzed using the Log-rank test. [106].

3.1.2. *Clec16a* silencing diminishes the severity of insulitis in pancreatic islets in NOD mice

After establishing that T cells were less diabetogenic in *Clec16a* KD mice, this project aimed to investigate whether there was a visible microscopic change in pancreatic islet inflammation. As described in Chapter 1.1.2, insulitis is a characteristic feature of autoimmune diabetes. To study inflammation of pancreatic islets in WT and *Clec16a* KD animals, lymphocyte infiltration was microscopically scored in pancreata of female NOD mice of each genotype (Chapter 2.3.3). Insulitis phenotype was manually scored and classified into three groups depending on

the level of lymphocyte infiltration. Figure 3 shows one example of each grade of insulitis in a WT NOD mouse, ranging from 'no insulitis' to 'severe insulitis'.

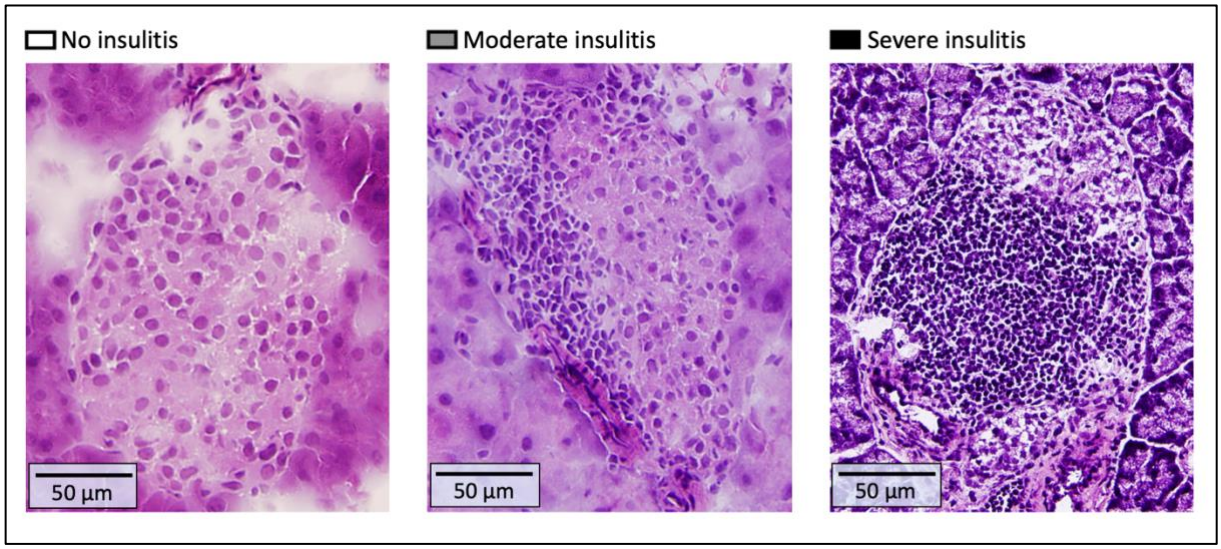

Figure 12 Insulitis subgroups in the NOD WT mouse

Microscopic scoring of insulitis in an exemplary female WT NOD mouse at 8 weeks of age. Pancreatic sections were 7 µm thick and stained with hematoxylin and eosin. Six sections (approximately 90 islets) were scored per animal. Insulitis was divided into three subgroups: no insulitis (left panel), moderate insulitis with <50 % lymphocyte infiltration or peripheral infiltration (middle panel) and severe insulitis with >50 % lymphocyte infiltration or central infiltration (right panel). Above, lymphocytes can be identified as small cells with spherical nuclei and an abundance of dark-staining chromatin (purple), and very little cytoplasm.

To see if *Clec16a* KD had any effect on the quality and severity of insulitis, pancreatic tissue samples of WT and *Clec16a* KD NOD mice were collected at four different developmental stages ranging from 4 to 10 weeks of age. There was no change in macroscopic pancreatic structure, weight and size. Also, there were no significant differences in number or size of pancreatic islets (data not shown). Overall, all stages of insulitis were found in both WT and *Clec16a* KD animals. Similar to insulitis in human, some pancreatic islets showed no signs of inflammation in WT NOD and *Clec16a* KD mice (Figure 4, left panels). Figure 4 shows the typical distribution of the varying stages of insulitis in WT NOD and *Clec16a* KD mice at 4, 6, 8 and 10 weeks of age. Strikingly, *Clec16a* KD reduced the severity of insulitis. Islet inflammation was more prominent in WT NOD mice with an earlier onset of insulitis as well as a more severe infiltration of lymphocytes at all stages of age, most prominently at 8 and 10 weeks of age. As seen in Figure 4, *Clec16a* KD delayed the onset of insulitis and reduced the severity of inflammation drastically.

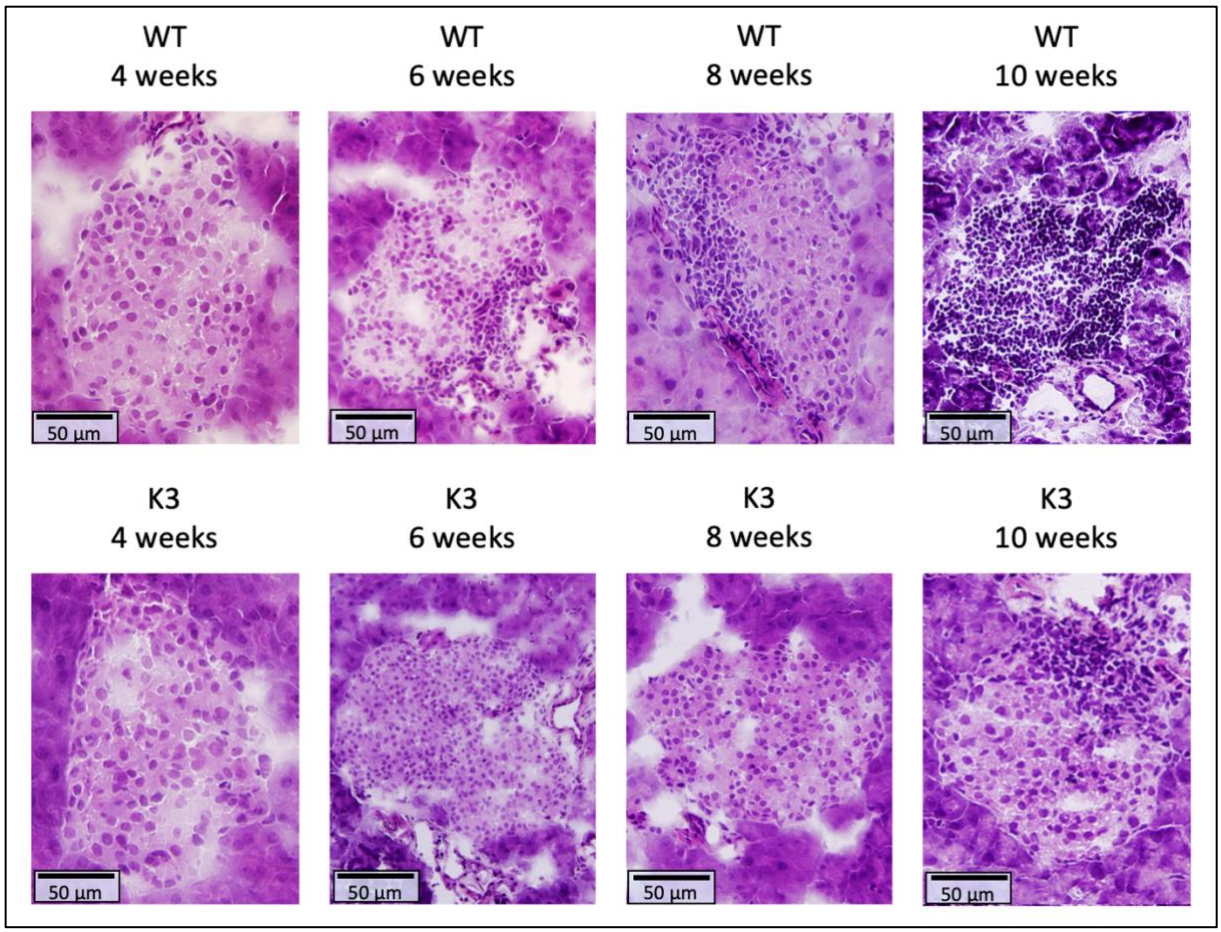

Figure 13 ***Clec16a*** **knockdown delays onset and reduces severity of insulitis in the NOD mouse**

Pancreatic islets of WT NOD and *Clec16a* K3 NOD mice at 4, 6, 8 and 10 weeks of age, stained with hematoxylin and eosin. Lymphocytes can be identified as small cells with little cytoplasm and an abundance of dark-staining chromatin. n = 2 – 5 animals were used for each age group. Six pancreatic sections per animal were analyzed manually. Approximately 10 – 15 islets were analyzed per section, n = 120 – 450 per age group. Shape and size of pancreas, as well as severity (stage) and onset of lymphocyte infiltration was studied. There are no differences in shape of pancreatic islets. (Top panels): Early onset of insulitis (6 w) in WT animals with severe inflammation (10 w), increasing with age. (Bottom panels): Delayed onset of insulitis in *Clec16a* KD animals with significantly less infiltration of lymphocytes (see Figure 5), even at high age. Displayed results are representative of K5 animals (second *Clec16a* KD line), with n = 2 – 5 animals and n = 120 – 450 islets, data not shown.

In addition to studying the quality of insulitis in WT and *Clec16a* KD animals, inflammatory lesions were also quantified in the same experiment. Overall, more than 3500 islets were analyzed and counted in a total of 24 animals. Figure 5 shows the distribution of the three stages of insulitis in WT NOD and *Clec16a* KD mice (pooled data from K3 and K5). With rising age, there was an increase in both moderately and severely inflamed islets in both groups. This increase was significantly greater in WT NOD mice, as the two insulitis stages became more prevalent at higher age. Strikingly, while the frequency of inflamed islets steadily

increased with age in WT NOD mice to a prevalence of up to 60 % at 10 weeks of age, the frequency of inflamed islets in *Clec16a* KD mice remained unchanged at approximately 15 %. Even after 10 weeks, up to 85 % of islets in *Clec16a* KD mice showed no sign of inflammation. While WT NOD mice suffered from an increased severity and rate of insulitis with older age, *Clec16a* KD mice were mostly protected from insulitis.

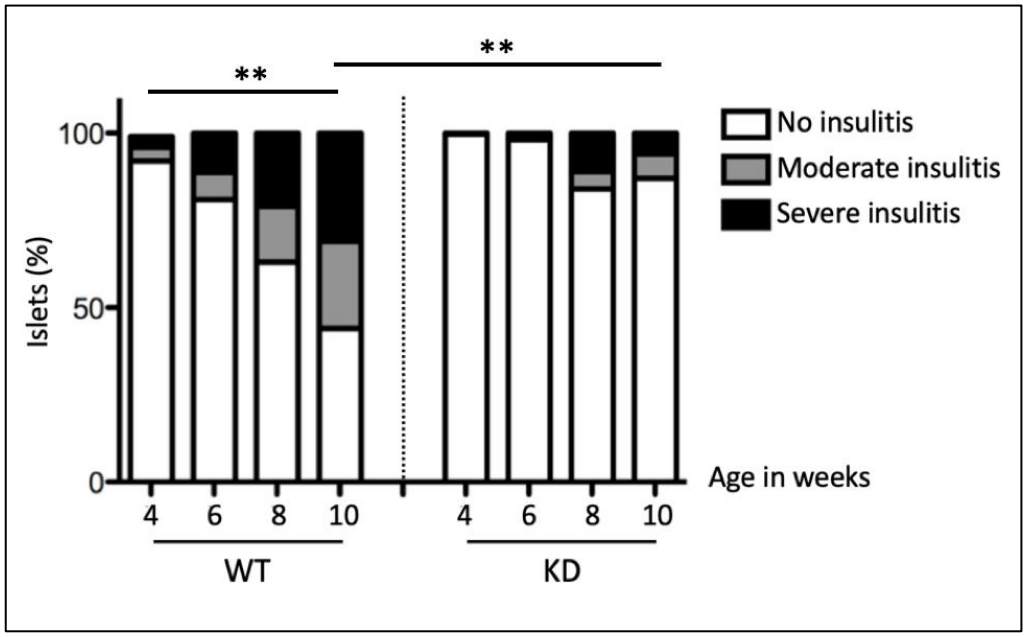

Figure 14 ***Clec16a* knockdown results in significantly less insulitis lesions in the NOD mouse**

Rate of Insulitis in WT NOD and *Clec16a* KD mice at 4, 6, 8 and 10 weeks of age. n = 60 – 90 islets per animal, n = 120 – 450 islets per age/genotype group, total islets analyzed n = 3600 – 4000. (Left panel): significantly increased rate of insulitis (moderate + severe) in WT animals of 4 weeks vs. 10 weeks of age, with 60% of all islets inflamed at 10 weeks of age, ** $p < 0.01$, two-tailed t-test. (Right panel): Significantly reduced rate of insulitis (moderate + severe) in *Clec16a* KD animals of 10 weeks of age vs. WT animals of 10 weeks of age, ** $p < 0.01$, two-tailed t-test.

3.1.3. * *Clec16a* knockdown causes T cell hyporeactivity

Further characterization of transgenic T lymphocytes in *Clec16a* KD animals by Schuster et al. is displayed in Figure 6 [106]. For this, proliferation rates of T cells were measured using a thymidine incorporation assay that quantified the amount of 3H-thymidin which was incorporated into new DNA strands during mitotic cell division. After stimulation of the TCR with CD3 antibody, polyclonal $CD4^+$ T cells in *Clec16a* KD animals showed less 3H-thymidin incorporation counts per minute and thus reduced proliferation compared to WT $CD4^+$ T cells (Figure 6A). This reduced responsiveness was confined to $CD4^+$ T cells, as transgenic $CD8^+$ T

cells showed no change in proliferation after stimulation with CD3 antibody (Figure 6B, middle panel). Normal reactivity of *Clec16a* KD CD4⁺ T cells was restored by circumventing TCR signalling via mitogen-mediated activation (data not shown), indicating that *Clec16a* KD reduces T cell responsiveness by affecting TCR signalling [106]. Notably, regulatory effector T cells (Tregs) in *Clec16a* KD mice showed no difference in suppressive function compared to WT Tregs (Figure 6B, right panel).

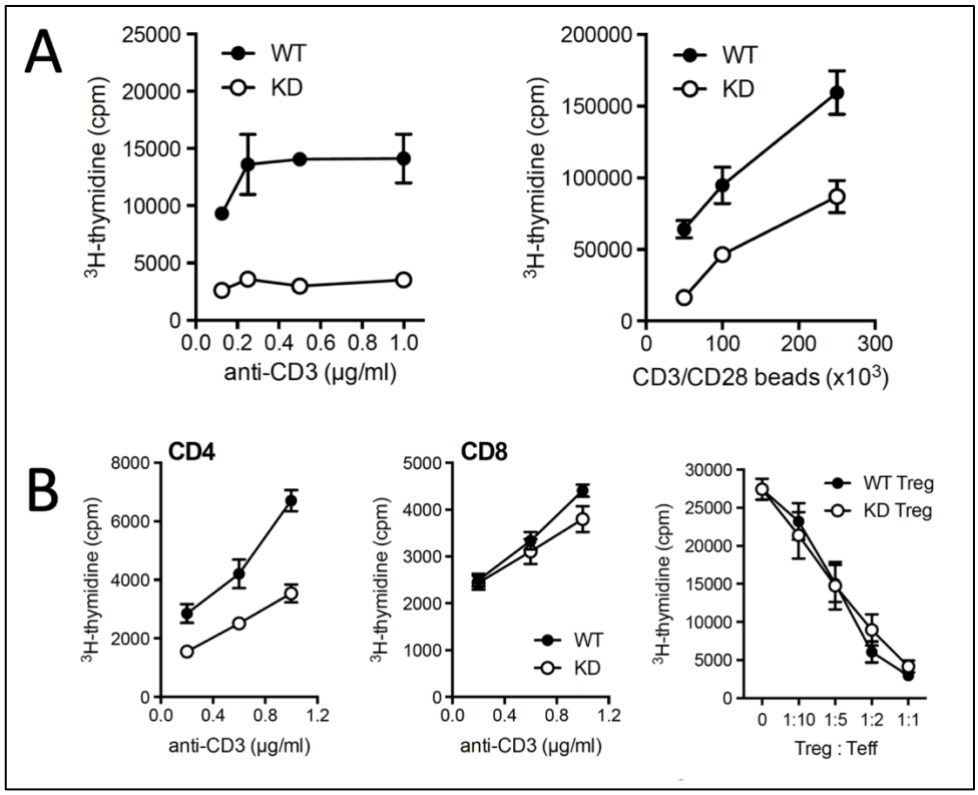

Figure 15 *** CD4⁺ T cells show reduced proliferation rates and are hyporeactive in *Clec16a* knockdown animals, as published by Schuster et al.**

Thymidine incorporation assay using 3H-thymidine, which is incorporated into new strands of DNA during mitotic cell division of T cells and can be measured as radioactive activity in counts per minute. (A) Reduced proliferation of *Clec16a* KD CD4⁺ T cells after stimulation with anti-CD3 (left panel) and CD3/CD28 covered beads (right panel). (B) Proliferation panels of CD4⁺ and CD8⁺ T cells of WT and *Clec16a* KD animals stimulated by anti-CD3 (left, middle panel), with reduced proliferation rates of *Clec16a* KD CD4⁺ T cells and unchanged proliferation rates of *Clec16a* KD CD8⁺ T cells. Suppression of WT CD4⁺ T cells by WT and *Clec16a* KD Tregs, with no change in suppressive function (right panel) [106].

3.1.4. * The effects of *Clec16a* knockdown are not T cell intrinsic

Previous results had suggested that autoimmune protection was mediated by hyporeactive T cells. Thus, further experiments were required to see whether these effects were caused by

gene KD and intrinsic changes within the cells. Due to the natural variegation of transgenesis after lentiviral infection, not every T cell expressed the transgene which included the reporter protein GFP. About 75% of all T cells in *Clec16a* KD mice were GFP^+ and therefore expected to express the transgene. To further characterize the behavior of transgenic T cells, both GFP^+ and GFP^- cells were stimulated with anti-CD3 by Schuster et al. . Strikingly, both subpopulations showed similarly reduced proliferation response, independent on their transgene expression (Figure 7A). As hyporesponsiveness was independent on transgene expression in T cells, the effects of *Clec16a* KD had to be conveyed by another tissue. To test if the effect of *Clec16a* KD on T cells was mediated by hematopoietic cells, bone marrow (BM) chimeras were generated by Schuster et al. (see Chapter 2.3.4.2). Transgenic T cells that developed in contact with WT TECs showed a similar reactivity as WT T cells in the same environment (Figure 7B). Notably, irradiated WT NOD animals were not protected from diabetes, regardless of whether they had been reconstituted with WT or *Clec16a* KD BM (Figure 7C). In contrast, irradiated *Clec16a* KD mice reconstituted with WT BM or *Clec16a* KD BM remained protected from diabetes over more than 40 days (Figure 7D), suggesting that disease protection was not owed to gene KD in hematopoietic cells but perhaps another tissue of the knockdown animal.

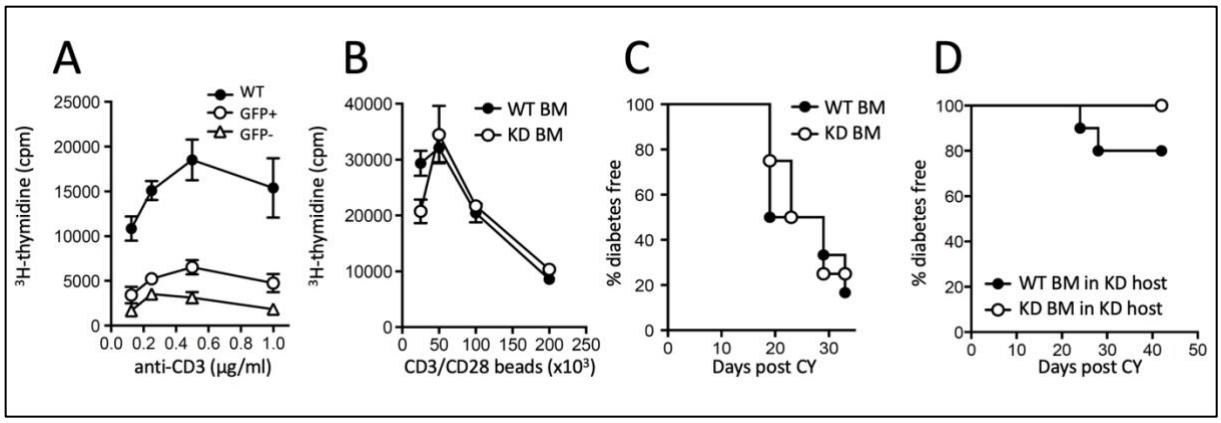

Figure 16 *** The effects of *Clec16a* knockdown are not conveyed by changes in T cells or hematopoietic cells, as published by Schuster et al.**

(A) Thymidine incorporation assay using 3H-thymidine. Reduced proliferation of GFP^+ and GFP^- *Clec16a* KD $CD4^+$ T cells after stimulation with anti-CD3, compared with WT $CD4^+$ T cells. (B) Proliferation of $CD4^+$ T cells in a WT BM chimeric mouse reconstituted with WT or *Clec16a* KD BM, stimulated by CD3/CD28 beads. (C) Diabetes frequency study. Rate of diabetes in WT BM chimeric mice reconstituted with WT or *Clec16a* KD BM. (D) Rate of diabetes in *Clec16a* KD BM chimeric mice reconstituted with WT or *Clec16a* KD BM, with disease protection of 80% of all animals [106].

3.1.5. The effects of *Clec16a* knockdown are thymus intrinsic

As part of this thesis, to test if the effects of *Clec16a* KD on T cells were perhaps conveyed by thymic epithelial cells during T cell selection, a thymic transplantation experiment was performed. For this, thymectomized and irradiated WT NOD animals were reconstituted with WT BM and subsequently transplanted with fetal thymi of either WT or *Clec16a* KD NOD embryos under the kidney capsule (see Chapter 2.3.4, and Figure 17). All animals survived anaesthesia and surgery with no follow-up mortality. After transplantation, a diabetes frequency study was conducted (see Chapter 2.3.4.5) to see which animals suffered from autoimmune diabetes.

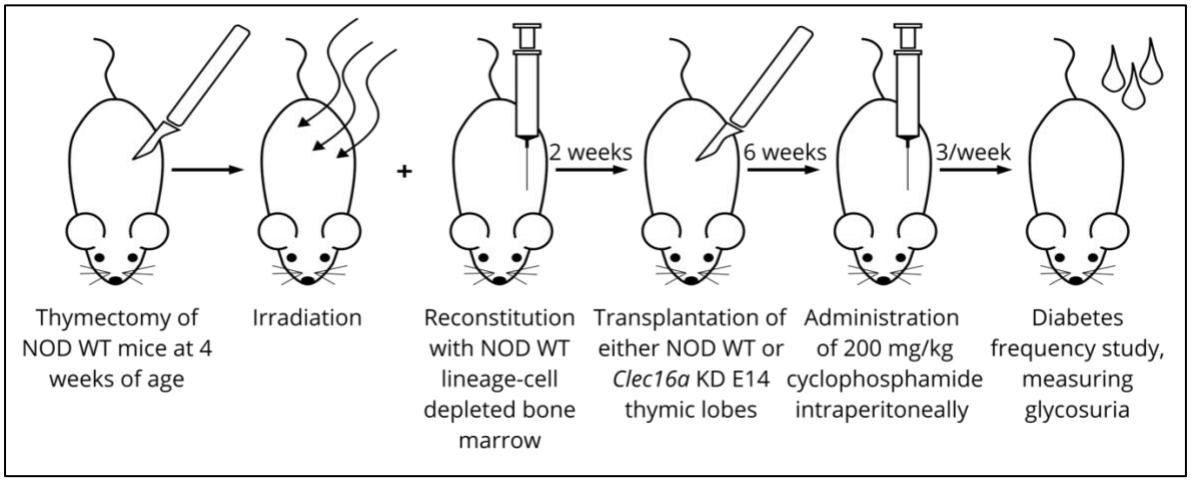

Figure 17 Thymic transplantation, schematic overview

Thymectomized NOD WT mice of 4 weeks of age were purchased from Jackson Laboratory. Subsequently, mice were irradiated and reconstituted with NOD WT lineage-cell depleted bone marrow. 2 weeks later, thymic transplantation was performed and E14 lobes were transplanted under the kidney capsule. 6 weeks later cyclophosphamide was injected to accelerate onset of diabetes. Thrice per week mice were tested for glycosuria.

Once completed, all animals were euthanized and dissected to study the success rate of thymic transplantation. All transplanted thymi had successfully grown underneath the kidney capsule (Figure 18). There was no organ rejection. At the time of dissection, all transplanted organs were well perfused and vital (Figure 18, left panel). Transplanted thymi did not show any macroscopic changes between the three test groups. The bottom right panel of Figure 18 shows representative examples of fully functional, successfully transplanted thymi in all three experimental groups. Additionally, there was no difference in T cell composition post transplantation at the time of diabetes onset (data not shown) [106].

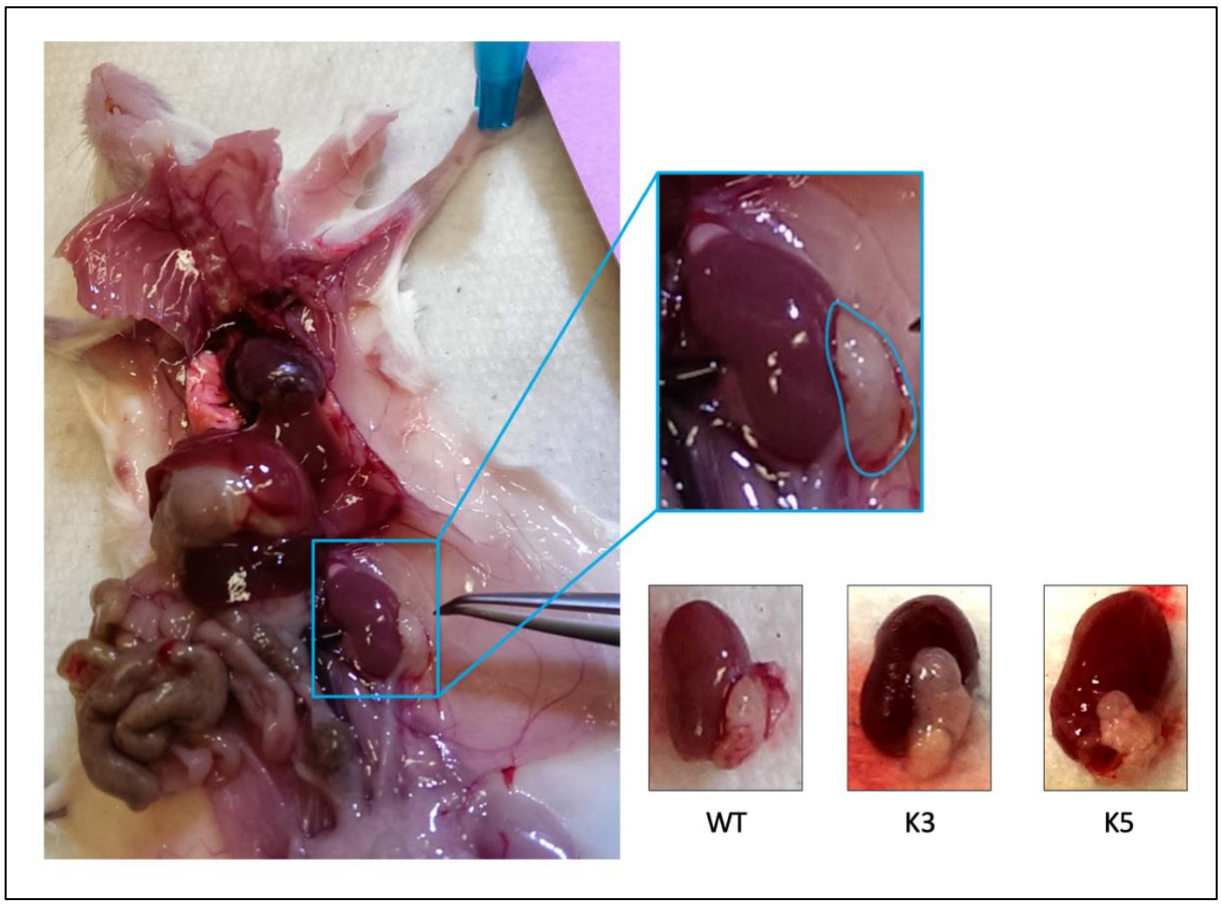

Figure 18 Transplantation of fetal thymi of WT or *Clec16a* knockdown NOD embryos

A dissected WT NOD mouse after thymectomy, irradiation and successful transplantation of WT BM and fetal thymus, after the concluded diabetes study. (Enlarged): Example of a fetal thymus transplant (indicated by the blue line) underneath the kidney capsule, adhesive to the left kidney, vital, well perfused, with no difference in macroscopic appearance. (Right bottom panel): Examples of successfully transplanted fetal thymi in all three experimental groups.

As expected, all WT NOD mice transplanted with WT BM and WT thymi developed autoimmune diabetes within 20 days. Most strikingly, WT NOD mice transplanted with WT BM, but *Clec16a* KD thymi, showed protection from autoimmune diabetes up to 40 days (Figure 19). Most notably, these findings suggested the effects of *Clec16a* KD were facilitated by changes within the thymus and perhaps a modified T cell selection.

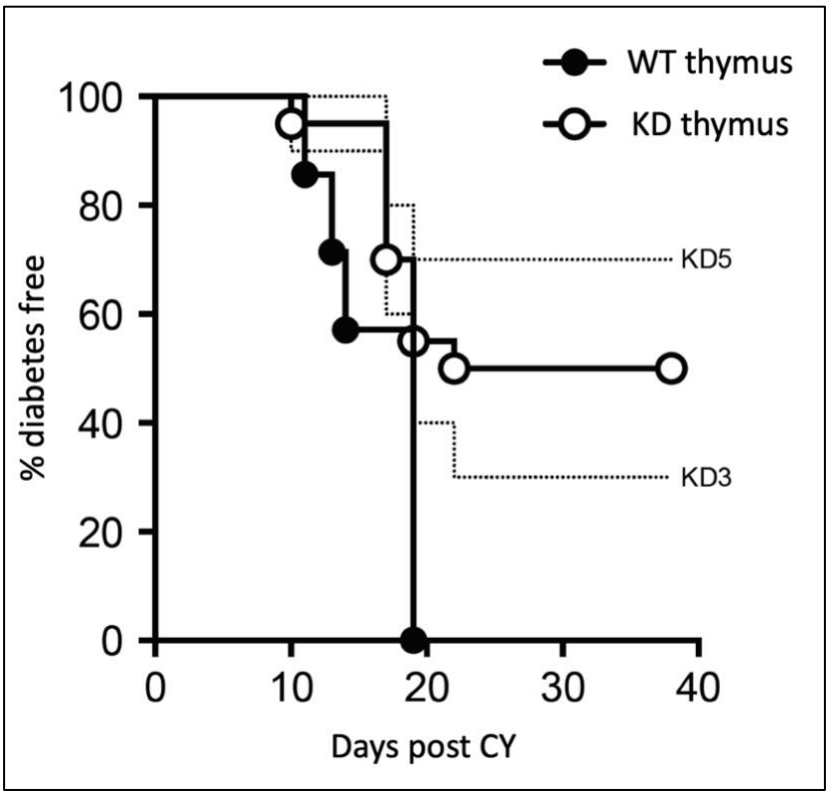

Figure 19 *** Disease protection is conveyed by changes in the thymic epithelium, as published by Schuster et al.**

Development of autoimmune diabetes in WT NOD mice, which were previously thymectomized at 4 weeks of age, irradiated and reconstituted with WT BM and subsequently transplanted with WT (n = 7) or *Clec16a* KD (K3 n = 10, K5 n = 10) fetal thymi (E14). WT vs. KD, pooled data, $p < 0.05$, Log-rank test [106].

3.1.6. *Clec16a* knockdown does not impair blood glucose homeostasis in NOD mice

It had previously been reported that islet-specific deletion of *Clec16a* in the pancreas led to a decrease in insulin secretion of pancreatic β cells and a reduction of blood glucose tolerance in mice, suggesting that perhaps a reduction of insulin as auto-antigen was contributing to disease protection [123]. To test whether impaired insulin secretion was contributing to disease protection in the *Clec16a* KD NOD mouse, pancreatic islets were isolated from WT and *Clec16a* KD NOD mice and analyzed as part of this thesis. As shown in Figure 20, there was a significantly reduced expression level of *Clec16a* mRNA in KD animals relative to WT, indicating an effective gene KD in pancreatic islets.

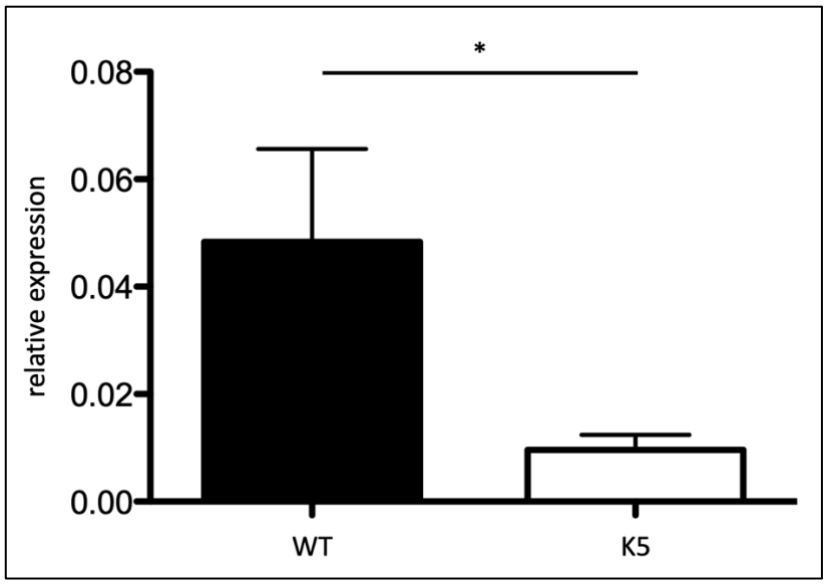

Figure 20 ***Clec16a* knockdown is effective in pancreatic islets of *Clec16a* knockdown NOD mice**

Relative expression of *Clec16a* mRNA in relation to *β-Actin* in pancreatic islets of K5 *Clec16a* KD NOD mice (n = 6) vs. WT animals (n = 6), data also representative of K3 animals (n = 6; data not shown), * $p < 0.05$, two-tailed t-test.

Insulin secretion and insulin content remained unchanged in pancreatic islets of *Clec16a* KD animals compared to WT mice (data not shown) [106]. Additionally, WT and *Clec16a* KD NOD mice were challenged by an intraperitoneal glucose tolerance test (IPGTT). Fasting blood glucose levels after overnight fast were comparable between WT and *Clec16a* KD animals as seen in Figure 21. Both groups showed physiological fasting blood glucose levels at t = 0 min. After glucose injection, there was an immediate and expected jump in blood glucose levels. Over time, WT and *Clec16a* KD animals showed no difference in blood glucose clearance with a similar blood sugar metabolism (Figure 21). These results highlight physiological blood glucose homeostasis in *Clec16a* KD animals with no direct effect on autoimmune diabetes, leaving the thymus as the pivotal organ involved in pathogenesis.

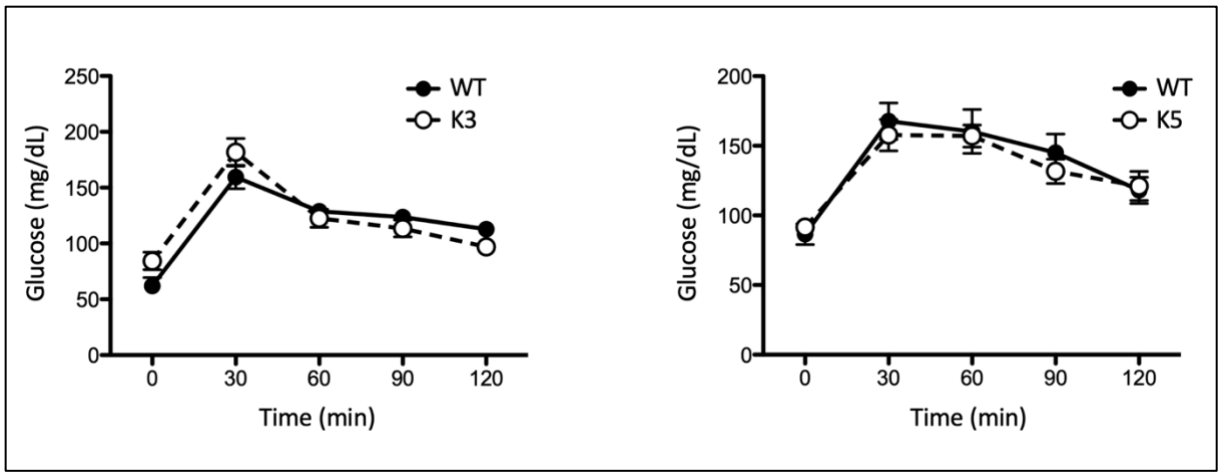

Figure 21 Blood glucose homeostasis remains unchanged in *Clec16a* knockdown animals

Intraperitoneal glucose tolerance test. Total blood glucose levels over time after intraperitoneal challenge with glucose in WT and *Clec16a* KD (K3 and K5) NOD mice. Physiological fasting blood glucose levels after overnight fast in all groups at t = 0 min. Initial jump in blood glucose levels after immediate challenge with glucose, with no difference in blood glucose clearance between WT and KD animals.

3.1.7. *Clec16a* and *Dexi* show similar expression patterns in the NOD mouse

Although *CLEC16A* contains most autoimmune disease associated SNPs in the 16p13 region, recent studies have also started to focus on its neighboring genes such as *SOCS1*, *CIITA* and *DEXI* (see Chapter 1.5.2). It was reported that intron 19 of *CLEC16A* may act as a regulatory sequence for its neighbor *DEXI*, as the intron interacts with the promoter region of *DEXI* and is located in close proximity to the gene [90]. Additionally, other studies could demonstrate that *CLEC16A* serves as an expression quantitative trait locus (eQTL) for itself in pancreatic β cells, for *DEXI* in monocytes and for *DEXI* and *SOCS1* in thymic tissue [124]. Based on these findings, the effects of *Clec16a* KD in the NOD mouse were investigated in regard to gene expression levels of the 16p13 gene cluster.

First, WT and *Clec16a* KD NOD mice were used to test detectability of all relevant 16p13 genes and to create an overview of gene expression levels in different tissues. Figure 22 serves as an example of first preliminary data collected in different murine tissues, presenting expression levels of the 16p13 gene cluster in kidney and liver produced with qPCR. As expected, *CIIta* shows only little expression in kidney and liver, as it is mostly expressed in tissues which harbor MHC class II carrying APCs [125]. *Socs1*, *Clec16a* and *Dexi* show expression levels similar to those previously reported in liver and kidney in various databases. Most notably, it appears as if *Clec16a* and *Dexi* show similar expression patterns independent of genotype.

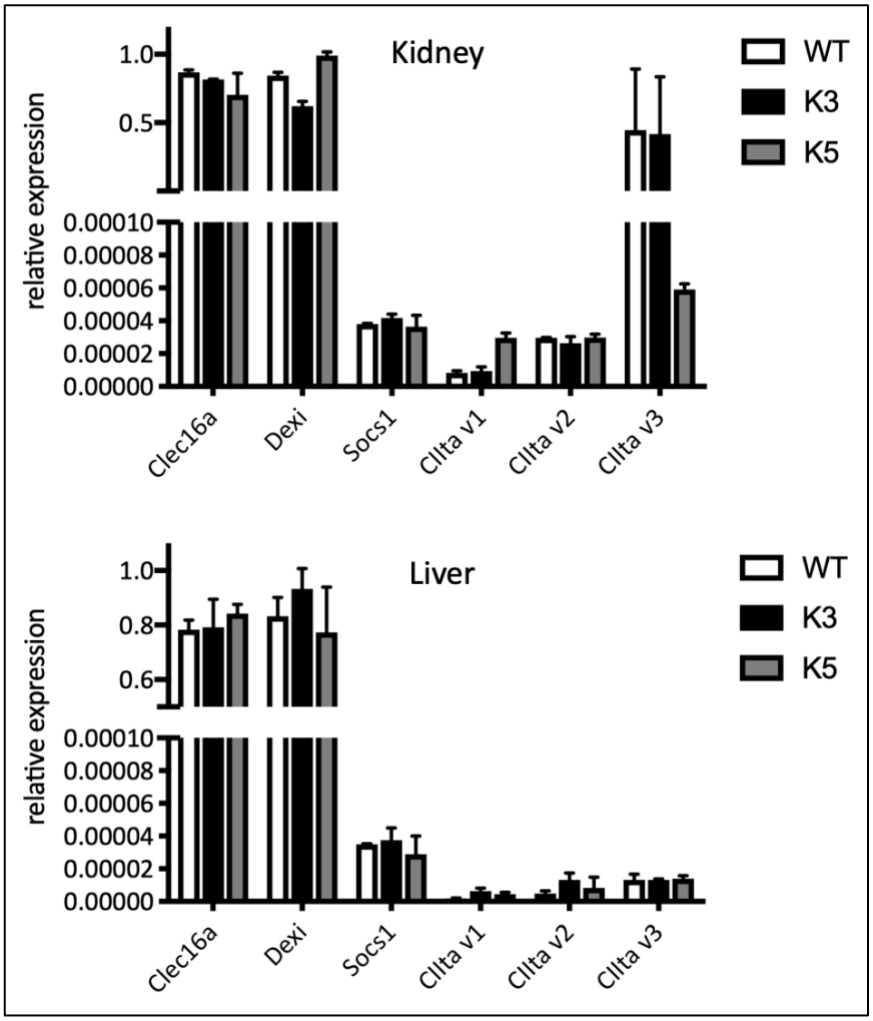

Figure 22 Relative expression of the 16p13 gene cluster in WT and *Clec16a* knockdown NOD mice

qPCR of liver and kidney samples from the NOD mouse. Expression of *CIIta, Dexi, Clec16a* and *Socs1* relative to *β-Actin* in WT (n = 3) and *Clec16a* KD (K3 n = 3, K5 n = 3) animals.

As there is no established link between *CLEC16A* risk SNPs and *CIITA* expression levels in literature, further experiments solely focused on *Clec16a*, *Dexi* and *Socs1*. WT NOD mice were used to establish a gene expression profile for these genes using qPCR. Among others, the cerebellum, liver and kidney have been reported to show relatively high expression levels of *Clec16a*, which is why these tissues were used as a reference point [84]. Additionally, due to the immunological nature of T1D, these experiments focused on lymphoid tissues such as thymus, spleen and lymph nodes, as well as the pancreas.

Matching the results reported in human, *Socs1* in the NOD mouse is mainly expressed in lymphoid tissue, especially the thymus and lymph nodes (Figure 23A) [126]. *Clec16a* and *Dexi*

mRNA expression in the NOD mouse is relatively high in brain, kidney and liver, which is also consistent with human data (Figure 23A) [127, 128]. While there is a clear difference in expression levels compared to *Socs1*, both *Clec16a* and *Dexi* show a distinctly similar gene expression pattern in almost all tested tissues (Figure 23B).

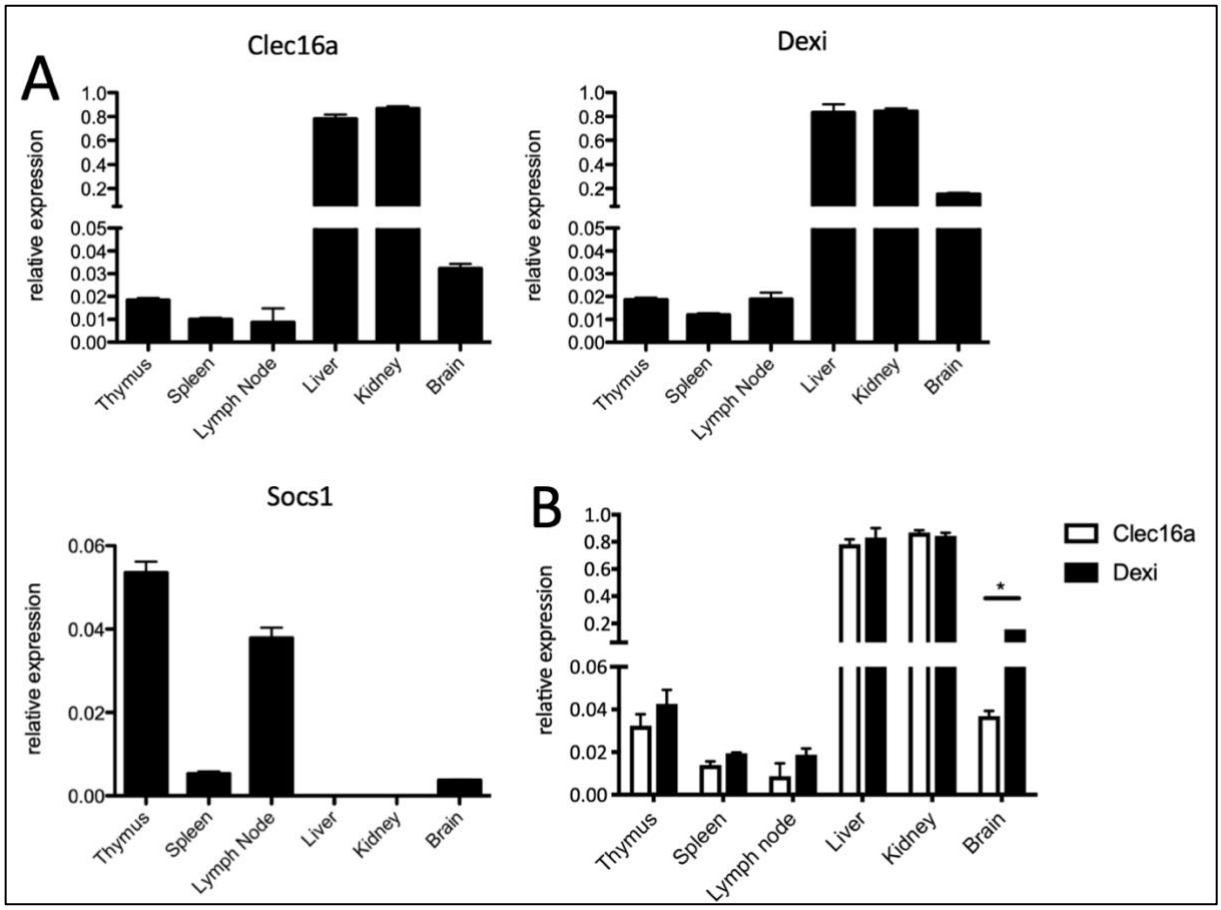

Figure 23 ***Clec16a* and *Dexi* share a gene expression pattern in the WT NOD mouse**

(A) Expression of *Clec16a*, *Dexi* and *Socs1* mRNA relative to *β-Actin* expression in WT NOD mice (n = 6) in thymus, spleen, pancreatic lymph node, liver, kidney and brain via qPCR. (B) Same data set as in (A), direct comparison of *Clec16a* and *Dexi* expression levels. No difference in expression patterns, except for a significantly increased expression of *Dexi* in the brain, * $p < 0.05$, two-tailed t-test.

3.1.8. *Clec16a*, *Dexi* and *Socs1* expression levels are reduced in *Clec16a* knockdown mice

As previously reported, *CLEC16A* and *CLEC16A* variations act as potential eQTLs for *DEXI* and *SOCS1* in the thymus [91, 124]. To test whether similar results could be found in the *Clec16a* KD NOD mouse, thymic tissue samples were analysed as part of this project. Real-time qPCR confirmed an effective gene KD with significantly decreased expression levels of *Clec16a* in the thymus (Figure 24). Additionally, with the successful *Clec16a* KD, there is a distinct

decrease in *Dexi* and *Socs1* gene expression, with a clear trend for *Dexi* (p = 0.054) and similar results for *Socs1* (Figure 24).

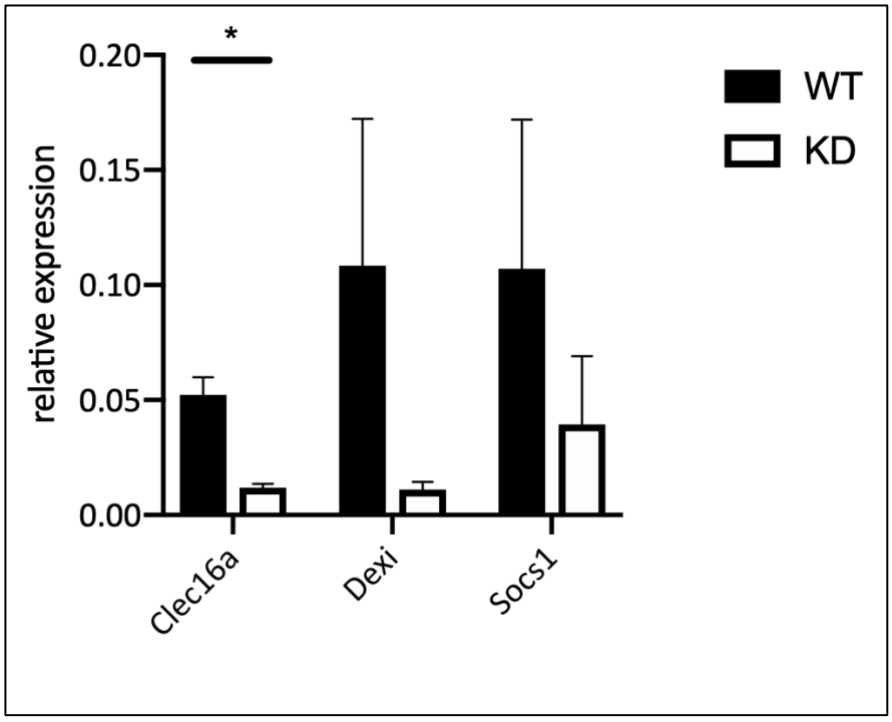

Figure 24 ***Clec16a* knockdown in the NOD mouse is accompanied by a decrease in *Dexi* and *Socs1* expression in the thymus**

Expression of *Clec16a*, *Dexi* and *Socs1* relative to *β-Actin* expression in thymic tissue of *Clec16a* KD NOD mice (n = 3 per group) via qPCR. Effective gene KD of *Clec16a*, * $p < 0.05$, two-tailed t-test. 90% reduction of *Dexi* expression in the *Clec16a* KD animals, p = 0.054, two-tailed t-test. 60% reduction of *Socs1* expression in the *Clec16a* KD mouse, p = 0.076, two-tailed t-test.

With regard to the pathogenesis of autoimmune diabetes, the previous experiment was also conducted in pancreatic islets. Interestingly, identical results were obtained for the expression patterns of *Clec16a*, *Dexi* and *Socs1* in the pancreas of NOD mice. As there is a statistically significant gene KD of *Clec16a* in pancreatic islets, *Dexi* and *Socs1* show a clear trend of reduced gene expression (Figure 25). Taken together, these results (Figure 24, Figure 25) suggest a possible regulatory role for *Clec16a* as an eQTL for *Dexi* and *Socs1* in the NOD mouse model.

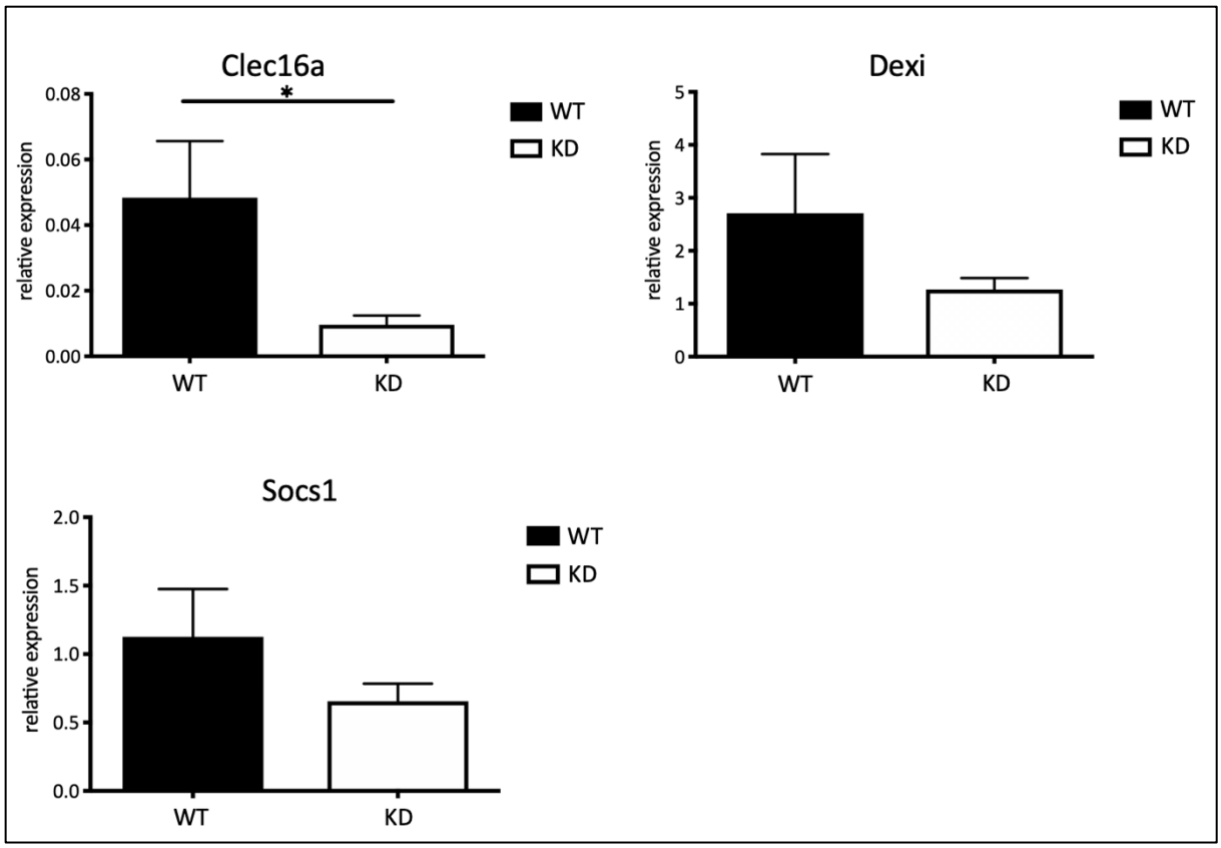

Figure 25 ***Clec16a* knockdown in the NOD mouse leads to reduced gene expression of *Dexi* and *Socs1* in pancreatic islets**

Expression of *Clec16a*, *Dexi* and *Socs1* relative to *β-Actin* expression in isolated pancreatic islets of *Clec16a* KD NOD mice (n = 3 per group) via qPCR. Effective gene KD of *Clec16a*, * $p < 0.05$, two-tailed t-test. Reduced relative expression of *Dexi* and *Socs1* in the *Clec16a* KD animals.

3.2. *In vitro* results

Based on the previously discussed *in vivo* results, it was hypothesized that the effects of *Clec16a* KD on T cell selection and T cell responsiveness were conveyed by changes in thymic epithelial cells. As previously reported and explained in Chapter 1, the drosophila ortholog of *CLEC16A ema* is implicated in autophagy. Autophagy, in turn, is required in thymic epithelium for antigen presentation and T cell selection. The following *in vitro* experiments were conducted to study the function of *Clec16a* in autophagy and to investigate a possible link between autophagy and T cell selection.

3.2.1. * *Clec16a* silencing impairs autophagy in thymic epithelial cells

Thymic epithelium is essential for T cell selection and the generation of a healthy T cell repertoire. As described in Chapter 1.4.3., TECs have been shown to use autophagy as a

pathway to load antigen into the MHC class II pathway. Here, Schuster et al. had investigated the effects of *Clec16a* KD on autophagy in thymic epithelial cells. For this, MJC1 cells were used, which had been derived from murine cortical thymic epithelium (see Chapter 2). Schuster et al. created *Clec16a* KD MJC1 cells, which showed effective gene KD (Figure 26A). Additionally, as a positive control for impaired autophagy, the autophagy-related gene *Atg5* was silenced in these cells. To investigate autophagy in TECs, the autophagy markers LC3 and p62 were quantified in *Clec16a* KD and *Atg5* KD MJC1 cells. Strikingly, *Clec16a* KD resulted in a reduced LC3-II/LC3-I ratio and accumulation of p62 in TECs, similar to *Atg5* KD, indicating impaired autophagy (Figure 26B) [106].

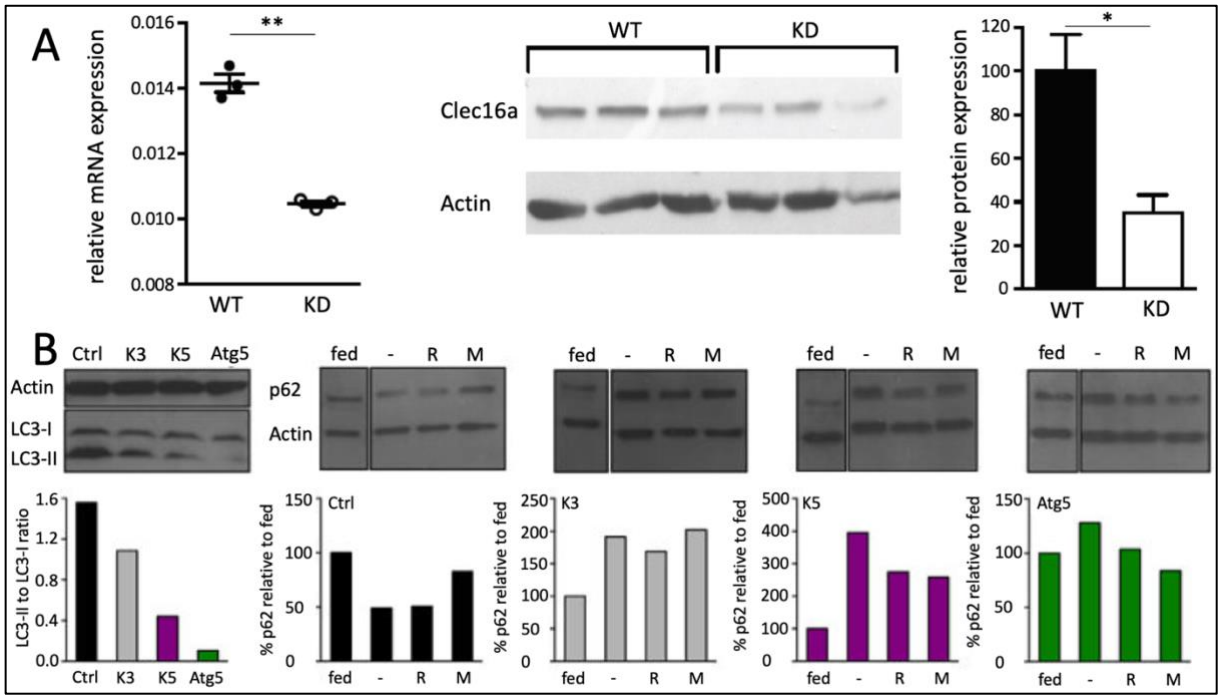

Figure 26 *** *Clec16a* knockdown in MJC1 cells results in impaired autophagic degradation and flux, as published by Schuster et al.**

(A) Relative expression of *Clec16a* mRNA in MJC1 cells in qPCR, significantly reduced with ** $p < 0.01$, two-tailed t-test (left panel). Protein expression levels via Western blot, significantly reduced with * $p < 0.05$ two-tailed t-test (middle and right panel). (B) Quantification of LC3-I, LC3-II and p62 via Western blot in control, *Clec16a* KD and *Atg5* KD MJC1 cells. Cells were starved and treated with autophagy inhibitor E64d to measure LC3 (left panel). For quantification of p62, cells were treated with autophagy inducer rapamycin (R) or autophagy inhibitor 3-methyladenine (M), or cells were without treatment (-) (right panels) [106].

3.2.2. *CLEC16A* knockdown alters autophagy in human cells

Based on these findings, the function of *CLEC16A* was tested in human cells as part of this thesis to see if its role in autophagy was evolutionarily preserved in human. For this, *CLEC16A*

KD HeLa cells were generated (see Chapter 2.1.3.). *CLEC16A* knockdown was induced in HeLa cells via lentiviral transgenesis to create two transgenic cell lines (K3 and K5). As a positive control, *ATG5* KD HeLa cells were generated as a reference for impaired autophagy. Figure 27 shows the effective gene knockdown of both *ATG5* and *CLEC16A* in HeLa cells (K3), with similarly effective results for the K5 cell line (data not shown).

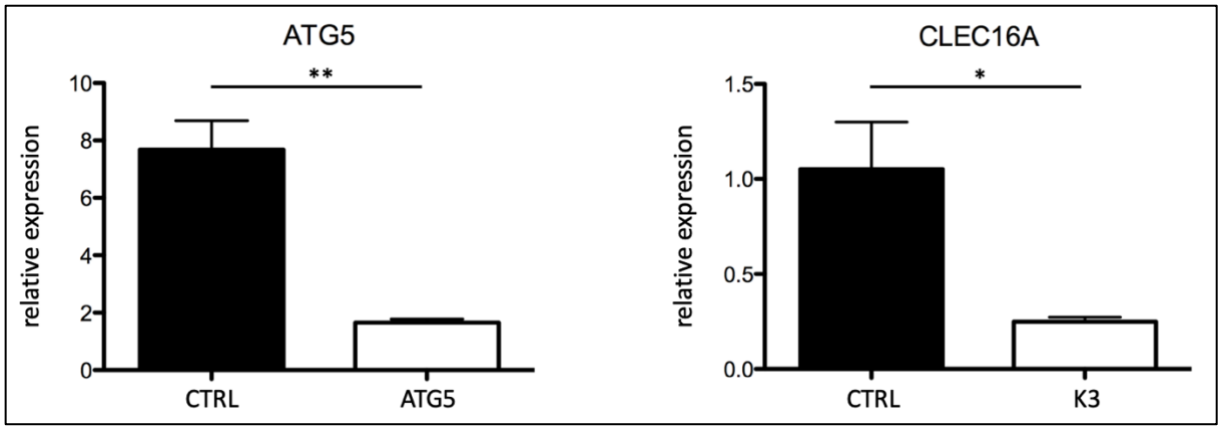

Figure 27 Effective knockdown of *ATG5* and *CLEC16A* in HeLa cells

qPCR of HeLa cells. Expression levels of *ATG5* mRNA in the *ATG5* KD HeLa cell line with a statistically significant reduction of expression, ** $p < 0.01$, two-tailed t-test (left panel). Relative expression levels of *CLEC16A* mRNA in the K3 KD HeLa cell line, with a statistically significant reduction of expression, * $p < 0.05$, two-tailed t-test (right panel). Data of K3 KD HeLa cells is representative of K5 KD HeLa cells.

To study the effect of *CLEC16A* KD on autophagy, p62 degradation was quantified via Western blot in *CTRL*, *CLEC16A* KD and *ATG5* KD HeLa cells. CTRL cells were transduced with shRNA targeting a luciferase not present in HeLa cells and served as a negative control. *ATG5* KD cells served as a positive control. All cells were starved over 24h to ensure induced autophagy. Remarkably, there was significantly more p62 accumulation in *CLEC16A* KD cells, with similar results in *ATG5* KD cells (Figure 28). As p62 is normally degraded under starved conditions by a functioning autophagy, the accumulation of p62 in *CLEC16A* KD HeLa cells is implicative of impaired autophagy. After treatment with autophagy inhibitors, similar results were observed with increased levels of p62, but no statistical significance (data not shown). These results are representative of three individual experiments.

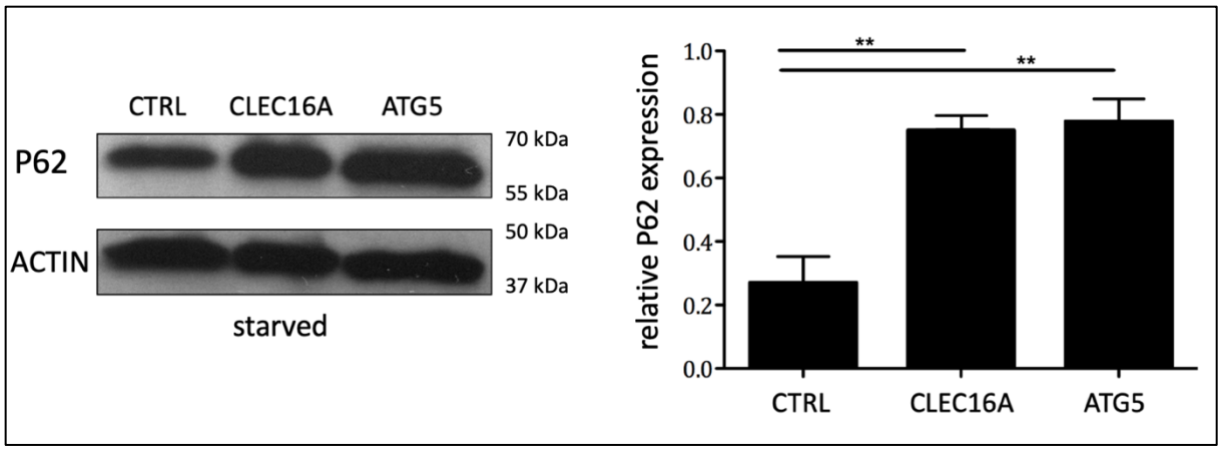

Figure 28 Accumulation of p62 in starved *CLEC16A* and *ATG5* knockdown HeLa cells

Western blot showing protein levels of the autophagy marker p62 in *CTRL*, *CLEC16A* KD and *ATG5* KD HeLa cells, under starved conditions (left panel), with ACTIN as loading control. Protein expression levels of p62 in *CTRL*, *CLEC16A* KD und *ATG5* KD HeLa cells after quantification relative to ACTIN levels (right panel), statistical significance ** $p < 0.01$, two-tailed t-test. Data is representative of three experiments.

To further investigate autophagy in *CLEC16A* KD HeLa cells, LC3 levels were measured as a marker for autophagic flux (see Chapter 1.4.4.1) in *CTRL*, *ATG5* KD and *CLEC16A* KD HeLa cells. After overnight starvation and treatment with the autophagy inhibitor E64d, autophagic flux was intact in *CTRL* HeLa cells as there was normal turnover of LC3-I to LC3-II, and LC3-II accumulated due to treatment with E64d (Figure 29). Remarkably, autophagic flux appeared to be impaired in *CLEC16A* KD HeLa cells with similar results in *ATG5* KD HeLa cells, as there was a significant reduction in LC3-II/LC3-I ratio with no apparent accumulation of LC3-II relative to LC3-I (Figure 29, top panel). In a second control, treatment with a different autophagy inhibitor called Pepstatin A resulted in similar results (Figure 29, bottom panel). In CTRL HeLa cells, LC3-I was converted to LC3-II, but LC3-II was not further degraded due to inhibition through Pepstatin A, resulting in a relatively high LC3-II/LC3-I ratio. In comparison, in *CLEC16A* KD and *ATG5* KD HeLa cells, there was less turnover of LC3-I to LC3-II, which resulted in reduced LC3-II/LC3-I ratios, indicating impaired autophagy. Taken together, there is no increase in LC3-II in starved *CLEC16A* KD HeLa cells after treatment with protease inhibitors, similar to the results in *ATG5* KD cells, which demonstrates reduced autophagic flux and confirms impaired autophagy. Based on these findings there is a clear role of *CLEC16A* in autophagy in human.

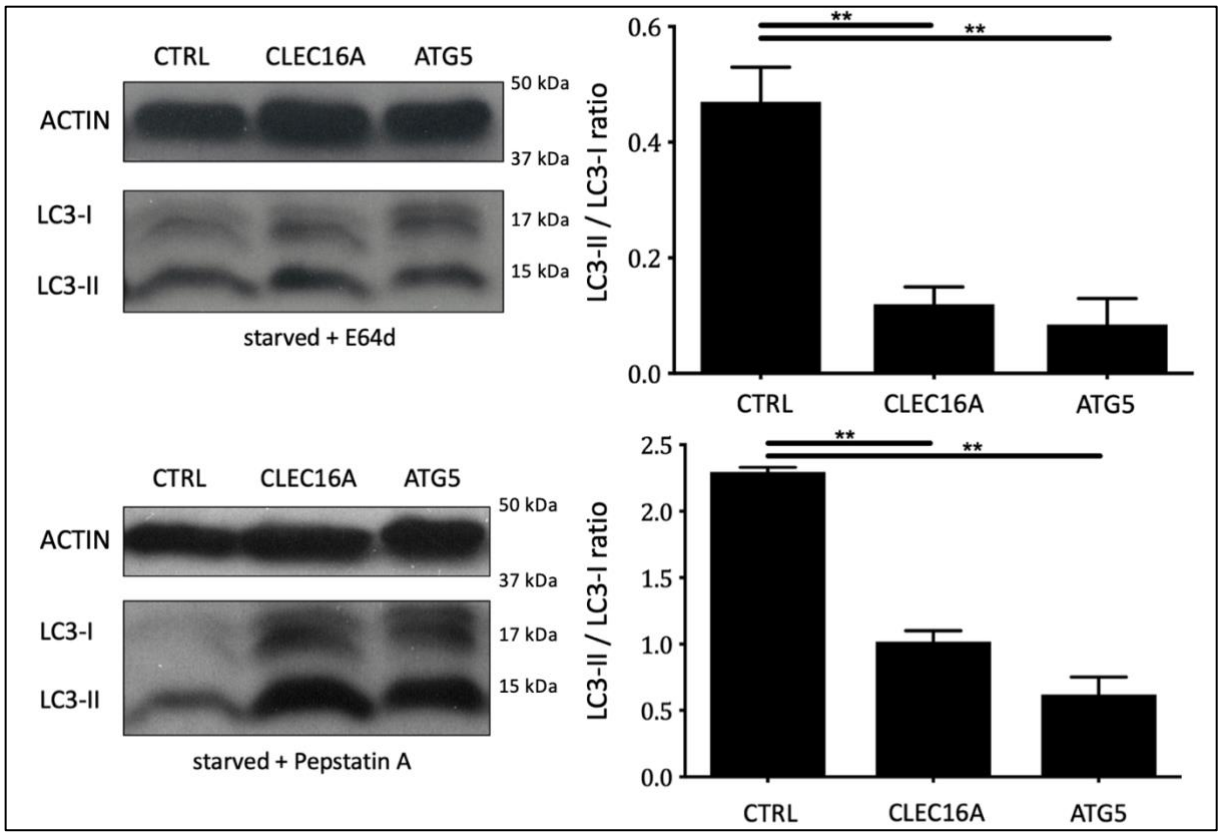

Figure 29 Reduced LC3-II / LC3-I ratios in *CLEC16A* and *ATG5* knockdown HeLa cells

Western Blot of LC3-I and LC3-II as a marker of autophagic flux in *CTRL*, *CLEC16A* KD and *ATG5* KD HeLa cells, under starved conditions. After treatment with autophagy inhibitor E64d (top panel) or Pepstatin A (bottom panel), there is less turnover of LC3-I to LC3-II in *CLEC16A* KD and *ATG5* KD HeLa cells, with a significantly reduced LC3-II/LC3-I ratio, ** $p < 0.01$, two-tailed t-test.

3.2.3. * *Clec16a* knockdown modifies thymocyte stimulation by MJC1 cells due to impaired autophagy

Finally, it was examined by Schuster et al. if there was a direct link between TEC autophagy and altered T cell selection owed to *Clec16a* KD. For this, Schuster et al. co-cultured the previously generated MJC1 cells with $CD69^{lo}$ DP thymocytes and found that the majority of immature thymocytes developed regularly into SP CD4 cells with an upregulation of the early activation marker CD69. However, when co-cultured with *Clec16a* KD MJC1 cells, developing thymocytes showed impaired upregulation of CD69 and reduced proliferation [106, 129].

In the scope of this thesis, to test if there is a direct link between impaired TEC autophagy and reduced T cell activation, MJC1 cells were transduced with an LC3 transgene that also encoded for $OVA_{323-339}$, a peptide tied to LC3 and to the autophagy-dependent antigen loading process of MHC class II molecules [130]. Thymocytes with a specific TCR for $OVA_{323-339}$, so called OT-II

thymocytes [131], were co-cultured with MJC1 cells expressing the $OVA_{323-339}$-LC3 construct. OT-II thymocytes stimulated by *Ctrl* MJC1 cells showed regular proliferation, while OT-II thymocytes stimulated by *Clec16a* KD and *Atg5* KD MJC1 cells demonstrated reduced activation (Figure 30). This indicated that *Clec16a* KD (similar to *Atg5* KD) modulated autophagy-dependent antigen presentation and reduced T cell stimulation. Hereafter, a mutation of the $OVA_{323-339}$-LC3 construct ($LC3_{G120A}$) cleavage site was introduced as part of this thesis, which prevented the peptide from being integrated into autophagosomes and the autophagy-dependent antigen presentation pathway. Finally, OT-II thymocytes stimulated by *Ctrl* MJC1 cells carrying the mutated construct displayed the same reduced proliferation pattern as seen after stimulation by *Clec16a* KD MJC1 cells without the mutated construct (Figure 30). This suggested that inhibition of autophagy-dependent antigen presentation via the mutated $OVA_{323-339}$-LC3 construct mirrored the effects of *Clec16a* KD. In summary, these results reveal a role of *Clec16a* in autophagy-related stimulation of thymocytes by TEC.

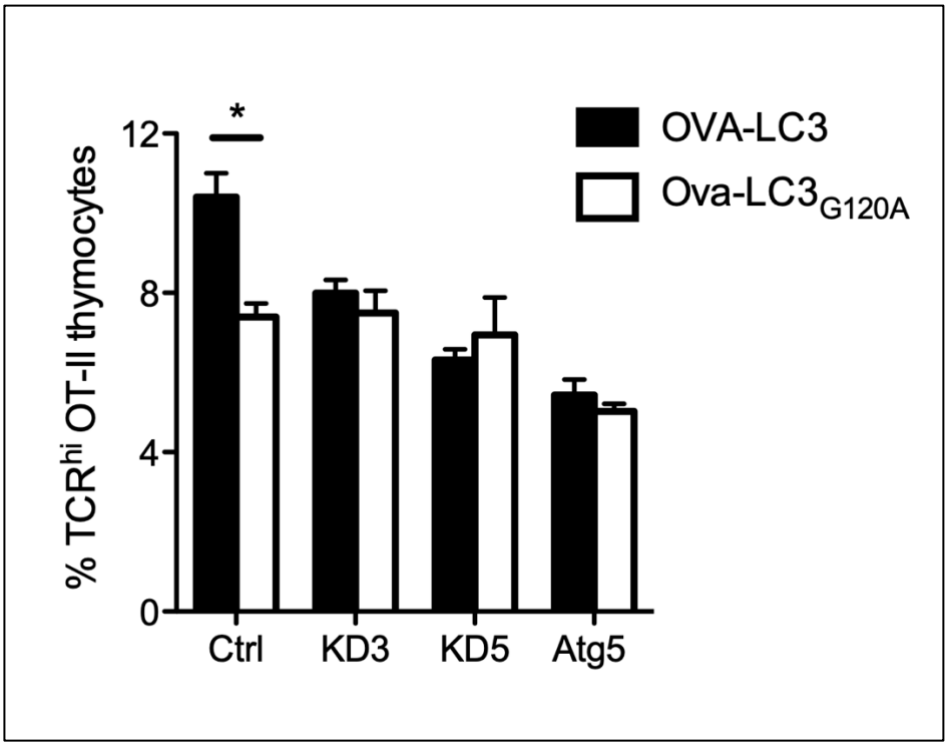

Figure 30 * *Clec16a* knockdown affects T cell stimulation by MJC1 cells, as published by Schuster et al.

Percentage of TCR^{hi} OT-II thymocytes after stimulation of immature OT-II thymocytes by *Crtl*, *Clec16a* KD or *Atg5* KD TECs. TECs had been transduced with $OVA_{323-339}$-LC3 constructs (black) or $OVA_{323-339}$-$LC3_{mut}$ constructs (white), respectively. Reduced thymocyte proliferation after stimulation with *Clec16a* KD and *Atg5* KD MJC1 cells compared to WT MJC1 cells (black bars). Significant decrease in thymocyte proliferation after stimulation with WT MJC1 cells carrying the $LC3_{G120A}$ mutation, mirroring the effects of *Clec16a* KD and *Atg5* KD (white bars). * $p < 0.05$, two-tailed t-test [106].

4. Discussion

4.1. *Clec16a* knockdown protects the NOD mouse from autoimmune diabetes

The NOD mouse is a common experimental model for the development and study of autoimmune diabetes [110]. Strikingly, knockdown of *Clec16a* protected almost all NOD mice from spontaneous diabetes (Results, Figure 11A). As the mechanisms of *Clec16a* KD remained unknown, and based on the autoimmune pathogenesis of T1D, this work investigated whether *Clec16a* KD affected autophagy in TECs, T cell selection and the immune system to convey disease protection. As seen in Figure 11, the transfer of *Clec16a* KD splenocytes protected from diabetes, while animals injected with WT splenocytes developed disease. This protective role of transgenic splenocytes indicates that disease protection is indeed conveyed by changes within the immune system. Further experiments demonstrated disease protection was mediated by transgenic T cells and independent of the genotype of B cells (Results, Figure 11D). Markedly, these results are in line with the widely accepted theory that T1D is a mostly T cell mediated autoimmune disease [132], and suggest a critical protective role of T cells in *Clec16a* KD NOD mice.

To further distinguish which specific immune cells were affected by *Clec16a* KD, T cell subpopulations were stimulated via TCR signaling and proliferation was measured. Interestingly, $CD4^+$ T cells of *Clec16a* KD animals were hyporeactive after TCR stimulation, while $CD8^+$ T cells of *Clec16a* KD animals showed normal proliferation (Results, Figure 15). Although cytotoxic $CD8^+$ T cells are regarded as the effectors of pancreatic β cell destruction [133] and constitute the majority cell population within insulitis lesions [19], $CD4^+$ T cells are of critical importance in the pathogenesis of T1D and immune tolerance. They stimulate B cells to produce (auto-)antibodies, stimulate effector $CD8^+$ T cells to destroy pancreatic β cells, and they release cytokines to induce macrophages [134]. Hence, hyporeactivity of $CD4^+$ T cells in *Clec16a* KD animals could be the underlying mechanism of disease protection. Markedly, $CD4^+$ T regulatory cells were not affected by *Clec16a* KD and displayed regular proliferation after TCR stimulation (Results, Figure 15B, right panel). This could be explained by their innately reduced dependency on TCR signaling [135].

Knowing that T cells were hyporeactive in *Clec16a* KD animals, pancreatic tissue of these animals was analyzed to see if there was a subsequent change in pancreatic inflammation. Strikingly, insulitis scoring showed that *Clec16a* KD reduced the severity of pancreatic inflammation and lymphocytic infiltration in the NOD mouse (Results, Figures 13 and 14). Nonetheless, all stages of insulitis were found in both WT and *Clec16a* KD groups, including '*no insulitis*'. Notably, there was an increase in severity of insulitis in WT NOD animals with older age. In contrast, while *Clec16a* KD animals also suffered from insulitis, the rate and severity of it were drastically reduced compared to WT mice of the same age (Results, Figure 14). Within the scope of this thesis, the investigator could not be blinded for this large experiment. To increase the power of this experiment and to compensate for a potential bias, more than 3500 individual islets were analyzed manually, and insulitis scoring was performed as reported and validated in literature [120]. Previous reports from human data have identified insulitis as a characteristic lesion in young T1D patients. Although it can be completely absent in T1D patients, it is regarded as a pathognomonic lesion [136]. Taken together, the results mentioned above match previous findings and serve as a potential histopathological explanation of disease protection in *Clec16a* KD mice. To increase the validity of this particular experiment, the analysis could be replicated with a blinded investigator in further studies.

4.2. The effects of *Clec16a* knockdown are thymus-intrinsic

Expression of lentiviral transgenes can vary depending on the integration site of the transgene, but this variegation can be improved greatly by using a superior lentiviral construct [94]. In *Clec16a* KD animals, approximately 75% of T lymphocytes expressed the transgene which included a GFP reporter protein. Strikingly, T cells in *Clec16a* KD animals were hyporeactive independent on whether they expressed the transgene (GFP^+) or not (GFP^-) (Results, Figure 16A). This suggests that T cells are not hyporeactive because of internal changes caused by *Clec16a* KD within the cell, but perhaps because of changes in other cell populations or tissues interacting with T cells. Following up on that, Schuster et al. could show that disease protection was surprisingly not conveyed by hematopoietic cells as WT NOD mice suffered from diabetes, regardless of whether they had been reconstituted with WT or *Clec16a* KD bone marrow (Results, Figure 16C). In contrast, the work for this thesis found almost all *Clec16a* KD animals protected from diabetes, no matter the genotype of the transplanted

bone marrow (Results, Figure 16D). This clearly indicates that disease protection is not conveyed by hematopoietic cells, but by changes in another tissue.

One study had reported that *Clec16a* KD affected pancreatic β cells and reduced insulin secretion [123]. To test whether T cells in *Clec16a* KD animals were hyporeactive because of changes in the pancreas and due to a lack of the insulin antigen, intraperitoneal glucose tolerance tests were performed. Notably, there was no difference in insulin secretion, and blood glucose metabolism in *Clec16a* KD animals was similar to WT animals (Results, Figure 21). As a next step, it would be interesting to repeat the experiment in animals with a complete gene knockout. Nevertheless, changes in insulin secretion or glucose metabolism could not be found in *Clec16a* KD mice used for this work and, therefore, cannot be accountable for disease protection in NOD mice.

Based on the autoimmune nature of T1D, the lymphatic tissue is known to play a vital part in disease pathogenesis. Namely, the thymus is known as the essential location for T cell maturation and selection [137, 138]. More specifically, in recent years it has become clear that interactions between thymic epithelial cells and self-peptide:MHC complexes are critical to positive and negative selection of developing thymocytes [42]. To test if T cell hyporeactivity in *Clec16a* KD animals was caused by changes within the thymus, a thymic transplantation experiment was performed on thymectomized, irradiated WT NOD mice, which had been reconstituted with lineage depleted WT bone marrow. Most strikingly, transplantation of *Clec16a* KD fetal thymus protected WT NOD mice from spontaneous diabetes, whereas transplantation of WT fetal thymus did not protect from disease (Results, Figure 19). This suggests firmly that disease protection derives from *Clec16a* KD in the thymus. Subsequent elaboration on this by Schuster et al. could show that indeed T cell selection was impaired in *Clec16a* KD animals, specifically the transition from DP to CD4 SP T cells [106].

4.3. *Clec16a* serves as a potential expression quantitative trait locus for its neighboring genes

GWAS have identified many susceptibility SNPs located on the chromosome 16p13 locus encompassing *CLEC16A*, *DEXI*, *SOCS1* and *CIITA*. These variants are in strong linkage disequilibrium. Some recent studies have reported that *CLEC16A* can act as a quantitative

expression trait locus for its neighboring genes such as *DEXI* and *SOCS1* in MS patients [90, 91, 124]. To this day, it remains quite difficult to understand each individual functional and causal contribution to disease pathogenesis. To see if there was any correlation between *Clec16a* and its neighboring genes under knockdown conditions in the NOD mouse, *Clec16a* KD tissues and cells were analyzed and gene expression levels were compared. The data shown in Figure 22 represents preliminary data in exemplary organs, and has to be interpreted with caution, as there is no clear gene KD detectable. Further refinement of these experiments resulted in more viable data, as seen in Figures 23-25. Most notably, in various tissues of WT NOD mice, *Clec16a* and *Dexi* show distinct similarity of mRNA expression levels (Results, Figure 23). With a focus on T1D, tissues such as the thymus and pancreatic islets were further analyzed. Interestingly, with *Clec16a* KD comes a remarkable reduction of *Dexi* and *Socs1* mRNA expression levels, both in the thymus and in the pancreas (Results, Figures 24, 25). As these preliminary qPCR results imply, there may be a direct correlation of expression levels of *Clec16a*, *Dexi* and *Socs1* in *Clec16a* KD animals. This, in turn, could mean that *Clec16a* indeed serves as an eQTL in the NOD mouse or perhaps serves a regulatory purpose for its neighboring genes. Obviously, these studies would need to be vastly expanded upon to better understand the functions and mechanisms of said genes. This, however, was not feasible within the scope and time limitations of this thesis. Nonetheless, the preliminary data acquired by this work was used to initiate further studies to characterize the neighboring gene *Dexi* by colleagues at the Kissler lab (unpublished data).

4.4. The role of *Clec16a* in autophagy is conserved in human cells

The preceding results from Schuster et al. and the experiments conducted for this thesis demonstrate that the effects of *Clec16a* KD originate from within the thymus and impair T cell selection. T cell selection is highly dependent on a functional thymic epithelium [42], which led to the assumption that perhaps *Clec16a* KD affected thymic epithelial cells and thereby altered T cell selection. Remarkably, recent studies discovered that *Clec16a* and its orthologs play a vital role in drosophila and mice autophagy [58, 106, 123, 139]. Additionally, autophagy has been identified as a prominent feature in TEC as a major contributor of peptide to the MHC class II loading process [46, 47, 62]. Building on the most recent finding that *Clec16a* KD indeed impaired autophagy in TEC of NOD mice [106], this study aimed to investigate a possible link between *CLEC16A* KD and impaired autophagy in human cells. To adequately

study the autophagic process in human cells, accumulation of p62 and the conversion of LC3-I to LC3-II were measured in HeLa cells via Western blot [63, 69].

To test autophagy in HeLa cells, at first, gene knockdowns of *CLEC16A* and *ATG5* were generated and confirmed via qPCR (Results, Figure 27), using *ATG5* as a positive control. Due to the lack of a reliable and thoroughly tested antibody for *CLEC16A* at the time, this work refrained from measuring protein levels via Western blot and relied on mRNA expression levels to detect knockdown, as is customary in experimental design after siRNA induced mRNA silencing [140]. To test the validity of p62 and LC3 as autophagy markers, HeLa cells were starved for autophagy induction, and protein levels were measured. HeLa cells carrying a control plasmid showed reduced levels of p62 (Results, Figure 28), which was interpreted as a sign of regular p62 clearance and intact autophagy [69]. Considering the difficulties of interpreting LC3 levels without the use of protease inhibitors, data of starved HeLa cells without treatment of protease inhibitors was not analyzed any further. Control HeLa cells treated with protease inhibitors, however, showed an increase in LC3-II/LC3-I ratio, which can be interpreted as a regular conversion of LC3-I to LC3-II with no further degradation of LC3-II owed to protease inhibitor treatment. As these findings were reproducible and consistent with literature, p62 and LC3 were confirmed as autophagy markers in HeLa cells.

Under starved conditions, p62 degradation was significantly reduced in *CLEC16A* KD HeLa cells compared to control cells, with equal results for *ATG5* KD (Results, Figure 28). Naturally, under starved conditions and induced autophagy, control cells would show an increased clearance of p62. Accumulation of p62 in *CLEC16A* KD cells suggests a dysfunctional autophagic process. To further increase a potential effect of *CLEC16A* KD on autophagy, protease inhibitors were added to these experiments. Unfortunately, results of treatment with protease inhibitors showed too much variance, which is why that data was not analyzed further. Optimally, the immunoblot for p62 could be repeated under starved conditions and with treatment of protease inhibitors. Considering that the first results were already of statistical significance, there was no scientific need to repeat these experiments with protease inhibitor treatmet in regard to the strict time limitations of this experimental work.

LC3 conversion rates were studied under starved conditions and treatment with protease inhibitors such as E64d and Pepstatin A. Bafilomycin A1 was also used as a protease inhibitor but did not yield any valid data. In WT cells, after treatment with protease inhibitors, LC3-II accumulates due to inhibition of LC3-II degradation, and the LC3-II/LC3-I ratio increases as LC3-I is converted to LC3-II. Strikingly, in *CLEC16A* KD cells, as well as *ATG5* KD cells, LC3-II/LC3-I ratios were significantly reduced compared with control cells (Results, Figure 29). This shows a reduced conversion of LC3-I to LC3-II and confirms impaired autophagic flux in *CLEC16A* KD cells. Taking these results together, the previous discovery of impaired autophagy in *Clec16a* KD TECs [106] could be reproduced in human cells. This underlines that the function of *Clec16a* is conserved in human and that there is a clear link between *CLEC16A*, impaired autophagy and autoimmune disease.

4.5. *Clec16a* knockdown alters autophagy in thymic epithelium and modulates T cell selection

Analogous to the effects of *CLEC16A* KD in HeLa cells, knockdown of *Clec16a* results in impaired autophagy in thymic epithelial cells of the NOD mouse [106]. This led to the question if the effects of *Clec16a* KD on TEC autophagy were directly linked to thymocyte stimulation. To further investigate this, TEC derived MJC1 cells were used to stimulate immature thymocytes [106]. Beforehand, MJC1 cells were transduced with an LC3 construct containing the $OVA_{323-339}$ peptide, which allowed for antigen presentation restricted only to autophagy-dependent MHC class II loading [130]. Additionally, a mutated construct was introduced which prevented autophagy-dependent presentation of the OVA antigen. Stimulation by *Clec16a* KD and *Atg5* KD MJC1 cells resulted in reduced proliferation of TCR^{hi} OT-II cells (Results, Figure 30). Strikingly, stimulation via control MJC1 cells carrying the mutated $OVA_{323-339}$-LC3 construct led to a similar reduction in proliferation (Results, Figure 30). This indicates that disruption (in this case via mutation) of the autophagy-dependent MHC class II loading process mirrors the effects of *Clec16a* KD and *Atg5* KD in thymic epithelial cells. This, in turn, emphasizes the direct link between *Clec16a* KD, impaired autophagy and thymocyte stimulation.

4.6. *CLEC16A* and its role in autoimmune disease

CLEC16A is associated with a variety of autoimmune diseases. This thesis demonstrates a crucial role for the gene in immune tolerance and regulation. Its effects on autophagy modulate antigen presentation in the thymus and lead to hyporeactive T cells and disease protection in the NOD mouse. Constitutive autophagy is a characteristic feature of TEC [141]. TEC autophagy is at least partially involved in generating the MHC class II ligandome [62, 142]. Additionally, it was shown that LC3 co-localizes with MHC class II loading proteins in epithelial cells [130], as well as that autophagy directly interacts with the MHC class II loading process in TECs [62]. It remains unanswered as to how exactly *CLEC16A* affects the selection and presentation of self-peptide in the thymus. However, there are a few possible explanations for this. First, the effects of *CLEC16A* KD could impair autophagy and antigen presentation in the thymic cortex and lead to reduced positive selection, which in turn would result in more 'death by neglect' at the early stages of thymocyte development. Notably, in *Clec16a* KD animals, there was a distinct reduction in thymocytes undergoing selection ($TCR^{int/hi}$ $CD69^{hi}$) and a relative over-expression of immature thymocytes (TCR^{lo} $CD69^{lo}$) [106]. As CD69+ is a marker for transitional cells between the DP and SP developmental stages, these findings would support the idea of reduced positive selection [129]. Secondly, the effects of *CLEC16A* KD could alter autophagy in the medullary thymic epithelium, which would modulate the presentation of tissue restricted antigen and perhaps, due to qualitative or quantitative changes of self-peptide, lead to increased negative selection. Indeed, members of the Kissler Lab could demonstrate an increase in negative selection after *Clec16a* KD by measuring the expression of *Helios*, a transcription factor that marks thymocytes undergoing deletion [106]. Third, it could be a combination of both, altered positive and negative selection, as well as additional effects conveyed by changes during the maturation process of thymocytes.

In order to better understand the function of *CLEC16A,* more experiments have to be conducted, especially in regard to T cell selection, and the molecular mechanisms of the gene. Several studies have tried to characterize *CLEC16A* in more detail. One group speculated that human *CLEC16A* regulated autophagy through mTOR [143], while other groups postulated that *Clec16a* is regulated by *Pdx1* and mediates mitophagy by regulation of an E3 ubiquitin ligase called *Nrdp1* in pancreatic β cells [144], as other groups declared *Clec16a* as an

expression quantitative trait locus for its neighboring genes *Dexi* and *Socs1* [91]. Clearly, further investigation of the gene is required to illuminate the function and role of *CLEC16A*.
In this respect, as part of this thesis, confocal microscopy experiments were initiated to investigate potential co-localization of CLEC16A with other molecules involved in autophagy and antigen presentation, i.e. LC3, LAMP1 and HLA (date not shown). Furthermore, this project initiated a test to see if changes in autophagy were consistent with different human risk SNPs. For this, the first steps of a functioning CRISPR/Cas9 system were established at the Kissler Lab as ground work for future studies. Additionally, the neighboring gene *Dexi* will actively be investigated by members of the Kissler Lab, to further characterize this potential immunoregulatory gene and its association with *Clec16a*.

In summary, this work confirms that the effects of *Clec16a* KD on autophagy are conserved in human, strengthening previous results of similar function in drosophila [58] and mice [106, 123]. As the mechanistical function of *CLEC16A* remains elusive, the functional role of *CLEC16A* provides a better understanding of TEC autophagy, T cell selection and disease protection. Establishing a link between impaired autophagy, altered antigen presentation and autoimmunity, this thesis suggests a vital role for *CLEC16A* as a regulator of immune tolerance and autoimmune disease in human.

5. Summary

Genome-wide association studies revealed *CLEC16A* as a candidate gene for Type 1 Diabetes and multiple other autoimmune disorders [72]. The function of *CLEC16A* remains unknown. However, previous work showed that the *CLEC16A* ortholog *ema* and the murine *Clec16a* were both implicated in autophagy, a process partially required for MHC class II loading and antigen presentation [58, 123]. Furthermore, studies could show that autophagy was required in thymic epithelial cells for antigen presentation during T cell selection, suggesting a possible role of *CLEC16A* in T cell selection in the thymus [46, 47]. Additionally, it was postulated that *CLEC16A* may function as an expression quantitative trait locus for its neighboring genes [91, 124] and that *Clec16a* KD was involved in pancreatic islet function and impaired insulin secretion and glucose homeostasis [144]. Prior to this work, Schuster et al. had created a *Clec16a* KD NOD mouse, which was protected from spontaneous autoimmune diabetes [106].

For this work it was hypothesized that *CLEC16A* variation serves as a Type 1 Diabetes risk gene by affecting autophagy in thymic epithelial cells, which modulates antigen presentation and shapes the T cell repertoire. To expand and complement previous findings by Schuster et al., this thesis aimed to investigate how *CLEC16A* modifies the function of thymic epithelial cells. For this purpose, *CLEC16A* KD was induced in human cells via RNA interference and autophagy was studied through immunoblotting. Additionally, inflammation of pancreatic tissue in *Clec16a* KD NOD mice was scored using H.E. stained pancreatic sections. Thymic transplantation experiments were conducted to test whether the effects of *Clec16a* KD were T cell intrinsic. Also, intraperitoneal glucose tolerance tests were performed to study glucose homeostasis in *Clec16a* KD NOD animals. Finally, using qPCR, gene expression levels of neighboring genes such as *Dexi* and *Socs1* were measured to study *Clec16a* as an expression quantitative trait locus.

In combination with the findings of Schuster et al., this thesis demonstrates that *Clec16a* KD reduces the severity of insulitis and protects from onset of spontaneous diabetes in the NOD mouse. Disease protection is conveyed by impaired autophagy in TEC, which leads to altered T cell selection and hyporeactive $CD4^+$ T cells. The effects of *Clec16a* KD in the NOD mouse are thymus intrinsic. Glucose homeostasis remains unchanged in the *Clec16a* KD NOD mouse and plays no role in disease protection. *Clec16a* and *Dexi* presented similar expression levels, but

further studies are required to investigate a clear link between these two genes. Finally, impaired autophagy could be replicated in human *CLEC16A* KD cells, which demonstrates a conserved function of *CLEC16A* and suggests a possible link between *CLEC16A* variation and risk of autoimmune disease in human.

6. Zusammenfassung

Genomweite Assoziationsstudien haben *CLEC16A* als ein Suszeptibilitätsgen für Typ 1 Diabetes und weitere Autoimmunerkrankungen identifiziert [72]. Die genaue Funktion von *CLEC16A* bleibt jedoch ungeklärt. Studien zeigten, dass sowohl das Drosophila Ortholog *ema* als auch das murine *Clec16a* eine Rolle in Autophagie spielen. Autophagie trägt zur Beladung der MHC-Klasse-II Moleküle und somit der Antigenpräsentation bei [58, 123]. Darüber hinaus konnten Studien belegen, dass Autophagie zur Antigenpräsentation während der T-Zell Selektion in Thymus-Epithelzellen benötigt wird [46, 47]. Dies schlägt eine mögliche Funktion von *CLEC16A* in Thymus-Epithelzellen während der T-Zell Selektion vor. Außerdem berichteten Arbeiten, dass *CLEC16A* als quantitativer Trait Locus für seine Nachbargene fungiert [91, 124] und dass *Clec16a* KD in Langerhans Inseln im Pankreas die Insulinsekretion und den Glukosestoffwechsel beeinträchtigt [144]. Dieser Arbeit vorausgehend hatten Schuster et al. eine *Clec16a* KD NOD Maus generiert, welche vor spontanem autoimmunem Diabetes geschützt war [106].

Für diese Arbeit wurde vermutet, dass *CLEC16A* als Suszeptibilitätsgen für Typ 1 Diabetes den Prozess der Autophagie in Thymus-Epithelzellen beeinträchtigt und somit Antigenpräsentation und das T-Zell Repertoire beeinflusst. Um auf der Vorarbeit von Schuster et al. aufzubauen und diese zu ergänzen, zielte diese Arbeit darauf ab, den Einfluss von *CLEC16A* auf Thymus-Epithelzellen zu untersuchen. Hierfür wurde ein *CLEC16A* KD in menschlichen Zellen mittels RNA Interferenz erzeugt und Autophagie durch Immunoblotting untersucht. Zusätzlich wurde die Entzündung im Pankreasgewebe von *Clec16a* KD NOD Mäusen mittels H.E. Färbung beurteilt und bewertet. Thymus-Transplanationen wurden durchgeführt, um zu sehen, ob der Einfluss von *Clec16a* KD T-Zell intrinsisch ist. Außerdem wurden intraperitoneale Glukosetoleranztests durchgeführt, um den Blutzuckerstoffwechsel in *Clec16a* KD Mäusen zu beurteilen. Schließlich wurden mittels qPCR Expressionslevel der

benachbarten Gene, wie zum Beispiel *Dexi* und *Socs1*, erhoben, um die Eigenschaften von *CLEC16A* als quantitativer Trait Locus einzuordnen.

Gemeinsam mit den Ergebnissen von Schuster et al. kann diese Arbeit aufzeigen, dass *Clec16a* KD die Ausprägung von Insulitis im Pankreas reduziert und *Clec16a* KD NOD Mäuse vor spontanem Autoimmundiabetes schützt. Dieser Schutz vor Erkrankung wird durch beeinträchtigte Autophagie in Thymus-Epithelzellen hervorgerufen, welche die T-Zell Selektion beeinflusst und die Reaktivität von T-Zellen reduziert. Der Einfluss des *Clec16a* KD ist innerhalb des Thymus wirksam. Der Blutzuckerstoffwechsel in *Clec16a* KD NOD Mäusen bleibt unverändert und kann deshalb als Ursache für den Schutz vor Type 1 Diabetes ausgeschlossen werden. *Clec16a* und *Dexi* zeigen ähnliche Expressionslevel auf, dennoch benötigt es weitere detaillierte Studien, um eine Beziehung zwischen den beiden Genen etablieren zu können. Letztlich konnte die Beeinträchtigung von Autophagie in menschlichen *CLEC16A* KD Zellen nachgewiesen werden, was bedeutet, dass die Funktion von *CLEC16A* evolutionär konserviert ist und ein möglicher Zusammenhang zwischen *CLEC16A* Polymorphismen und einem erhöhten Risiko für Typ 1 Diabetes im Menschen besteht.

7. Bibliography

1. Zheng, Y., S.H. Ley, and F.B. Hu, *Global aetiology and epidemiology of type 2 diabetes mellitus and its complications.* Nat Rev Endocrinol, 2018. **14**(2): p. 88-98.
2. BÄK, K., AWMF. *Nationale Versorgungsleitlinie Therapie des Typ-2-Diabetes* 2013 [cited 2019; Available from: http://www.deutsche-diabetes-gesellschaft.de/fileadmin/Redakteur/Leitlinien/Evidenzbasierte_Leitlinien/dm-therapie-1aufl-vers4-kurz.pdf.
3. Atkinson, M.A., G.S. Eisenbarth, and A.W. Michels, *Type 1 diabetes.* Lancet, 2014. **383**(9911): p. 69-82.
4. Atkinson, M.A., *The pathogenesis and natural history of type 1 diabetes.* Cold Spring Harb Perspect Med, 2012. **2**(11).
5. Hex, N., et al., *Estimating the current and future costs of Type 1 and Type 2 diabetes in the UK, including direct health costs and indirect societal and productivity costs.* Diabet Med, 2012. **29**(7): p. 855-62.
6. Sundberg, F., P. Sand, and G. Forsander, *Health-related quality of life in preschool children with Type 1 diabetes.* Diabet Med, 2015. **32**(1): p. 116-9.
7. Copenhaver, M. and R.P. Hoffman, *Type 1 diabetes: where are we in 2017?* Transl Pediatr, 2017. **6**(4): p. 359-364.
8. Maahs, D.M., et al., *Epidemiology of type 1 diabetes.* Endocrinol Metab Clin North Am, 2010. **39**(3): p. 481-97.
9. Reinehr, T., *Type 2 diabetes mellitus in children and adolescents.* World J Diabetes, 2013. **4**(6): p. 270-81.
10. Morran, M.P., et al., *Immunogenetics of type 1 diabetes mellitus.* Mol Aspects Med, 2015. **42**: p. 42-60.
11. Noble, J.A., et al., *HLA class I and genetic susceptibility to type 1 diabetes: results from the Type 1 Diabetes Genetics Consortium.* Diabetes, 2010. **59**(11): p. 2972-9.
12. Jaidane, H., et al., *Enteroviruses and type 1 diabetes: towards a better understanding of the relationship.* Rev Med Virol, 2010. **20**(5): p. 265-80.
13. Hober, D. and P. Sauter, *Pathogenesis of type 1 diabetes mellitus: interplay between enterovirus and host.* Nat Rev Endocrinol, 2010. **6**(5): p. 279-89.
14. Paschou, S.A., et al., *On type 1 diabetes mellitus pathogenesis.* Endocr Connect, 2018. **7**(1): p. R38-r46.
15. Knip, M., et al., *Dietary intervention in infancy and later signs of beta-cell autoimmunity.* N Engl J Med, 2010. **363**(20): p. 1900-8.
16. Lerner, A., P. Jeremias, and T. Matthias, *The World Incidence and Prevalence of Autoimmune Diseases is Increasing.* International Journal of Celiac Disease, 2015. **3**(4): p. 151-155.
17. Hu, C., F.S. Wong, and L. Wen, *Type 1 diabetes and gut microbiota: Friend or foe?* Pharmacol Res, 2015. **98**: p. 9-15.
18. Keenan, H.A., et al., *Residual insulin production and pancreatic ss-cell turnover after 50 years of diabetes: Joslin Medalist Study.* Diabetes, 2010. **59**(11): p. 2846-53.
19. Willcox, A., et al., *Analysis of islet inflammation in human type 1 diabetes.* Clin Exp Immunol, 2009. **155**(2): p. 173-81.
20. Paschou, S.A., et al., *Type 1 diabetes as an autoimmune disease: the evidence.* Diabetologia, 2014. **57**(7): p. 1500-1.
21. Winter, W.E. and D.A. Schatz, *Autoimmune markers in diabetes.* Clin Chem, 2011. **57**(2): p. 168-75.

22. Pescovitz, M.D., et al., *Rituximab, B-lymphocyte depletion, and preservation of beta-cell function.* N Engl J Med, 2009. **361**(22): p. 2143-52.
23. van Belle, T.L., K.T. Coppieters, and M.G. von Herrath, *Type 1 diabetes: etiology, immunology, and therapeutic strategies.* Physiol Rev, 2011. **91**(1): p. 79-118.
24. Li, M., L.J. Song, and X.Y. Qin, *Advances in the cellular immunological pathogenesis of type 1 diabetes.* J Cell Mol Med, 2014. **18**(5): p. 749-58.
25. Katz, J., C. Benoist, and D. Mathis, *Major histocompatibility complex class I molecules are required for the development of insulitis in non-obese diabetic mice.* Eur J Immunol, 1993. **23**(12): p. 3358-60.
26. Rasche, S., R.Y. Busick, and A. Quinn, *GAD65-Specific Cytotoxic T Lymphocytes Mediate Beta-Cell Death and Loss of Function.* Rev Diabet Stud, 2009. **6**(1): p. 43-53.
27. Stavroula A. Paschou, S.T.K.N.G.K.P. and T. Agathocles, *The Role of T regulatory Cells (Tregs) in the Development and Prevention of Type 1 Diabetes.* Journal of Clinical & Cellular Immunology, 2013. **0**(0): p. 1-7.
28. Kordonouri, O., T. Hartmann R Fau - Danne, and T. Danne, *Treatment of type 1 diabetes in children and adolescents using modern insulin pumps.* (1872-8227 (Electronic)).
29. Mendez, C.E. and G.E. Umpierrez, *Management of Type 1 Diabetes in the Hospital Setting.* (1539-0829 (Electronic)).
30. Chaplin, D.D., *Overview of the immune response.* J Allergy Clin Immunol, 2010. **125**(2 Suppl 2): p. S3-23.
31. Nicholson, L.B., *The immune system.* Essays Biochem, 2016. **60**(3): p. 275-301.
32. Medina, K.L., *Overview of the immune system.* Handb Clin Neurol, 2016. **133**: p. 61-76.
33. Murphy, K., et al., *Janeway's immunobiology.* New York, Garland Science, 2012.
34. Cooper, G.S., M.L. Bynum, and E.C. Somers, *Recent insights in the epidemiology of autoimmune diseases: improved prevalence estimates and understanding of clustering of diseases.* J Autoimmun, 2009. **33**(3-4): p. 197-207.
35. The, D.P.G., *Incidence and trends of childhood Type 1 diabetes worldwide 1990–1999.*
36. Tao, B., et al., *Estimating the Cost of Type 1 Diabetes in the U.S.: A Propensity Score Matching Method.* PLoS One, 2010. **5**(7).
37. Ebers, G.C., et al., *A population-based study of multiple sclerosis in twins.* N Engl J Med, 1986. **315**(26): p. 1638-42.
38. Ebers, G.C., A.D. Sadovnick, and N.J. Risch, *A genetic basis for familial aggregation in multiple sclerosis. Canadian Collaborative Study Group.* Nature, 1995. **377**(6545): p. 150-1.
39. Peng, J., et al., *Long term effect of gut microbiota transfer on diabetes development.* J Autoimmun, 2014. **53**: p. 85-94.
40. Floreani, A., P.S. Leung, and M.E. Gershwin, *Environmental Basis of Autoimmunity.* Clin Rev Allergy Immunol, 2016. **50**(3): p. 287-300.
41. Xing, Y. and K.A. Hogquist, *T-cell tolerance: central and peripheral.* Cold Spring Harb Perspect Biol, 2012. **4**(6).
42. Klein, L., et al., *Antigen presentation in the thymus for positive selection and central tolerance induction.* Nat Rev Immunol, 2009. **9**(12): p. 833-44.
43. Murata, S., et al., *Regulation of CD8+ T cell development by thymus-specific proteasomes.* Science, 2007. **316**(5829): p. 1349-53.
44. Gommeaux, J., et al., *Thymus-specific serine protease regulates positive selection of a subset of CD4+ thymocytes.* Eur J Immunol, 2009. **39**(4): p. 956-64.

45. Nakagawa, T., et al., *Cathepsin L: critical role in Ii degradation and CD4 T cell selection in the thymus.* Science, 1998. **280**(5362): p. 450-3.
46. Nedjic, J., et al., *Autophagy in thymic epithelium shapes the T-cell repertoire and is essential for tolerance.* Nature, 2008. **455**(7211): p. 396-400.
47. Nedjic, J., et al., *Macroautophagy, endogenous MHC II loading and T cell selection: the benefits of breaking the rules.* Curr Opin Immunol, 2009. **21**(1): p. 92-7.
48. Peterson, P., T. Org, and A. Rebane, *Transcriptional regulation by AIRE: molecular mechanisms of central tolerance.* Nat Rev Immunol, 2008. **8**(12): p. 948-57.
49. Gallegos, A.M. and M.J. Bevan, *Central tolerance to tissue-specific antigens mediated by direct and indirect antigen presentation.* J Exp Med, 2004. **200**(8): p. 1039-49.
50. Oukka, M., et al., *Medullary thymic epithelial cells induce tolerance to intracellular proteins.* J Immunol, 1996. **156**(3): p. 968-75.
51. Klein, L., et al., *Positive and negative selection of the T cell repertoire: what thymocytes see (and don't see).* Nat Rev Immunol, 2014. **14**(6): p. 377-91.
52. Sprent, J. and H. Kishimoto, *The thymus and central tolerance.* Philos Trans R Soc Lond B Biol Sci, 2001. **356**(1409): p. 609-16.
53. Kurd, N. and E.A. Robey, *T-cell selection in the thymus: a spatial and temporal perspective.* Immunol Rev, 2016. **271**(1): p. 114-26.
54. Boya, P., F. Reggiori, and P. Codogno, *Emerging regulation and functions of autophagy.* Nat Cell Biol, 2013. **15**(7): p. 713-20.
55. Mizushima, N. and M. Komatsu, *Autophagy: renovation of cells and tissues.* Cell, 2011. **147**(4): p. 728-41.
56. Mizushima, N., T. Yoshimori, and Y. Ohsumi, *The role of Atg proteins in autophagosome formation.* Annu Rev Cell Dev Biol, 2011. **27**: p. 107-32.
57. Shaid, S., et al., *Ubiquitination and selective autophagy.* Cell Death Differ, 2013. **20**(1): p. 21-30.
58. Kim, S., S.A. Naylor, and A. DiAntonio, *Drosophila Golgi membrane protein Ema promotes autophagosomal growth and function.* Proc Natl Acad Sci U S A, 2012. **109**(18): p. E1072-81.
59. Yoshii, S.R. and N. Mizushima, *Monitoring and Measuring Autophagy.* Int J Mol Sci, 2017. **18**(9).
60. Dengjel, J., et al., *Autophagy promotes MHC class II presentation of peptides from intracellular source proteins.* Proc Natl Acad Sci U S A, 2005. **102**(22): p. 7922-7.
61. Paludan, C., et al., *Endogenous MHC class II processing of a viral nuclear antigen after autophagy.* Science, 2005. **307**(5709): p. 593-6.
62. Kasai, M., et al., *Autophagic compartments gain access to the MHC class II compartments in thymic epithelium.* J Immunol, 2009. **183**(11): p. 7278-85.
63. Klionsky, D.J., et al., *Guidelines for the use and interpretation of assays for monitoring autophagy (3rd edition).* Autophagy, 2016. **12**(1): p. 1-222.
64. Mizushima, N. and T. Yoshimori, *How to interpret LC3 immunoblotting.* Autophagy, 2007. **3**(6): p. 542-5.
65. Schaaf, M.B., et al., *LC3/GABARAP family proteins: autophagy-(un)related functions.* Faseb j, 2016. **30**(12): p. 3961-3978.
66. Kimura, S., et al., *Monitoring autophagy in mammalian cultured cells through the dynamics of LC3.* Methods Enzymol, 2009. **452**: p. 1-12.
67. Liu, W.J., et al., *p62 links the autophagy pathway and the ubiqutin-proteasome system upon ubiquitinated protein degradation.* Cell Mol Biol Lett, 2016. **21**: p. 29.

68. Rogov, V., et al., *Interactions between autophagy receptors and ubiquitin-like proteins form the molecular basis for selective autophagy.* Mol Cell, 2014. **53**(2): p. 167-78.
69. Bjorkoy, G., et al., *p62/SQSTM1 forms protein aggregates degraded by autophagy and has a protective effect on huntingtin-induced cell death.* J Cell Biol, 2005. **171**(4): p. 603-14.
70. Kabeya, Y., et al., *LC3, a mammalian homologue of yeast Apg8p, is localized in autophagosome membranes after processing.* Embo j, 2000. **19**(21): p. 5720-8.
71. Kabeya, Y., et al., *LC3, GABARAP and GATE16 localize to autophagosomal membrane depending on form-II formation.* J Cell Sci, 2004. **117**(Pt 13): p. 2805-12.
72. Hakonarson, H., et al., *A genome-wide association study identifies KIAA0350 as a type 1 diabetes gene.* Nature, 2007. **448**(7153): p. 591-4.
73. Tomlinson, M.J.t., et al., *Fine mapping and functional studies of risk variants for type 1 diabetes at chromosome 16p13.13.* Diabetes, 2014. **63**(12): p. 4360-8.
74. Hirschfield, G.M., et al., *Association of primary biliary cirrhosis with variants in the CLEC16A, SOCS1, SPIB and SIAE immunomodulatory genes.* Genes Immun, 2012. **13**(4): p. 328-35.
75. Hafler, D.A., et al., *Risk alleles for multiple sclerosis identified by a genomewide study.* N Engl J Med, 2007. **357**(9): p. 851-62.
76. Jagielska, D., et al., *Follow-up study of the first genome-wide association scan in alopecia areata: IL13 and KIAA0350 as susceptibility loci supported with genome-wide significance.* J Invest Dermatol, 2012. **132**(9): p. 2192-7.
77. Skinningsrud, B., et al., *A CLEC16A variant confers risk for juvenile idiopathic arthritis and anti-cyclic citrullinated peptide antibody negative rheumatoid arthritis.* Ann Rheum Dis, 2010. **69**(8): p. 1471-4.
78. Skinningsrud, B., et al., *Polymorphisms in CLEC16A and CIITA at 16p13 are associated with primary adrenal insufficiency.* J Clin Endocrinol Metab, 2008. **93**(9): p. 3310-7.
79. Marquez, A., et al., *Specific association of a CLEC16A/KIAA0350 polymorphism with NOD2/CARD15(-) Crohn's disease patients.* Eur J Hum Genet, 2009. **17**(10): p. 1304-8.
80. Dubois, P.C., et al., *Multiple common variants for celiac disease influencing immune gene expression.* Nat Genet, 2010. **42**(4): p. 295-302.
81. Gateva, V., et al., *A large-scale replication study identifies TNIP1, PRDM1, JAZF1, UHRF1BP1 and IL10 as risk loci for systemic lupus erythematosus.* Nat Genet, 2009. **41**(11): p. 1228-33.
82. Database. *Uniprot (Internet)*. 2019; Available from: https://www.uniprot.org/uniprot/Q2KHT3.
83. Database. *Ensembl Genome Browser (Internet)*. 2019; Available from: https://www.ensembl.org/Homo_sapiens/Gene/Summary?g=ENSG00000038532;r=16:10944488-11182189.
84. Berge, T., I.S. Leikfoss, and H.F. Harbo, *From Identification to Characterization of the Multiple Sclerosis Susceptibility Gene CLEC16A.* Int J Mol Sci, 2013. **14**(3): p. 4476-97.
85. McGreal, E.P., L. Martinez-Pomares, and S. Gordon, *Divergent roles for C-type lectins expressed by cells of the innate immune system.* Mol Immunol, 2004. **41**(11): p. 1109-21.
86. Bezbradica, J.S., et al., *A role for the ITAM signaling module in specifying cytokine-receptor functions.* Nat Immunol, 2014. **15**(4): p. 333-42.
87. Barrett, J.C., et al., *Genome-wide association study and meta-analysis find that over 40 loci affect risk of type 1 diabetes.* Nat Genet, 2009. **41**(6): p. 703-7.

88. Chang, C.H. and R.A. Flavell, *Class II transactivator regulates the expression of multiple genes involved in antigen presentation.* J Exp Med, 1995. **181**(2): p. 765-7.
89. Fenner, J.E., et al., *Suppressor of cytokine signaling 1 regulates the immune response to infection by a unique inhibition of type I interferon activity.* Nat Immunol, 2006. **7**(1): p. 33-9.
90. Davison, L.J., et al., *Long-range DNA looping and gene expression analyses identify DEXI as an autoimmune disease candidate gene.* Hum Mol Genet, 2012. **21**(2): p. 322-33.
91. Leikfoss, I.S., et al., *Multiple sclerosis-associated single-nucleotide polymorphisms in CLEC16A correlate with reduced SOCS1 and DEXI expression in the thymus.* Genes Immun, 2013. **14**(1): p. 62-6.
92. *Human Genome Resources at NCBI*. CLEC16A 2019 [cited 2019; Available from: https://www.ncbi.nlm.nih.gov/genome/gdv/browser/?cfg=NCID_1_24981646_130.14.22.10_9146_1553523213_3147728562.
93. Kim, S., et al., *The novel endosomal membrane protein Ema interacts with the class C Vps-HOPS complex to promote endosomal maturation.* J Cell Biol, 2010. **188**(5): p. 717-34.
94. Kissler, S., *From genome-wide association studies to etiology: probing autoimmunity genes by RNAi.* Trends Mol Med, 2011. **17**(11): p. 634-40.
95. Chipman, L.B. and A.E. Pasquinelli, *miRNA Targeting: Growing beyond the Seed.* Trends Genet, 2019.
96. Levanova, A. and M.M. Poranen, *RNA Interference as a Prospective Tool for the Control of Human Viral Infections.* Front Microbiol, 2018. **9**: p. 2151.
97. Database. *NCBI Probe Database*. 2019; Available from: https://www.ncbi.nlm.nih.gov/probe/docs/techrnai/.
98. Birmingham, A., et al., *3' UTR seed matches, but not overall identity, are associated with RNAi off-targets.* Nat Methods, 2006. **3**(3): p. 199-204.
99. Website. *The Jackson Laboratory*. [cited 2019; Available from: https://www.jax.org/personalized-medicine/why-mouse-genetics#.
100. Perlman, R.L., *Mouse models of human disease: An evolutionary perspective.* Evol Med Public Health, 2016. **2016**(1): p. 170-6.
101. Website. *hek293.com*. [cited 2019; Available from: http://www.hek293.com/.
102. Lucey, B.P., W.A. Nelson-Rees, and G.M. Hutchins, *Henrietta Lacks, HeLa cells, and cell culture contamination.* Arch Pathol Lab Med, 2009. **133**(9): p. 1463-7.
103. Ye, X., X.J. Zhou, and H. Zhang, *Exploring the Role of Autophagy-Related Gene 5 (ATG5) Yields Important Insights Into Autophagy in Autoimmune/Autoinflammatory Diseases.* Front Immunol, 2018. **9**: p. 2334.
104. Tuzmen, S., J. Kiefer, and S. Mousses, *Validation of short interfering RNA knockdowns by quantitative real-time PCR.* Methods Mol Biol, 2007. **353**: p. 177-203.
105. Sheen, J.H., et al., *Defective regulation of autophagy upon leucine deprivation reveals a targetable liability of human melanoma cells in vitro and in vivo.* Cancer Cell, 2011. **19**(5): p. 613-28.
106. Schuster, C., et al., *The Autoimmunity-Associated Gene CLEC16A Modulates Thymic Epithelial Cell Autophagy and Alters T Cell Selection.* Immunity, 2015. **42**(5): p. 942-52.
107. Morel, E., et al., *Autophagy: A Druggable Process.* Annu Rev Pharmacol Toxicol, 2017. **57**: p. 375-398.

108. Foster, D.A. and A. Toschi, *Targeting mTOR with rapamycin: one dose does not fit all.* Cell Cycle, 2009. **8**(7): p. 1026-9.
109. Kim, K.W., et al., *Autophagy upregulation by inhibitors of caspase-3 and mTOR enhances radiotherapy in a mouse model of lung cancer.* Autophagy, 2008. **4**(5): p. 659-68.
110. Makino, S., et al., *Breeding of a non-obese, diabetic strain of mice.* Jikken Dobutsu, 1980. **29**(1): p. 1-13.
111. Anderson, M.S. and J.A. Bluestone, *The NOD mouse: a model of immune dysregulation.* Annu Rev Immunol, 2005. **23**: p. 447-85.
112. Lieberman, S.M. and T.P. DiLorenzo, *A comprehensive guide to antibody and T-cell responses in type 1 diabetes.* Tissue Antigens, 2003. **62**(5): p. 359-77.
113. Wicker, L.S., J.A. Todd, and L.B. Peterson, *Genetic control of autoimmune diabetes in the NOD mouse.* Annu Rev Immunol, 1995. **13**: p. 179-200.
114. Greeley, S.A., et al., *Elimination of maternally transmitted autoantibodies prevents diabetes in nonobese diabetic mice.* Nat Med, 2002. **8**(4): p. 399-402.
115. Bach, J.F., *Insulin-dependent diabetes mellitus as an autoimmune disease.* Endocr Rev, 1994. **15**(4): p. 516-42.
116. Kikutani, H. and S. Makino, *The murine autoimmune diabetes model: NOD and related strains.* Adv Immunol, 1992. **51**: p. 285-322.
117. Jansen, A., et al., *Immunohistochemical characterization of monocytes-macrophages and dendritic cells involved in the initiation of the insulitis and beta-cell destruction in NOD mice.* Diabetes, 1994. **43**(5): p. 667-75.
118. Gerold, K.D., et al., *The soluble CTLA-4 splice variant protects from type 1 diabetes and potentiates regulatory T-cell function.* Diabetes, 2011. **60**(7): p. 1955-63.
119. Li, D.S., et al., *A protocol for islet isolation from mouse pancreas.* Nat Protoc, 2009. **4**(11): p. 1649-52.
120. Funda, D.P., et al., *Gluten-free but also gluten-enriched (gluten+) diet prevent diabetes in NOD mice; the gluten enigma in type 1 diabetes.* Diabetes Metab Res Rev, 2008. **24**(1): p. 59-63.
121. Caquard, M., et al., *Diabetes acceleration by cyclophosphamide in the non-obese diabetic mouse is associated with differentiation of immunosuppressive monocytes into immunostimulatory cells.* Immunol Lett, 2010. **129**(2): p. 85-93.
122. Vladutiu, A.O., *The severe combined immunodeficient (SCID) mouse as a model for the study of autoimmune diseases.* Clin Exp Immunol, 1993. **93**(1): p. 1-8.
123. Soleimanpour, S.A., et al., *The diabetes susceptibility gene Clec16a regulates mitophagy.* Cell, 2014. **157**(7): p. 1577-90.
124. Leikfoss, I.S., et al., *Multiple Sclerosis Risk Allele in CLEC16A Acts as an Expression Quantitative Trait Locus for CLEC16A and SOCS1 in CD4+ T Cells.* PLoS One, 2015. **10**(7): p. e0132957.
125. Pai, R.K., et al., *Regulation of class II MHC expression in APCs: roles of types I, III, and IV class II transactivator.* J Immunol, 2002. **169**(3): p. 1326-33.
126. NCBI. *SOCS1 suppressor of cytokine signaling 1 [Homo sapiens (human)]*. 2019; Available from: https://www.ncbi.nlm.nih.gov/gene/8651#gene-expression.
127. NCBI. *CLEC16A C-type lectin domain containing 16A [Homo sapiens (human)]*. 2019; Available from: https://www.ncbi.nlm.nih.gov/gene/23274.
128. NCBI. *DEXI Dexi homolog [Homo sapiens (human)]*. 2019; Available from: https://www.ncbi.nlm.nih.gov/gene/28955.

129. Yamashita, I., et al., *CD69 cell surface expression identifies developing thymocytes which audition for T cell antigen receptor-mediated positive selection.* Int Immunol, 1993. **5**(9): p. 1139-50.
130. Schmid, D., M. Pypaert, and C. Munz, *Antigen-loading compartments for major histocompatibility complex class II molecules continuously receive input from autophagosomes.* Immunity, 2007. **26**(1): p. 79-92.
131. Robertson, J.M., P.E. Jensen, and B.D. Evavold, *DO11.10 and OT-II T cells recognize a C-terminal ovalbumin 323-339 epitope.* J Immunol, 2000. **164**(9): p. 4706-12.
132. Roep, B.O., *The role of T-cells in the pathogenesis of Type 1 diabetes: from cause to cure.* Diabetologia, 2003. **46**(3): p. 305-21.
133. Varanasi, V., et al., *Cytotoxic mechanisms employed by mouse T cells to destroy pancreatic beta-cells.* Diabetes, 2012. **61**(11): p. 2862-70.
134. Burrack, A.L., T. Martinov, and B.T. Fife, *T Cell-Mediated Beta Cell Destruction: Autoimmunity and Alloimmunity in the Context of Type 1 Diabetes.* Front Endocrinol (Lausanne), 2017. **8**: p. 343.
135. Plesa, G., et al., *TCR affinity and specificity requirements for human regulatory T-cell function.* Blood, 2012. **119**(15): p. 3420-30.
136. In't Veld, P., *Insulitis in human type 1 diabetes: The quest for an elusive lesion.* Islets, 2011. **3**(4): p. 131-8.
137. Takaba, H. and H. Takayanagi, *The Mechanisms of T Cell Selection in the Thymus.* Trends Immunol, 2017. **38**(11): p. 805-816.
138. Griesemer, A.D., E.C. Sorenson, and M.A. Hardy, *The role of the thymus in tolerance.* Transplantation, 2010. **90**(5): p. 465-74.
139. Kim, S. and A. DiAntonio, *A role for the membrane Golgi protein Ema in autophagy.* Autophagy, 2012. **8**(8): p. 1269-70.
140. Holmes, K., et al., *Detection of siRNA induced mRNA silencing by RT-qPCR: considerations for experimental design.* BMC Res Notes, 2010. **3**: p. 53.
141. Crotzer, V.L. and J.S. Blum, *Autophagy and adaptive immunity.* Immunology, 2010. **131**(1): p. 9-17.
142. Brazil, M.I., S. Weiss, and B. Stockinger, *Excessive degradation of intracellular protein in macrophages prevents presentation in the context of major histocompatibility complex class II molecules.* Eur J Immunol, 1997. **27**(6): p. 1506-14.
143. Tam, R.C., et al., *Human CLEC16A regulates autophagy through modulating mTOR activity.* Exp Cell Res, 2017. **352**(2): p. 304-312.
144. Soleimanpour, S.A., et al., *Diabetes Susceptibility Genes Pdx1 and Clec16a Function in a Pathway Regulating Mitophagy in beta-Cells.* Diabetes, 2015. **64**(10): p. 3475-84.

8. Appendix

8.1. Affidavit

Affidavit

I hereby confirm that my thesis entitled "How *CLEC16A* modifies the function of thymic epithelial cells" is the result of my own work. I did not receive any help or support from commercial consultants. All sources and / or materials applied are listed and specified in the thesis.

Furthermore, I confirm that this thesis has not yet been submitted as part of another examination process neither in identical nor in similar form.

Wuerzburg, _____ _____
Place, Date Signature

Eidesstattliche Erklärung

Hiermit erkläre ich an Eides statt, die Dissertation "Wie *CLEC16A* die Funktion von Thymus-Epithelzellen beeinflusst" eigenständig, d.h. insbesondere selbständig und ohne Hilfe eines kommerziellen Promotionsberaters, angefertigt und keine anderen als die von mir angegebenen Quellen und Hilfsmittel verwendet zu haben.

Ich erkläre außerdem, dass die Dissertation weder in gleicher noch in ähnlicher Form bereits in einem anderen Prüfungsverfahren vorgelegen hat.

Würzburg, den _____ _____
Ort, Datum Unterschrift

8.2. List of publications and posters

8.2.1. Publication

Cornelia Schuster, Kay D. Gerold, Kilian Schober, Lilli Probst, Kevin Boerner, Mi-Jeong Kim, Anna Ruckdeschel, Thomas Serwold, Stephan Kissler. The Autoimmunity-Associated Gene *CLEC16A* Modulates Thymic Epithelial Cell Autophagy and Alters T Cell Selection. *Immunity* (2015).

8.2.2. Poster Presentation

Kevin Boerner, Cornelia Schuster, Stephan Kissler.
How *CLEC16A* modifies the function of thymic epithelial cells.
Eureka! - 10th International GSLS Students Symposium, Wuerzburg, Germany, 2015.

8.3. Acknowledgment

First, I would like to express my sincere gratitude to my advisor and mentor Prof. Dr. Stephan Kissler for his continuous support and guidance over the past five years. I am grateful for all the patience and motivation, and thankful for the incredible knowledge and insight he constantly shared with me in all the time of research and writing of this thesis. This project would not have been possible without Prof. Dr. Stephan Kissler, who generously invited me into his Lab and the United States of America.

Besides my advisor, I would like to thank the rest of my thesis committee: Prof. Dr. Thomas Hünig for making this unusual project possible by supervising me as my advisor from abroad, and Prof. Dr. med. Hans-Peter Tony for completing the committee without hesitation. Thank you for the insightful and critical comments, which helped me focus on my research and broaden my scientific horizon.

A special thank you to my brilliant supervisor and dear friend Dr. Cornelia Schuster, for her unwavering patience, for teaching me everything I now know about science and being a great friend.

Of course, I want to thank my fellow lab mates Dr. Celia Caballero-Franco, Dr. Chin-Nien Lee, Dr. Dominika Nowakowska and Janice Nieves-Bonilla for always helping me out, and for the inspiring discussions and all the fun we had. I also want to thank my friends and colleagues from the 4th floor, especially Dr. Mi-Jeong Kim for providing the MJC1 cell line, Dr. Russel Eason for his valuable input and the good laughs, and of course Halina Polishuk, for never letting coffee run out and making life at the lab a little bit more enjoyable every day.

A special thank you to the Medical Faculty of the University of Wuerzburg and the Graduate School of Life Sciences for supporting me with a scholarship and providing the framework for this project.

Thank you, Boston, for being the most incredible and beautiful city.

Last, I would like to thank my friends and family for everything. Thank you for being with me all the way through, for accompanying me on this journey, and for never giving up on me. Thank you for letting me go and thank you for letting me come back. Anna Ruckdeschel, for being my partner in crime during this time. And, always, my parents Dietmar Börner and Birgit Koj, my grandmother Elvira Hartenberger and my brother Kenneth Börner, for guiding me with love and providing the foundation needed to complete this work.

Thank you.